INVESTIGATION ON THE EFFECTS OF ULTRA-HIGH PRESSURE AND TEMPERATURE ON THE RHEOLOGICAL PROPERTIES OF OIL-BASED DRILLING FLUIDS

A Thesis

by

CHIJIOKE STANLEY IBEH

Submitted to the Office of Graduate Studies of
Texas A&M University
in partial fulfillment of the requirements for the degree of

MASTER OF SCIENCE

December 2007

Major Subject: Petroleum Engineering

INVESTIGATION ON THE EFFECTS OF ULTRA-HIGH PRESSURE AND TEMPERATURE ON THE RHEOLOGICAL PROPERTIES OF OIL-BASED DRILLING FLUIDS

A Thesis

by

CHIJIOKE STANLEY IBEH

Submitted to the Office of Graduate Studies of
Texas A&M University
in partial fulfillment of the requirements for the degree of

MASTER OF SCIENCE

Approved by:

Co-Chairs of Committee,	Jerome J. Schubert
	Catalin Teodoriu
Committee Members,	Kenneth R. Hall
	Hans C. Juvkam-Wold
Head of Department,	Steve Holditch

December 2007

Major Subject: Petroleum Engineering

ABSTRACT

Investigation on the Effects of Ultra-High Pressure and Temperature on the Rheological Properties of Oil-based Drilling Fluids. (December 2007)

Chijioke Stanley Ibeh, B.Eng., Federal University of Technology Owerri, Nigeria

Co-Chairs of Advisory Committee: Dr. Jerome J. Schubert
Dr. Catalin Teodoriu

Designing a fit-for-purpose drilling fluid for high-pressure, high-temperature (HP/HT) operations is one of the greatest technological challenges facing the oil and gas industry today. Typically, a drilling fluid is subjected to increasing temperature and pressure with depth. While higher temperature decreases the drilling fluid's viscosity due to thermal expansion, increased pressure increases its viscosity by compression. Under these extreme conditions, well control issues become more complicated. Also current logging tools are at best not reliable because the anticipated bottom-hole temperature is often well above their operating limit. The literature shows limited experimental data on drilling fluid properties beyond 350°F and 20,000 psig. The practice of extrapolation of fluid properties at some moderate level to extreme-HP/HT (XHP/HT) conditions is obsolete and could result in significant inaccuracies in wellbore hydraulics calculations.

This research is focused on developing a methodology for testing drilling fluids at XHP/HT conditions using a state-of-the-art viscometer capable of accurately measuring drilling fluids properties up to 600°F and 40,000 psig. A series of factorial experiments were performed on typical XHP/HT oil-based drilling fluids to investigate their change in rheology at these extreme conditions (200 to 600°F and 15,000 to 40,000 psig). Detailed statistical analyses involving: analysis of variance, hypothesis testing, evaluation of residuals and multiple linear regression are implemented using data from

the laboratory experiments. I have developed the *FluidStats* program as an effective statistical tool for characterizing drilling fluids at XHP/HT conditions using factorial experiments. Results from the experiments show that different drilling fluids disintegrate at different temperatures depending on their composition. In summary, the combined pressure-temperature effect on a drilling fluid's rheology is complex.

This research is vital because a proper drilling fluids design is a necessary first step towards curtailing the high well control incident rate (25 times that of non-HP/HT wells) often associated with HP/HT operations. According to the Minerals Management Service (MMS), over 50% of proven oil and gas reserves in the United States lie below 14,000 ft subsea. Thus drilling in HP/HT environment is fast becoming common place especially in the Gulf of Mexico where HP/HT resistant drilling fluids are increasingly being used to ensure safe and successful operations.

DEDICATION

First I am grateful to God for his guidance and dedicate this work to my loving parents (Dominic and Agnes Ibeh), my special brother (Obi), my darling (Nkem) and adorable sisters (Chioma and Chika) for all their love and support.

ACKNOWLEDGEMENTS

This project would not have been a success without the opportunity and support given to me by Dr. Jerome Schubert. I remain thankful for his guidance throughout this project and most of all his friendship.

I would like to thank Dr. Hans C. Juvkam-Wold and Dr. Hall for serving on my graduate committee and giving advice. I also thank Dr. Catalin Teodoriu for his technical support especially in setting-up and trouble-shooting the XHP/HT viscometer and Vivek Gupta for his assistance with the lab experiments.

I am particularly grateful to Baker Hughes Drilling Fluids (BHDF) for sponsoring this research and providing the XHP/HT viscometer, drilling fluid samples and technical support. I thank Bill Gusler for devoting his time to train me on how to program and use of the XHP/HT viscometer.

I would also like to thank the faculty and staff in the Department of Petroleum Engineering at Texas A&M University especially Dr Steve Holditch for his unique leadership.

Finally I would like to express my appreciation to all the members of Aggie Drilling Research and friends here at Texas A&M University.

TABLE OF CONTENTS

LIST OF FIGURES

FIGURE Page

FIGURE Page

LIST OF TABLES

CHAPTER I

INTRODUCTION: HP/HT DRILLING FLUIDS DESIGN

Formulating a drilling fluid system that can adequately withstand drilling in a high pressure and high temperature environment is very challenging, but very often little attention is given to proper fluids design. Hallan Marsh (inventor of the Marsh Funnel viscometer) made this assertion in the early twentieth century thus:

> *The subject of mud sounds so simple, uninteresting and unimportant that it has failed to receive the attention that it deserves, at least as applied to the drilling of oil wells. As a matter of fact, it is one of the most complicated, technical, important and interesting subjects in connection with rotary drilling.*

Basically a drilling fluid experiences two opposing effects as the temperature and pressure of a mud column increases with depth. Increase in pressure tends to increase the fluid's viscosity due to its compressibility, whereas the increase in temperature increases the Brownian motion of the macromolecules (particles) dissolved in the fluid matrix. As a consequence, there is reduced molecular interaction and hence reduced viscosity (values of other rheological properties are also reduced). However for a particular temperature and pressure profile, these two opposite effects cancel out, leaving uniform mud viscosity / density along the depth of the well that is equal to that at surface.

The general practice is to measure a fluid's flow characteristics under ambient surface conditions and extrapolate these measurements in some way to the downhole conditions. This requires a reliable model of how the rheology of the fluid changes with the cyclical variations in temperature, pressure and shear history which it experiences during circulation inside the wellbore.

_____

This thesis follows the style and format of *SPE Drilling & Completion*.

Despite a considerable experimental study over the years, for both water- and oil-based fluids, there is relatively little systematic understanding of how their flow behavior changes with downhole conditions for the following reasons,[1]:

1. It has been common practice to make measurements of shear rheology at relatively few shear rates and to represent shear stress/shear rate curves (rheograms) by simple two-parameter constitutive models, such as the Bingham Plastic or Power Law models which are not adequate especially in HP/HT situations.

2. The rheology of the fluid is influenced by many factors including temperature, pressure, shear history, composition and the electrochemical character of the components and of the continuous fluid phase. These effects can be summarized as follows:

Physical: Decreases in temperature and increases in pressure both affect the mobility of the systems and lead to an increase of apparent viscosities and visco-elastic relaxation times. The effect of pressure is expected to be greater with oil based systems owing to the oil phase compressibility.

Electrochemical: An increase in temperature augments the ionic activity of any electrolyte, and the solubility of any partially soluble salt that may be present in the fluid. This could alter the balance between the inter-particle attractive and repulsive forces and so the degree of dispersion and flocculation of the mud systems.

Chemical: At temperatures above 200ºF all hydroxides react with clay minerals. With many mud systems, this can result in a change of the structure and therefore also in a change of the mud rheological properties.

In recent years there has been an increasing awareness of the first point, and a study of oil-based fluids in the laboratory has shown that an equation initially proposed by Casson,[2] for ink pigments can be a good representation of these fluids and that its parameters vary with temperature and pressure in a systematic way describable by a simple engineering model.

The temperature at the bottom of the hole increases as the depth of the well increases because the earth's core is hotter than its crust with a continuous flow of heat from the center towards the surface. The geothermal gradient will vary depending on the geological conditions, such as the thickness of the earth's crust, thermal conductivity properties of the rocks and geological features such as volcanoes or fault zones. Naturally, the drilling fluid temperature will approach the geothermal gradient when it is not being circulated during a trip or on logging runs. However the mud temperature is always in a transient state strongly sensitive to the flow rate as presented by Karstad and Aadnoy.[3] Recent advances in temperature modeling have led to a better understanding and development of some brilliant interpretation techniques. The determination of effective mud viscosity/density is critical to the analysis of drilling and completion operations. Also without thorough knowledge of the actual pressures occurring in the system, it is sometimes difficult to prevent a gas kick or circulation losses in fractured formation. Therefore a drilling fluid's viscosity is directly related to the downhole variations in pressure and temperature and is a very important part of drilling engineering.

According to the Minerals Management Service (MMS),[4] an HP/HT completion or workover project is one where the well will:

1. Require completion equipment or well control equipment with either a pressure rating greater than 15,000 psig or a temperature rating greater than 350°F.
2. Have a maximum anticipated surface pressure (MASP) greater than 15,000 psig.
3. Have a shut-in tubing pressure (SITP) greater than 15,000 psig.

4. Have a flowing temperature greater than 350°F at the seafloor or at the surface.

For the purpose of this research, I collectively classify HP/HT and XHP/HT conditions to be in the range 200 to 600°F and 10,000 to 40,000 psig.

Oil-based drilling fluids have some advantages when compared to water based fluids in HP/HT applications. These include maintaining stable rheology and filtration control for extended periods of time and increased lubricity. In addition, oil base drilling fluids can be used to drill through most troublesome shale formations due to their inherent inhibitive nature and temperature stability. However, most commercial oil base drilling fluid systems have limitations such as reduced rheology and filtration control if the fluid is exposed to temperatures higher than 300°F for prolonged periods of time. Also there is the issue of hydrogen sulfide and methane absorption.

In HP/HT wells, only a small hydrostatic overbalance can be tolerated due to the reduced margin between pore and fracture gradients, Therefore it is vital that both the hydrostatic overbalance and the dynamic pressures are accurately modeled and managed. Otherwise, either losses or influx may result. Due to the small margin stated above, the effects of pressure and temperature on a drilling fluid's viscosity under downhole conditions and on the equivalent circulating density (ECD) cannot be ignored. Therefore the main objectives of this research are:

1. Develop a methodology for testing drilling fluids using the automated Chandler model 7600 XHP/HT viscometer.
2. Statistically quantify the main and interaction effects of ultra-high temperature and pressure on the rheological properties of oil-based drilling fluids.
3. Develop a Visual Basic algorithm for statistical analysis and modeling to facilitate easy application.

The approach adopted was first to review all relevant literature on HP/HT drilling fluids and rheological models. Then a series of factorial experiments were performed on the

oil-based drilling fluids using the automated XHP/HT viscometer. For each test, the initial dial reading values at 150°F and ambient pressure (14.7 psia) where compared with those of the Fann 35 viscometer for proper quality control and to ensure consistency in results. Finally, using statistical tools the results of the tests were analyzed and conclusions / recommendations made.

CHAPTER II

LITERATURE REVIEW

2.1 THE HP/HT ENVIRONMENT

The future of oil and gas exploration and production lies greatly in deepwater wells drilled in HP/HT and XHP/HT environments. The petroleum industry has been working to identify and bridge gaps between currently available technology and what is required to drill, complete, and produce wells in HP/HT deepwater environments. Deep resources represent approximately 158 Tcf (at depths greater than 14,000 ft), and are one of the sources of natural gas that will play an important role in meeting the growing need for natural gas in the United States. The Energy Information Agency estimated that 7% of U.S gas production came from deep formations in 1999. This contribution is expected to increase to 14% by 2010. Much of this deep gas production will come from the Rocky Mountain, Gulf Coast, and GOM sedimentary basins.

Data from a typical HP/HT field in the GOM is presented in **Table 2.1**. The conditions defined are wells drilled 27,000 ft below mud line with reservoir temperatures in excess of 400°F and reservoir pressures of 24,500 psig. It is explicitly recognized that reservoir temperatures on the order of 500°F are ultimately possible.

Table 2.1–Typical HP/HT field data in Gulf of Mexico[4]

Field Parameters	Data
Water Depth in Field	4,000ft
Number of Producing Wells	6 (Non-subsalt)
Hydrocarbon Type	Dry gas with contaminants
Net Reservoir Thickness	300 ft to 600 ft (Single production zone)
Reservoir Rock	Very fine medium grain subarkoses
Reservoir Type	Dune (50%); Sheet Sand (30%) with jigsaw puzzle discontinuous faults.
Reservoir Depth	27,000 ft BML
Bottom Hole Pressure	24,500 psi
Pressure Gradient (from mudline)	0.84 psi/ft
Bottom Hole Temperature	400°F
Temperature Gradient (from mudline)	15°F/1000 ft
Shut-In Wellhead Pressure	21,000psi
Producible Reserves	600 bcfg (≈75% RF)
Typical Reserves Per Well	100 bcfg
Natural Drive Mechanism	Pressure Depletion
Production Well Spacing	Approx. 700 acres
Initial Production Rate Per Well	100 MMscf/d
Typical Production Rate Per Well	100 MMscf/d and 10 bbl/MMscf liquids.

(Courtesy MMS Project No.: 519, DeepStar CTR 7501, Table 2)

Proper drilling fluids planning and execution play a major role in preventing adverse events and increasing the success of deep gas drilling. Since HP/HT drilling is inherently expensive, the choice of drilling fluids and technologies requires careful evaluation to handle the HP/HT challenges. These challenges include elevated temperatures and pressures that limit tool and downhole equipment selection, downhole pressure determination, lost circulation, low penetration rates, acid gases, and compliance with safety and environmental regulations as detailed below.

2.2 REALITIES OF DRILLING A HP/HT WELL

Challenges for drilling and completing deep HP/HT wells are significant. Future technologies and advances in current technology must adequately address the three issues at the heart of HP/HT drilling safety: kick prevention, kick detection and well control. For example, the volume of an HP/HT gas kick remains virtually unchanged as

it rises in the annulus from 14,000 to 10,000 ft. From 10,000 to 2,000 ft its volume triples. But from 2,000 ft to the surface, there is a 100-fold expansion.[4] There are other safety concerns that have a similar exponential increase of exposure that must be taken into account while new protocols are developed to drill wells in HP/HT deepwater environments. Health safety and environment (HSE) issues with regard to hot drilling fluids and tripping hot drill strings are also critical to the success of future operations.

Development of new approaches to drilling deep HP/HT wells is required to meet engineering requirements while keeping projects economically viable. Developing optimum drilling technologies and techniques must also take place within the framework of completion requirements. For example, casing-while-drilling could significantly decrease the time spent on downhole problems not associated with actual drilling processes (e.g., stuck pipe, lost circulation, and well control situations). This in turn leads to a safer and less expensive drilling operation (fewer people, less pipe handling, fewer trips, and less mud). Issues listed below represent primary concerns of drillers when planning HP/HT deep wells. As the state of the art advances, additional concerns will surface that merit evaluation.

2.2.1 Limited Evaluation Capabilities

- Most tools work to 425°F on wireline; very limited tool availability from 425°F to 600°F on wireline.
- Currently battery technology works to 400°F for MWD applications.
- Sensor accuracy decreases with increasing temperature.
- LWD/MWD tools are reliable to 275°F with an exponential decrease in dependability to 350°F.

2.2.2 Slow Rate of Penetration in Producing Zone

- Bits typically remove 10% of the rock per bit rotation in this environment compared to normal drilling conditions for Gulf of Mexico wells.

- Crystalline structure breaks down in polycrystalline diamond compact (PDC) bits at these conditions. (Boron expansion is an issue.)
- Roller-cone bits are unsuitable for HP/HT environment.
- Impregnated cutter drilling is often slow.

2.2.3 Well Control

- Pore pressure is near fracture gradient causing potential well control problems.
- Mud loss is an issue due to lithology and geopressure.
- Hole ballooning causes mud storage problems. The walls of the well expand outward because of increased pressure during pumping. When pumping stops, the walls contract and return to normal size. Excess mud is then forced out of the well.
- Methane (CH_4) and hydrogen sulfide (H_2S) are soluble in oil-base mud and are released from the solution as pressure decreases. The fluid column in the annulus is thereby lightened.
- Wellhead design for above 25,000 psig and 450°F is needed. Current rating is 15,000 psig, 350°F H_2S service with work in progress for 20,000 psig, 350°F equipment. Similar concerns with Blow-Out Prevention Equipment (BOPE).

2.2.4 Non-Productive Time

- Stuck pipe and twisting off
- Trip Time – caused by tool failure (LWD/MWD) and bit trips
- Suboptimal decision making caused by lack of HP/HT experience (the “learning curve”)
- Safety issues associated with handling hot drilling fluids, hot drill strings

2.3 DEVELOPMENTS IN HP/HT DRILLING FLUIDS

A review of the literature showed that for non-HP/HT wells, the effects of pressure and temperature on mud weight is minimal and can be ignored. However, for HP/HT wells the effects of pressure and temperature on surface mud weight, the equivalent downhole

mud weight, and the equivalent circulating density (ECD) must be taken into consideration.

Early investigations into the effects of temperature on the flow properties of drilling fluids were performed by Bartlett,[1] and published by AIME in 1967. The study showed significant decrease in viscosity (by half) of a particular ligno-sulfonate mud when its temperature was increased from 80°F to 140°F. Alderman *et al.*[5] made measurements of the rheology of a range of water-based drilling fluids at temperatures up to 266°F and pressure up to 14,500 psig. The data was then fitted using a three-parameter Herschel-Bulkley yield/power-law model. However in some cases the two-parameter Casson[2] equation gave a more acceptable fit. In both models, it was observed that the behavior of the high-shear viscosity reflected the viscous nature of the continuous phase: a weak pressure dependence and exponential temperature dependence similar to that of water. Yield stress was essentially independent of pressure and remained constant at some characteristic temperature in contrast to oil-based fluid behavior.

Combs and Whitmire[6] showed that the change in viscosity of the continuous phase is the main factor in controlling the change in the viscosity of the mud with pressure. McMordie *et al.*[7] concluded that the power law model gives the best mathematical description of the viscosity of an oil base fluid at constant temperature and pressure. They found that the logarithm of shear stress is proportional to the pressure. De Wolfe *et al.*[8] reported a close correlation of the results from their study of less toxic oils to the Herschel-Bulkley model. It was also observed that the magnitude of viscosity difference between oils tend to decrease with temperature in spite of pressure indicating that temperature was the more dominant factor. The fluids composition is also very important. The limitation is that their results are presented as apparent viscosities thereby masking the evaluation of other temperature and pressure dependent rheological properties.

During various phases of drilling, static pressures exerted by a fluid column are usually calculated by assuming a constant mud viscosity and density at all depths in the borehole. Fluids at different depths experience different temperatures and pressures. Thus mud viscosity at downhole condition can be significantly different from those measured at the surface especially in HP/HT wells. But inability to accurately quantify these effects has perpetuated the age-long practice of using rheological parameters measured at the surface.

Houwen,[9] described the pressure behavior of invert emulsion muds as exponential which can be represented by a two-parameter Casson model. The two Casson parameters are given as the viscosity at infinitely high shear rate, and the apparent yield stress which are analogous to the plastic viscosity and yield point of the Bingham Plastic model. The advantage of the Casson model over the Bingham model being that the Casson model reproduces the curvature of the rheograms at low shear rates above about $1s^{-1}$.

Drilling a HP/HT well means effectively managing the very narrow margin between the formation pore and fracture pressures. Therefore it is necessary to maintain the down-hole mud pressure within this ‘‘safe operating window,’’ in order to avoid any kick or loss problems. Through a recent survey conducted in the Norwegian sector of North Sea oil fields, it was observed HP/HT deep wells were prone to more kicks and well-control problems when compared to the other deep wells drilled in the same area. The accuracy of pressure prediction is dependent on the accuracy of the mud rheology measurements, the mud density, and on true pipe, casing and hole diameters. In practice, the stand pipe pressure variations could be used to monitor the down-hole rheological behavior of the mud.

There is a direct relationship between viscosity and density as increase in density results in increase in viscosity. Several authors have done some work on density-pressure-temperature modeling but not within the vicinity of XHP/HT conditions as defined

earlier. Babu,[10] measured data of different muds whose weights varied up to 18 lbm/gal and temperatures up to 400°F and pressures up to 15,000 psig and showed that mud weight variations of the magnitude of 1.5 lbm/gal occurred for both water as well as oil-based muds. He concluded that if these variations are not accounted for properly during the estimation of static pressures, they can cause well control problems during deep and hot well drilling. Karstad and Aadnoy[11] presented an analytical model for the density-pressure-temperature dependence of drilling fluids. This paper couples a transient temperature model with a fluid density model. The result is the determination of the effective wellbore pressure taking effects of compression and thermal expansion into account. Osman and Aggour[12] proposed an Artificial Neural Networks (ANN) model to predict mud density as a function of mud type, pressure and temperature. Data used were for temperature and pressure ranges up to 400°F and 14,000 psig respectively. The study showed the effect of temperature and pressure on the density of oil-base and water-base drilling fluids and presented experimental measurements of densities in the temperature range of 70 to 400°F and pressure range of 0 to 14,000 psig. Their finding was that the change in mud density with pressure and temperature is independent of the initial mud density (at 70°F and 0 psig). They also concluded that for equal densities at the surface conditions, oil-base drilling fluids become denser than water-base drilling fluids at high temperatures and pressures.

Oil based drilling fluids have definite advantages when compared to water based fluids. These include maintaining stable rheology and filtration control for extended periods of time and increased lubricity. In addition, oil base drilling fluids can be used to drill through most troublesome shale formations due to their inherent inhibitive nature and temperature stability.

More recently formate brines,[13] have been introduced into the HP/HT market to provide drilling and completion fluids that are free of the troublesome components like barite found in conventional fluids. The temperature stability of common drilling fluid polymers is enhanced when dissolved in aqueous solutions containing high levels of

sodium and/or potassium formates. Since entering service in 1999, cesium formate brines have been used in over 100 HP/HT operations in 21 different fields around the world. Rigorous field-testing has shown that cesium formates are thermally stable up to 420°F. Some of the many advantages of formate brines include: minimal formation damage, better thermal stability, elimination of barite sag, low gas solvency, low ECDs, reduced torque and drag, compatibility with elastomers and biodergradability. Formate brines make for perfect drilling and completion fluids for difficult well construction projects where extraordinary fluid performance is critical for economic success. Hence the demand for formate brines has been growing steadily at a compound rate of approximately 30% per annum over the past decade. The major disadvantage of formate brines is that they are relatively more expensive than traditional OBM and there is increased complexity in the reservoir log analysis.

In summary, there is little information on the rheological properties of the various drilling fluids described above at extreme HP/HT conditions (in the vicinity 300 to 600°F and 20,000 to 40,000 psig). Investigating the rheological behavior of various oil-based drilling fluids at these extreme conditions is the main focus of this research. It will be interesting to evaluate the behavior of other fluid types like formate brines in future research work.

2.4 SCOPE AND ORGANIZATION OF RESEARCH

The scope of this research is covered in the following three phases:

1. **Preliminary Studies**: This involves all studies relating to: literature review, drilling fluids fundamentals, measuring devices (viscometers and rheometers), and design of experiments.
2. **Experimentation**: This refers to fluid sampling, preparation and laboratory testing of oil-based drilling fluids.
3. **Analyses / Interpretation:** This final phase focuses on analyzing results, modeling and then conclusions / recommendations.

This report is organized into seven (7) chapters. Chapter III covers the fundamentals of drilling fluids describing in details the various types of rheological models available. Chapter IV highlights the methodology proposed and test design employed in this research. Results of these tests are presented in Chapter V while Chapter VI covers detailed statistical analyses of the results and modeling. Chapter VII discusses conclusions together with recommendations.

CHAPTER III

DRILLING FLUIDS FUNDAMENTALS

3.1 DRILLING FLUID TYPES

Drilling fluids can be broadly classified into three based on their constituents as shown in **Fig. 3.1**. Only diesel and mineral oil-based fluids are investigated in this research.

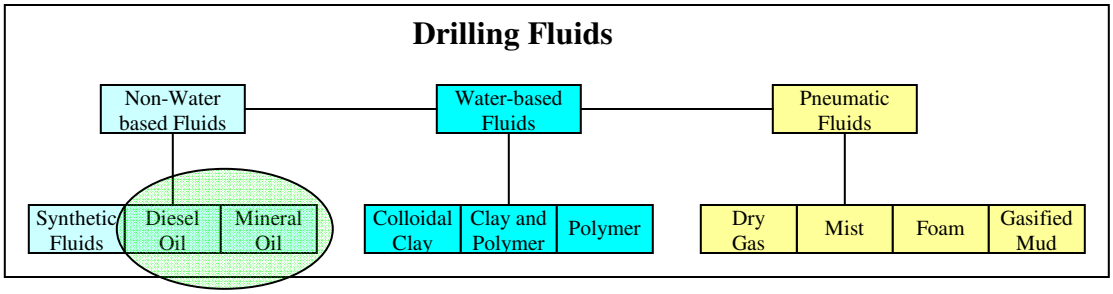

Fig. 3.1–Drilling fluids classification by composition

Fluids in general can be grouped into two according to their flow behavior: Newtonian and non-Newtonian. **Fig. 3.2** illustrates the two groupings with examples.

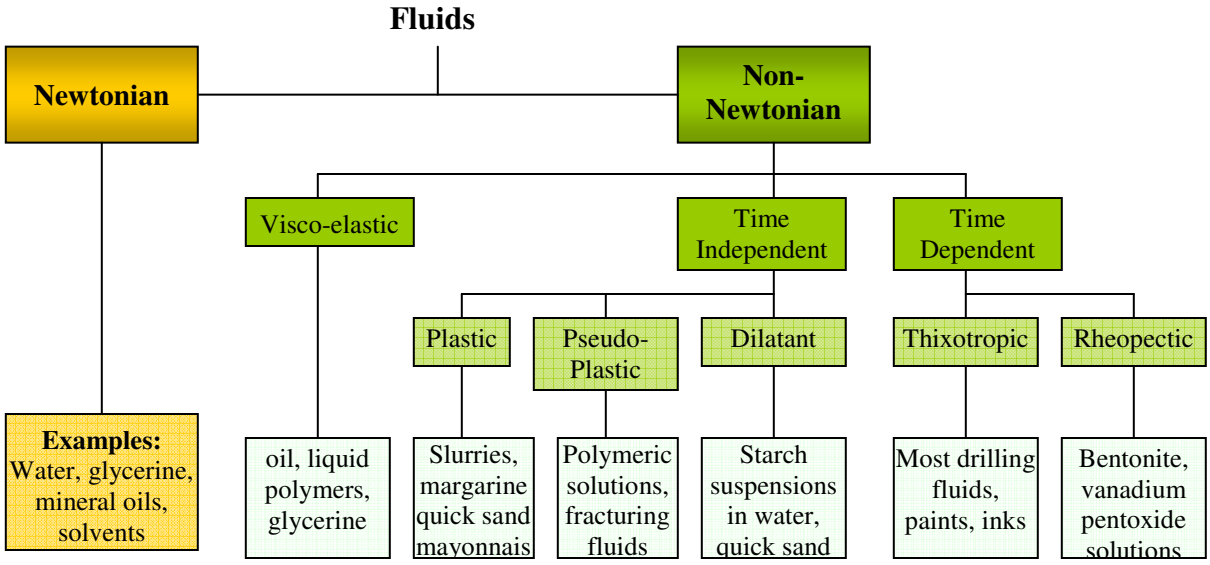

Fig. 3.2–General fluid grouping by flow behavior.

Newtonian fluids exhibit constant viscosity irrespective of the shear stress. For non-Newtonian, time independent fluid, shear stress is a function of shear rate. For time dependent fluids, stress – strain relationship depends on how the fluid has been sheared and on the previous history. Visco-elastic fluids are predominantly viscous but exhibit partial elastic recovery after deformation. Fluids exhibiting elastic properties are often referred to as *memory fluids*.

Most drilling fluids are non-Newtonian i.e. they have a viscosity value that is dependent on the rate of shear. Non-Newtonian, time independent fluids fall into 3 basic categories: Bingham plastics, pseudoplastics and dilatants fluids. A pseudoplastic fluid is one whose apparent viscosity or consistency decreases gradually with increase in rate of shear also known as shear thinning. For plastic fluids, shear force is not proportional to the shear rate and a finite shear stress is required to start and maintain flow. The direct opposite is a dilatant (shear thickening) fluid. Thixotropic fluids are characterized by increase in viscosity with time at constant shear rate. The reverse is true for rheopectic fluids. Examples of all these fluids are given in Fig. 3.2 above.

3.2 RHEOLOGY

Rheology is simply defined as the science of the deformation and flow of matter. The term comes from two Greek words; “rheo” meaning to flow and “logos” meaning science or logic. The term rheology is generally applicable to all materials from gases to solids. When applied to drilling fluids, rheology deals with the relationship between flowrate and flow pressure/temperature and their combined influence on the flow characteristics of the fluid. It is interesting to note the viscosity of some common fluids as shown in **Table 3.1**.

Table 3.1: Viscosity of some common fluids[14]

Fluids used in daily life	Viscosity (cP) at 68°F
Methyl Alcohol	0.597
Water	1.002
Mercury	1.554
Motor oil (SAE 30)	150 - 200
Pancake Syrup	2,500
Honey	10,000
Chocolate Syrup	25,000
Ketchup	50,000
Peanut Butter	250,000

The prevailing flow regime (either laminar or turbulent as illustrated in **Fig 3.3**) is also important in predicting the behavior of a fluid system and its ability to perform as desired. Laminar flow is generally associated with low fluid velocities typical of the annular regions of a wellbore and with fluid movement in uniform layers. The fluid particles tend to move in straight lines parallel to the flow direction. The layer nearest to the wall of the flow channel tends to move a lower velocity than the layer immediately next to it with the highest velocity at the center. The flow profile resembles a parabolic stack of thin as shown in **Fig. 3.4**.

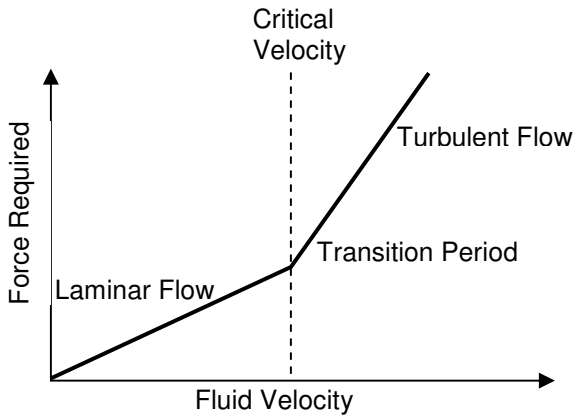

Fig. 3.3–Pressure versus viscosity on a flow regime

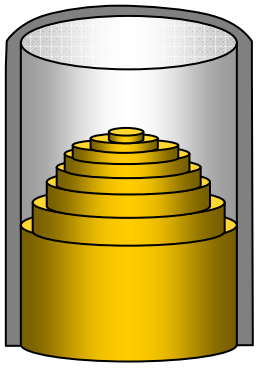

Fig. 3.4–Telescoping concentric cylinders of a laminar fluid flow

Turbulent flow occurs at high fluid velocities and is characterized by random movement of the drilling fluid particles. Although a flowing fluid is considered to be in either laminar or turbulent flow, there usually exists a transition period in which the movement of fluid particles is neither completely laminar nor random. This occurs at the critical velocity which is governed by the ratio of the fluid's inertia forces to its viscous forces which defines the Reynolds Number, N_{re}.

$$N_{re} = \frac{7745.8Du}{v} \quad \text{……...……...…} \quad (3.1)$$

Where $D =$ diameter of the flow channel, in

$u =$ average flow velocity, ft/s

$v =$ kinematic viscosity, cSt

The onset of turbulent flow is generally thought to occur at a Reynold's Number between 2000 and 3000 although other values may suffice in some special cases.

3.2.1 Viscosity Definitions

3.2.1.1 Dynamic Viscosity

This is the ratio of shear stress to the rate of shear under steady flow conditions. Dynamic viscosity is measured in units of **poise** which is defined as the force in **dynes** between parallel plates 1 square cm in area, 1 cm apart, moving with a relative velocity of 1cm/second. With the SI unit, paschal second (Pa-s) can be expressed as:

1 Pa-s = 10 poise

1 millipascal second (mPa.s) = 1 centipoise (cP) = 10^{-2} dyne-s/cm^2

The dynamic viscosity of water is 0.890 cP at 77°F, and 1.002 cP at 68°F. This is the globally accepted standard for viscosity. Dynamic viscosity can simply be said to be the resistance of a fluid to flow or deform under shear stress. This is represented mathematically as:

Dynamic viscosity; $\mu = \frac{\tau}{\gamma}$ (measured in centipoise, cP)……..... (3.2)

Where;

Shear stress; $\tau = \frac{Force\ \ Applied\,(\,dynes\,)}{Surface\ \ Area\,(\,cm^2\,)}$ (units in dynes/cm^2)

Shear rate; $\gamma = \frac{Velocity\,(\,cm/\,sec)}{Dis\,tan\,ce\,(\,cm\,)}$ (units in sec^{-1})

3.2.1.2 Kinematic Viscosity

This is defined as the dynamic viscosity divided by the density of the material. This results in units with dimensions of area per unit of time. When the units are mm^2/s they are known as centistokes (cSt). However in SI unit, kinematic viscosity is measured in m^2/s. Conversion between kinematic and dynamic viscosity, is given by: $v\rho = \mu$. Note that the parameters must be given in SI units not in P, cP or St.

For example, if kinematic viscosity, v = 1 St (=0.0001 m^2-s^{-1}) and ρ = 1000 kg m^{-3}
Then dynamic viscosity, $\mu = v\rho$ = 0.1 kg-m^{-1}-s^{-1} = 0.1 Pa-s = 100 cP

This research is based on laboratory measurements of dynamic viscosity so henceforth the term "viscosity" will be used to mean dynamic viscosity.

3.3 RHEOLOGICAL MODELS

A number of rheological models, based on mathematical equations relating shear stress and shear rate in laminar flow condition, have been developed in order to predict fluid behavior at shear rates other than those actually tested. However most drilling fluids are too complex to allow a single set of equations to be used in determining their behavior under all conditions. Therefore the utilization of the appropriate rheological model together with shear stress/shear rate data obtained from a suitable instrument allows accurate determination of the fluid behavior under varying flow conditions found in the oilfield. This data then forms the basis for further calculations used to determine several important aspects related to the drilling fluid's performance such as:

1. Calculation of system pressure losses
2. Calculation of surge and swab pressures
3. Bit and jet nozzle hydraulics
4. Equivalent circulating density
5. Relative hole cleaning efficiency
6. Bottom hole pressure management / well control
7. Estimation of the relative extent of hole erosion

Thus proper understanding and application of rheological principles is vital in determining the dynamic performance of a drilling fluid, in order to establish and maintain the most effective fluid properties for efficient, safe and economical drilling operation. For the purpose of this thesis the Newtonian, Bingham Plastic, Power Law and Herschel-Bulkley Models are illustrated in detail. Each of these models relate flow rate (shear rate) to flow pressure (shear stress) while the fluid is in laminar flow.

3.3.1 Newtonian Model

In a Newtonian fluid such as water, glycerine or oil, shear stress is directly proportional to shear rate with a slope equal to the viscosity of the fluid.

$$\tau = \mu\gamma \quad \text{..... (3.3)}$$

Where: $\tau =$ shear stress, lbf/100 ft^2

$\mu =$ viscosity, cP

$\gamma =$ shear rate, sec^{-1}

Most drilling fluids do not conform to the Newtonian Model and as such it is limited in predicting the behavior or drilling fluids.

3.3.2 Bingham Plastic Model

The Bingham Plastic Model assumes that the fluid behaves as an elastic solid up to some stress level known as the yield stress (τ_y) beyond which the fluid flow will be Newtonian. Bingham Plastic fluids therefore approach Newtonian behavior at very high

shear rates and approximate the behavior of a solid at low shear rates. This is a two-parameter model involving: yield point (stress) and plastic viscosity that is independent of shear rate. The constitutive equation for Bingham plastic fluids is:

$$\tau = \tau_y + \mu_p \gamma \quad \text{.....} \quad (3.4)$$

Where τ_y = yield stress, lbf/100 ft^2

μ_p = plastic viscosity, cP

γ = shear rate, sec^{-1}

Plastic viscosity and yield point are calculated from the 600 RPM and 300 RPM readings measured by the Couette viscometer as follows:

Plastic viscosity, $\mu_p = \theta_{600} - \theta_{300}$ ..... (3.5)

Yield point, $\tau_y = \theta_{300} - \mu_p$ ..... (3.6)

3.3.3 Power Law Model

The Power Law model accurately demonstrates the behavior of a drilling fluid at low shear rates; however, it does not include yield stress and therefore, can give poor results at extremely low shear rates. This model assumes that all fluids are pseudo-plastic in nature and may be defined by the following equation:

$$\tau = k\gamma^n \quad \text{.....} \quad (3.7)$$

Where k = consistency index, Pa-s^n

n = flow behavior index (dimensionless)

γ = shear rate, sec^{-1}

Pseudo-plastic fluids begin to flow as soon as any pressure is applied. They have no yield point and do not exhibit a linear consistency curve, although it may approach linearity at high shear rates.

The parameters n and k are obtainable from log-log plot of the shear stress versus shear rate. For pseudoplastic fluids, the exponent n is less than one. As the shear rate increases, the slope of the graph decreases. In other words, the apparent viscosity decreases with

increase in shear rate and such fluids are also known as shear thinning. Dilatant fluids tend to obey power law relationship; however, in this case n is greater than one. As a result, the curve for a dilatant fluid looks the same as for a pseudoplastic fluid, except that it is concave upwards because the apparent viscosity increases as shear rate increases. **Fig. 3.5** shows an idealized Power Law fluid.

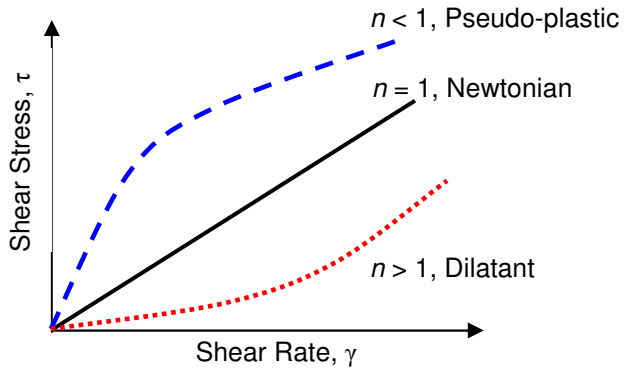

Fig. 3.5–Flow curves for a Power Law fluid

3.3.4 Herschel-Bulkley Model

The Hershel Bulkley model, describes the behavior of yield pseudo-plastics reasonably well. Pseudo-plastic flow curve is characterized by a non-linear relationship between shear rate, γ and shear stress, τ. This model is useful for describing a wide range of fluids used in oil field applications. It is given by the following equation:

$$\tau = \tau_y + k\gamma^n \quad \text{.....} \quad (3.8)$$

Where τ_y = yield stress, lbf/100 ft^2

k = consistency index, Pa-s^n

n = flow behavior index (dimensionless)

γ = shear rate, sec^{-1}

The model is reduced to the power law model if there is no yield point and to Bingham model if n is equal to one. The above 3 models are widely used to design the drilling fluids hydraulic program. A plot of their flow curves is presented in **Fig. 3.6** below.

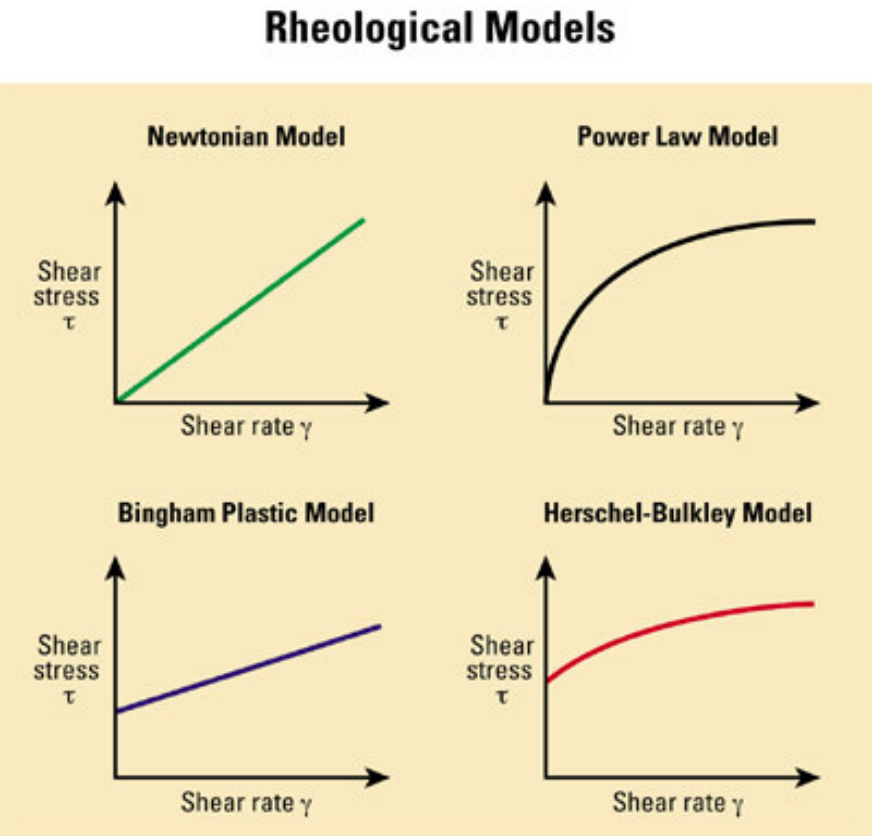

Fig. 3.6–Shear stress versus shear rate for various rheological models[15]

3.3.5 Other Models

The other rheological models,[2,15,16] are less popular and are defined by three or more adjustable parameters. Parameters are included to better describe the flow behavior of the fluid in the upper and lower Newtonian region. These models have been developed such that at low shear rates, they exhibit behavior intermediate between that of the Bingham and Power law models. A typical drilling fluid exhibits a yield stress and shear thinning. At high shear rate, all models represent a typical drilling fluid reasonably well. However the difference between the fluid models is most pronounced at low and at very high shear rates. The other models are Casson, Ellis, Sisko, Carreau, Robertson-Stiff, Cross and Meter model.

3.3.5.1 Casson Model

This model was originally developed for ink pigments but has been shown to give a good match for some oil-based fluid systems,[16]:

$$\tau^{\frac{1}{2}} = \tau_o^{\frac{1}{2}} + k^{\frac{1}{2}}\gamma^{\frac{1}{2}} \quad \text{..... (3.9)}$$

Where $k =$ Casson model constant ($\gamma = 0$ when $\tau \le \tau_o$)

$\tau_0 =$ Yield Stress, lbf/100 ft^2

$\gamma =$ Shear Rate, sec^{-1}

A plot of $\tau^{\frac{1}{2}}$ versus $\gamma^{\frac{1}{2}}$ gives an intercept of $\tau_o^{\frac{1}{2}}$ and a slope of $k^{\frac{1}{2}}$. The parameters of this model can be obtained using non-linear regression. This model combines a yield stress with greater shear thinning behavior than the Bingham plastic model. In general, it has limited application because of the difficulty in using it to predict pressure losses.

3.3.5.2 Ellis Model

Ellis constitutive law is given as,[17]:

$$\tau = \eta\gamma \quad \text{..... (3.10)}$$

$$\frac{1}{\eta} = \frac{1}{\eta_0}\left[1 + \left(\frac{\tau}{\tau_{\frac{1}{2}}}\right)^{\alpha-1}\right] \quad \text{..... (3.11)}$$

Here η is the viscosity, η_0 is the viscosity at zero shear stress, $\tau_{\frac{1}{2}}$ is the shear stress at which the viscosity is reduced by a factor of ½, and α is a power law index. When α = 1, the liquid is Newtonian, while for α >1, the liquid is shear thinning. The Ellis viscosity model incorporates power law behavior at high shear stress, while allowing for a Newtonian plateau at low shear stress. **Fig. 3.7** shows an idealized Ellis model.

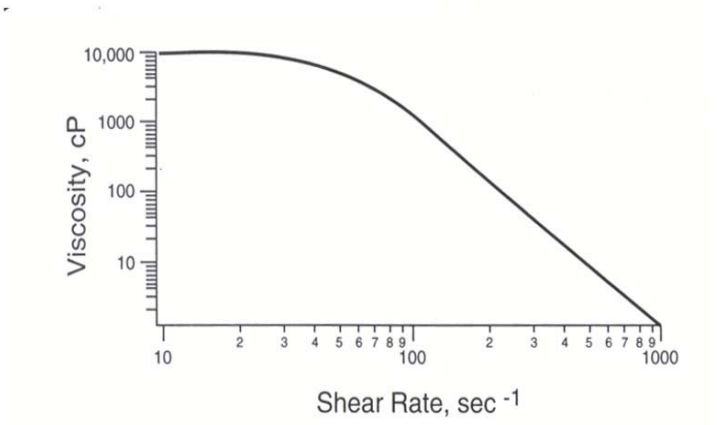

Fig. 3.7–Flow curve for an Ellis model fluid[16]

3.3.5.3 Sisko Model

The Sisko model,[16,17] is another three-parameter model, which is useful in describing flow in the power law and upper Newtonian regions. It is given as:

$$\eta = \eta_{\infty} + k\gamma^{n-1} \quad \text{.....} \quad (3.12)$$

The Sisko model is best suited to describe the flow behavior of fluids in the high shear rate region (1000 to 10,000 sec^{-1}). This model may be useful in evaluating fluid behavior at high flow rates to determine the impact of viscosity on pressure drops. **Fig. 3.8** shows an idealized Sisko model.

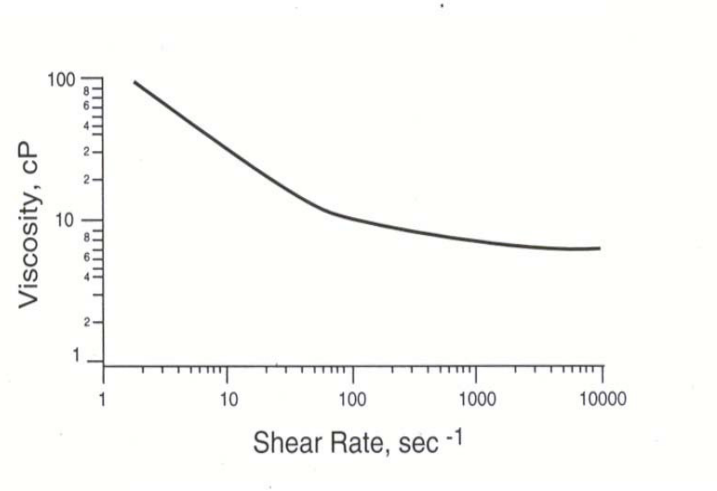

Fig. 3.8–Idealized Sisko model fluid.[16]

3.3.5.4 Carreau Model

This is an example of a four-parameter model that should describe the flow behavior over the entire range of shear rates. It is given as:

$$\frac{\eta-\eta_\infty}{\eta_0-\eta_\infty}=\left[1+(\lambda\gamma)^2\right]^{\frac{(n-1)}{2}} \quad \text{……...……...…} \quad (3.13)$$

The parameter λ is a time constant, calculated from the point on the viscosity versus shear rate curve where the flow changes from the lower Newtonian region to the power law region. This model has received a lot of attention in rheological literature; however, it has not been extensively used in describing oil field fluids due to difficulties in obtaining data to define upper and lower Newtonian regions.

Some other rheological models and their constitutive equations are,[16]:

1. Robertson-Stiff Model $\tau=k(\gamma_o+\gamma)^n$ …….. (3.14)

2. Cross Model $$\frac{\eta-\eta_\infty}{\eta_0-\eta_\infty}=\frac{1}{\left[1+(\lambda\gamma)^m\right]} \quad \text{…….....} \quad (3.15)$$

3. Meter Model $$\frac{\eta-\eta_\infty}{\eta_0-\eta_\infty}=\frac{1}{\left[1+\left(\frac{\tau}{\tau_{\frac{1}{2}}}\right)^{(\alpha-1)}\right]} \quad \text{……..…….....} \quad (3.16)$$

3.4 MEASUREMENT OF FLUID FLOW PROPERTIES

The measurement of fluid flow properties can be done with a variety of viscometric instruments. Two instruments are commonly used to measure viscometric properties,[18,19,20]. These are the capillary rheometer and rotating sleeve viscometers.

Using the capillary rheometer, fluid is pumped through a horizontal pipe at a measured rate and fluid pressure is measured at two points along the pipe. The difference between

these pressure readings is a measure of shear stress at the pipe wall, while shear rate at the wall is a function of flow rate and fluid properties. It describes flow curve completely.

There are different types of viscometers. The most common is the Fann viscometer. The Fann viscometer is of the rotational coaxial cylinder or Couette type. Readings from the Fann viscometer is used for this study. The common commercial models have two rotational speeds (300 and 600 RPM), six rotational speeds (3, 6, 100, 200, 300, 600 RPM) and twelve rotational speeds (0.9, 1.8, 3, 6, 30, 60, 90, 100, 180, 200, 300, 600 RPM). The shear stress (scale reading) is determined as a function of the shear rate (from the speed of rotation). The next chapter discusses in the details the various types of viscometers, their limitations and applications with emphasis on the automated XHP/HT viscometer.

CHAPTER IV

EQUIPMENT AND METHODOLOGY

4.1 VISCOMETERS AND RHEOMETERS

Viscometers can be broadly classified into two categories: dynamic and kinematic viscometers. A dynamic viscometer is one where the shear rate can both be controlled and measured (e.g rotational viscometer). It is the only type of viscosity measurement that is relevant to fluids where the viscosity is related to the shear rate (ie non-Newtonian fluids).

A kinematic viscometer on the other hand is one where the shear rate can neither be controlled nor measured, for example capillary viscometers. Sir George Gabriel Stokes in the late 19th century proposed a classical method of measuring viscosity which consisted of measuring the time for a fluid to flow through a capillary tube. Refined by Cannon, Ubbelohde and others, the glass tube (capillary) viscometer is still the master method for the standard determination of the kinematic viscosity of water. Capillary viscometers can have a reproducibility of nearly 0.1% under ideal conditions, which means when immersed in a high-precision fluid bath, but are not ideally suited for measuring fluids with high solids contents, or viscosity. Further, they are impossible to use to characterize non-Newtonian fluids, which include most fluids of technical interest. There are international standard methods for making measurements with a capillary instrument, such as ASTM D445 or ISO 3104.

Rheometers are viscometers which are able to measure visco-elastic properties of materials rather than viscosity alone. A rheometer, therefore, measures material behavior such as yield stress, kinetic properties, complex viscosity, modulus, creep, and recovery. Most rheometer models belong to three specific categories. These are the rotational rheometer, the capillary rheometer, and the extensional rheometer. The most commonly

used of these is the rotational rheometer, which is also called a stress/strain rheometer, followed by the capillary rheometer. Having differentiated viscometers from rheometers, for simplicity we will use the term “viscometer” through out this work to refer to both viscometers and rheometers alike.

For the purpose of this research, the family of dynamic viscometers will be discussed highlighting a few like the vibrational viscometer, marsh funnel viscometer but focusing more on the Couette or coaxial cylinder viscometer. This is because all laboratory experiments were performed with the Couette viscometer.

4.1.1 Vibrational Viscometers

Vibrational viscometers date back to the 1950’s Bendix instrument, which is of a class that operates by measuring the damping of an oscillating electromechanical resonator immersed in a fluid whose viscosity, is to be determined. The resonator generally oscillates in torsion or transversely (as a cantilever beam or tuning fork). The higher the viscosity, the larger the damping imposed on the resonator. The resonator's damping may be measured by one of several methods:

1. Measuring the power input necessary to keep the oscillator vibrating at constant amplitude. The higher the viscosity, the more power is needed to maintain the amplitude of oscillation.
2. Measuring the decay time of the oscillation once the excitation is switched off. The higher the viscosity, the faster the signal decays.
3. Measuring the frequency of the resonator as a function of phase angle between excitation and response waveforms. The higher the viscosity, the larger the frequency change for a given phase change.

Various companies have developed devices based on vibrating blades or other vessels, following the original designs patented by SOFRASER, a French Company. The active part of the viscometer is a vibrating rod excited by a constant electrical power. The vibration amplitude varies according to the viscosity of the fluid in which the rod is

immersed. These viscosity meters are suitable for measuring clogging fluid and high-viscosity fluids (up to 1,000,000 cP). Currently, many industries around the world consider these viscometers as the most efficient system to measure viscosity, contrasted to rotational viscometers, which require more maintenance, inability to measure clogging fluid, and frequent calibration after intensive use. Vibrating viscometers have no moving parts, no weak points and the sensitive part is very small. Some companies have electronic sensors that can work in the most difficult conditions up to 572°F. The downside is that vibrational viscometers suffer from a lack of a defined shear field, which makes them unsuited to measuring the viscosity of a fluid whose flow behavior is not known before hand.

4.1.2 Marsh Funnel Viscometers

The Marsh funnel is a simple device used for routine quick measurements of fluid viscosity. It is an excellent indicator of changes in drilling fluid properties. The marsh funnel is conical in shape, 6 inches in diameter at the top and 12 inches long with a capacity of 1.5 liters. A 12-mesh screen covers half of the top and is designed to remove any foreign matter and drilled cuttings from the fluid. The fluid runs through a fixed orifice at the end of the funnel and is 2 inches by 3/16 inches in size. **Fig. 4.1** shows a Marsh funnel.

Procedure:

1. Hold the funnel in an upright position with the index finger over the outlet.
2. Pour a freshly obtained sample of the fluid to be tested through the screen until the fluid level reaches the bottom of the screen.
3. Immediately remove the finger from the outlet tube and measure the number of seconds for a quart (0.946 liters) of mud to flow into the measuring cup.
4. Measure the temperature of the fluid in °F.
5. Record time in seconds as "funnel viscosity." Note: Calibration time for fresh water at 70°F is 26 seconds/quart.

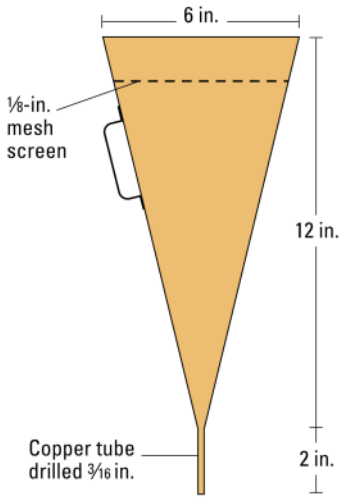

Fig. 4.1–Marsh funnel[21]

The funnel viscosity measurement obtained is influenced considerably by the gelation rate of the mud sample and its density. Because of these variations, the viscosity values obtained with the Marsh Funnel cannot be correlated directly with other types of viscometers.

4.1.3 Rotational Viscometers

Rotational viscometers are based on the principle that the torque required to turn an object in a fluid, can indicate the viscosity of that fluid.

4.1.3.1 Cone and Plate Viscometers

These viscometers use a cone of very shallow angle in bare contact with a flat plate. With this system the shear rate beneath the plate is constant to a modest degree of precision and deconvolution of a flow curve; a graph of shear stress (torque) against shear rate (angular velocity) yields the viscosity in a straightforward manner.

4.1.3.2 Stormer Viscometer

The Stormer viscometer is a rotation instrument used to determine the viscosity of paints, commonly used in paint industries. It consists of a paddle-type rotor that is spun

by an internal motor, submerged into a cylinder of viscous substance. The rotor speed can be adjusted by changing the amount of load supplied onto the rotor. For example, in one brand of viscometers, pushing the level upwards decreases the load and speed, downwards increases the load and speed. The viscosity can be found by adjusting the load until the rotation velocity is 200 rotations per minute. By examining the load applied and comparing tables found on ASTM D562, one can find the viscosity in Krebs units (KU), unique only to the Stormer type viscometer. This method is intended for paints applied by brush or roller only.

4.1.3.3 Cup and Bob Viscometers

The mode of operation is by first defining the exact volume of sample which is to be sheared within a test cell, then the torque required to achieve a certain rotational speed is measured and plotted. There are two classical geometries in "cup and bob" viscometers, known as either the "Couette" or "Searle" systems - distinguished by whether the cup or bob rotates. The rotating cup or Couette system is preferred in some cases, because it reduces the onset of Taylor vortices, but is more difficult to thermostat accurately. We shall now focus on the Couette system.

4.1.3.4 Couette Flow

In fluid dynamics, Couette flow refers to the laminar flow of a viscous liquid in the space between two surfaces, one of which is moving relative to the other. Friction between the fluid and the moving boundaries causes the fluid to shear. The force required for this action is a measure of the fluid's viscosity as shown in **Fig. 4.2**. This type of flow is known as a Couette flow named in honor of Maurice Marie Alfred Couette, a Professor of Physics at the French university of Angers in the late 19th century.

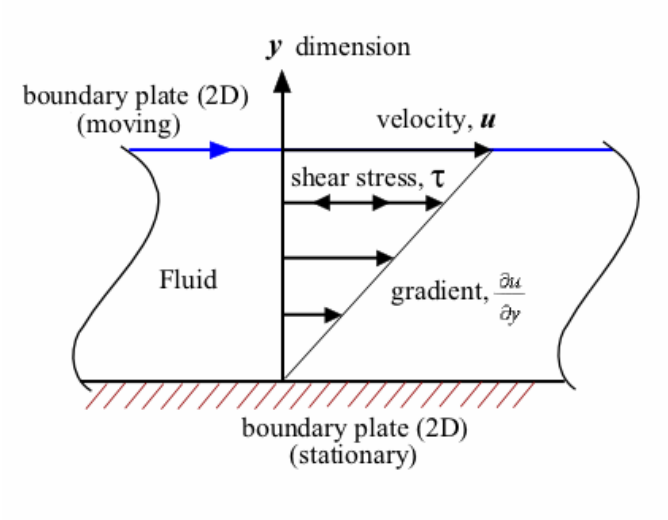

Fig. 4.2–Deformation of a fluid by simple shear[22]

A Couette viscometer is made up of an outer cylinder (or rotor) that rotates around a stationary inner cylinder (or bob). A simple schematic of the Couette viscometer is presented in **Fig. 4.3** below to illustrate its principles of operation.

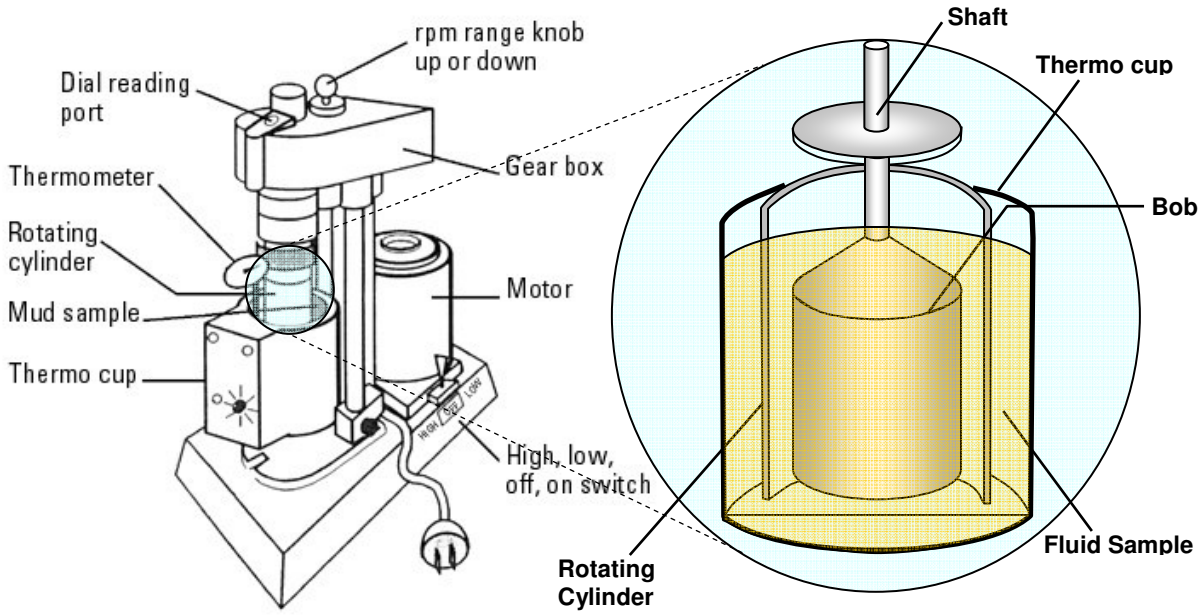

Fig. 4.3–Parts of a Couette viscometer

The fluid to be tested fills the space between the bob and the outer sleeve. The outer sleeve is then rotated at a constant velocity and the rotational force (shear rate) produces torque (shear stress) that is transmitted to the bob. The torsion spring acts a restraining force. As this restraining force is overcome, the bob is deflected to some degree which is a measure of the shear stress. The torque transducer connected to the bob is calibrated to indicate shear stress using known viscosities of Newtonian oils over the desired range of shear rates. Six-speed Couette viscometers like the Fann 35 are designed to allow for easy determination of the rheological parameters. It provides data at speeds of 3, 6, 100, 200, 300, 600 RPM. **Table 4.1** shows the RPM / shear rate relationships and how they relate to drilling fluid performance in a circulating system.

Table 4.1–RPM / Shear rate for different circulating systems

Couette Viscometer		**Circulating System**	
RPM	**Equivalent Shear Rate (sec^{-1})**	**Location**	**Shear Rate Range (sec^{-1})**
3	5.11	Tanks	1-5
6	10.22	Annulus	10-500
100	170	Pipe	100-700
200	341	Collar	700-3,000
300	511	Nozzles	10,000-100,000
600	1022		

Couette Flow Assumptions: The following assumptions (in line with Macosko,[23] 1994) are necessary when using Couette geometry to ensure accurate measurement of fluid flow properties:

1. The fluid is in steady, lamina, isothermal flow
2. The fluid velocity at the bob is zero (ie $v_r = v_z = 0$ but $v_\theta = r\omega$)
3. The fluid system is in equilibrium
4. There is a negligible gravity and end effect,[24].

5. Symmetry in θ, where $v_i =$ the velocity component in the i-coordinate direction, cm/s; $r =$ radial distance from centerline, cm; and $\omega =$ angular velocity, rad/sec.
6. The fluid behavior is not time-dependent.

It is often difficult to fully satisfy all these assumptions especially when working with solids-laden drilling fluids and torsion-measurement devices. For instance the assumption that there is only laminar flow in the annular clearance may be difficult to achieve since secondary flows like Taylor,[24] vortices are known to occur under certain situations.

Couette viscometers are widely used in the oil industry to determine the rheological properties of drilling fluids, fracturing fluids and even cement slurries. The American Petroleum Institute (API) and International Standards Organization have defined standards (ISO 10414-2:2002, ISO 10414-1:2002, API RP 13B-2 (2005)) that stipulate the recommended test procedures, conditions, bob and rotor geometries and shear rates for determining fluid characteristics. Couette viscometers are now available in high temperature-high pressure models like the Chandler model 7600 XHP/HT viscometer used extensively for fluid testing during this research.

4.2 THE CHANDLER MODEL 7600 XHP/HT VISCOMETER

The Chandler model 7600 Ultra-High Pressure High Temperature viscometer,[25] is a concentric cylinder (Couette) viscometer that uses a rotor and bob geometry accepted by the energy industry. The model 7600 design meets the requirements set forth in ISO and API standards for viscosity measurement of completion fluids at high pressure and high temperature.

4.2.1 Features and Benefits

- External Digital Torque Measurement
- 600°F and 40,000 psig

- Removable sample vessel assembly with vessel elevator mechanism
- Sample/Oil separation zone
- High strength, corrosion resistant, steel super-alloys
- Programmable Temperature and Pressure Controllers
- Microsoft® Windows® XP based program
- Temperature and Pressure control time-based profiles
- Configurable multiple axis plots of all variables
- Automatic calibration
- Data export in CSV format
- Ability to capture peak gel values.
- Pause, Resume, Jump feature for profile steps

4.2.2 Specifications

Sample Environment:

Pressure, Maximum ..... 40,000 psig

Temperature, Maximum ..... 600°F

Maximum Sample Heat-up Rate ..... 3°F/min

Sample Rheology:

Minimum Shear Stress .....20.0 dyne/cm^2

Maximum Shear Stress .....1533 dyne/cm^2

Minimum Viscosity .....2 cP at 600 RPM

Maximum Viscosity .....300 cP at 300 RPM

Shear Stress Resolution .....0.1 degree, 0.51 dyne/cm^2, 1 cP at 300 RPM

Shear Stress Accuracy ..... ±0.50% of F.S. from 51.1- to 1533-dyne/cm^2

Shear Rate Range ..... 1.7- to 1022-sec^{-1} (1- to 600-RPM with B1/R1 Bob and Rotor) ±0.1 RPM

Sample Gel Strength ..... Peak values at 3 RPM

Couette Geometry:

Bob Radius (R_i).....1.7245 cm (B1)

Rotor Radius (R_o) .....1.8415 cm (R1)

Bob Length (L) .....3.805 cm

Rheology Equations: The following equations are used to calculate the values for shear stress, shear rate and viscosity in the XHP/HT viscometer.

Shear Rate, $\gamma = 2\omega \frac{R_o^2}{R_o^2 - R_i^2}$, $\sec^{-1}$ ..... (4.1)

Shear Stress, $\tau = \frac{M}{2\pi R_i^2 L}$, $\frac{dyne}{cm^2}$ ..... (4.2)

Viscosity, $\mu = \frac{\tau}{\gamma}$, $\frac{dyne - \sec}{cm^2}$, $Poise$ ..... (4.3)

Angular Velocity, $\omega = RPM \times \frac{2\pi}{60}$, $\sec^{-1}$ ..... (4.4)

Plastic Viscosity, $PV = \theta_{600} - \theta_{300}$, cP ..... (4.5)

Yield Point, $YP = \theta_{300} - PV$, $lbf/100\,ft^2$ ..... (4.6)

Apparent Viscosity, $= \frac{\theta_{600}}{2}$ ..... (4.7)

Where; M = torque on bob shaft (dyne-cm)

L = bob height, cm

R_i = bob Radius, cm

R_o = rotor radius, cm

γ = shear rate, sec^{-1}

τ_y = yield stress, lbf/100 ft^2

μ_p = plastic viscosity, cP

k = consistency index, Pa-s^n

n = flow behavior index (dimensionless)

Pressure Vessel: Comprises of a removable sample vessel (test cell) assembly with support bracket, elastomer, Viton O-rings, and metal backup ring seals. **Fig. 4.4** is a schematic of the test cell showing the various parts.

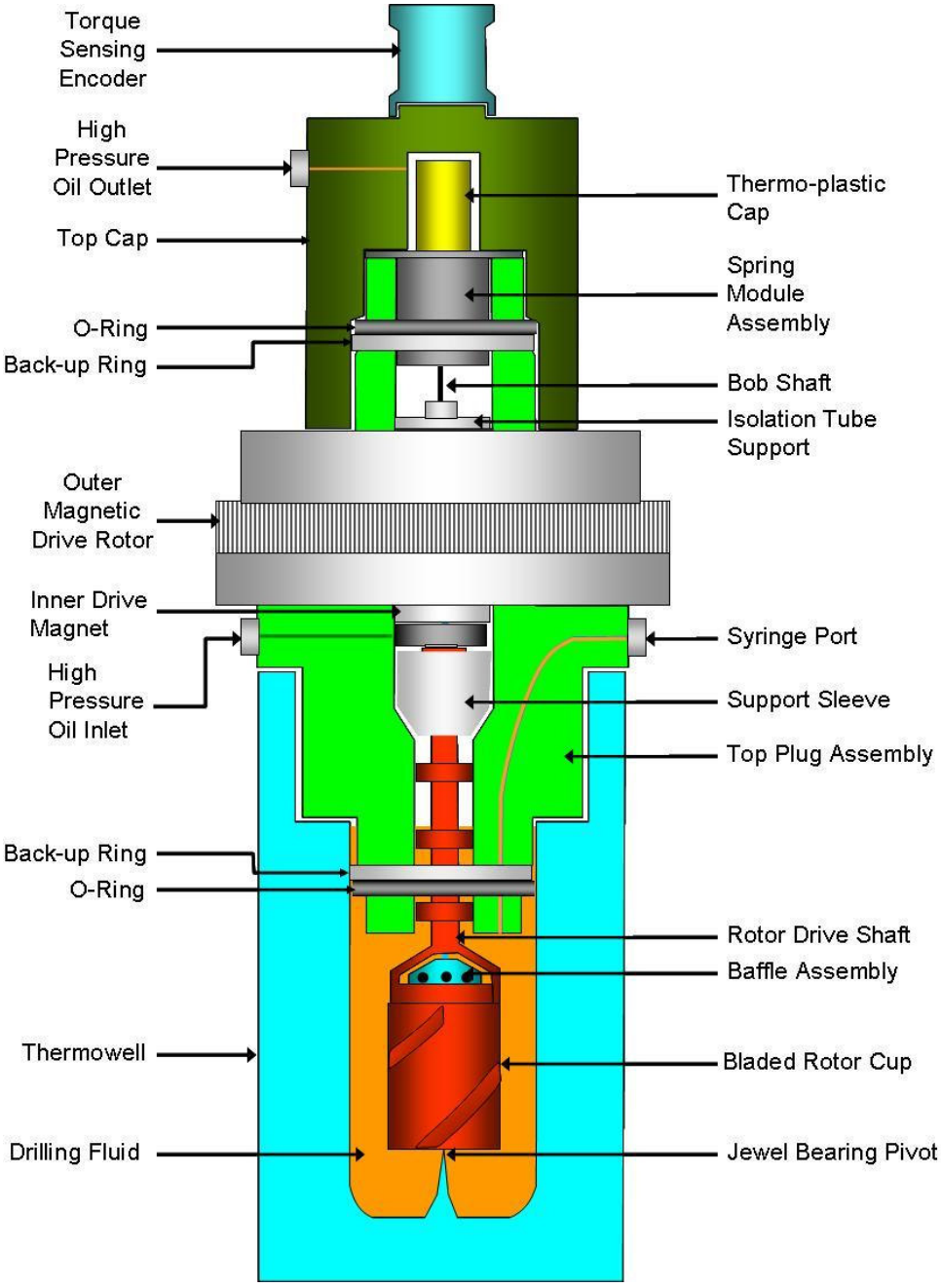

Fig. 4.4–Test cell schematic

4.2.3 Control System

- Microsoft® Windows® XP based program
- Temperature and Pressure control time-based profiles with data collection
- Motor RPM (shear rate) time or temperature based profiles providing standard speeds (600, 300, 200, 100, 6, 3) or user-defined speeds
- Configurable multiple axis plots of all variables (T, P, Shear Rate, Shear Stress, Viscosity, Dial Reading, n', K', etc…)
- Automatic calibration with Newtonian oil at multiple shear rates
- Data export in CSV format, compatible with Microsoft Excel
- Ability to capture peak gel value
- Configurable alarms for maximum shear stress, temperature, pressure
- Pause, Resume, Jump feature for profile steps

Instrument Utilities:

Power .....220 VAC, ±10%, 60Hz

Instrument Air .....100- to 140-psig (filtered and dry)

Coolant .....Water, chilled ethylene glycol/water mixture optional

4.2.4 Other Lab Equipments

The following equipments were used during the course of this research;

- Air Compressor: To supply steady 100- to 140-psig pressure to the oil pump in the XHP/HT viscometer.
- Fann 35 (6-speed) and Fann 286 (variable-speed) viscometers with thermo-cup
- ES Meter
- 3 Hamilton Beach mixers.
- Washing Bath
- Oven
- Hand tools.
- Stop Clock

Fig. 4.5 is a picture of the XHP/HT viscometer and lab set-up while running one of the constant temperature-variable pressure tests.

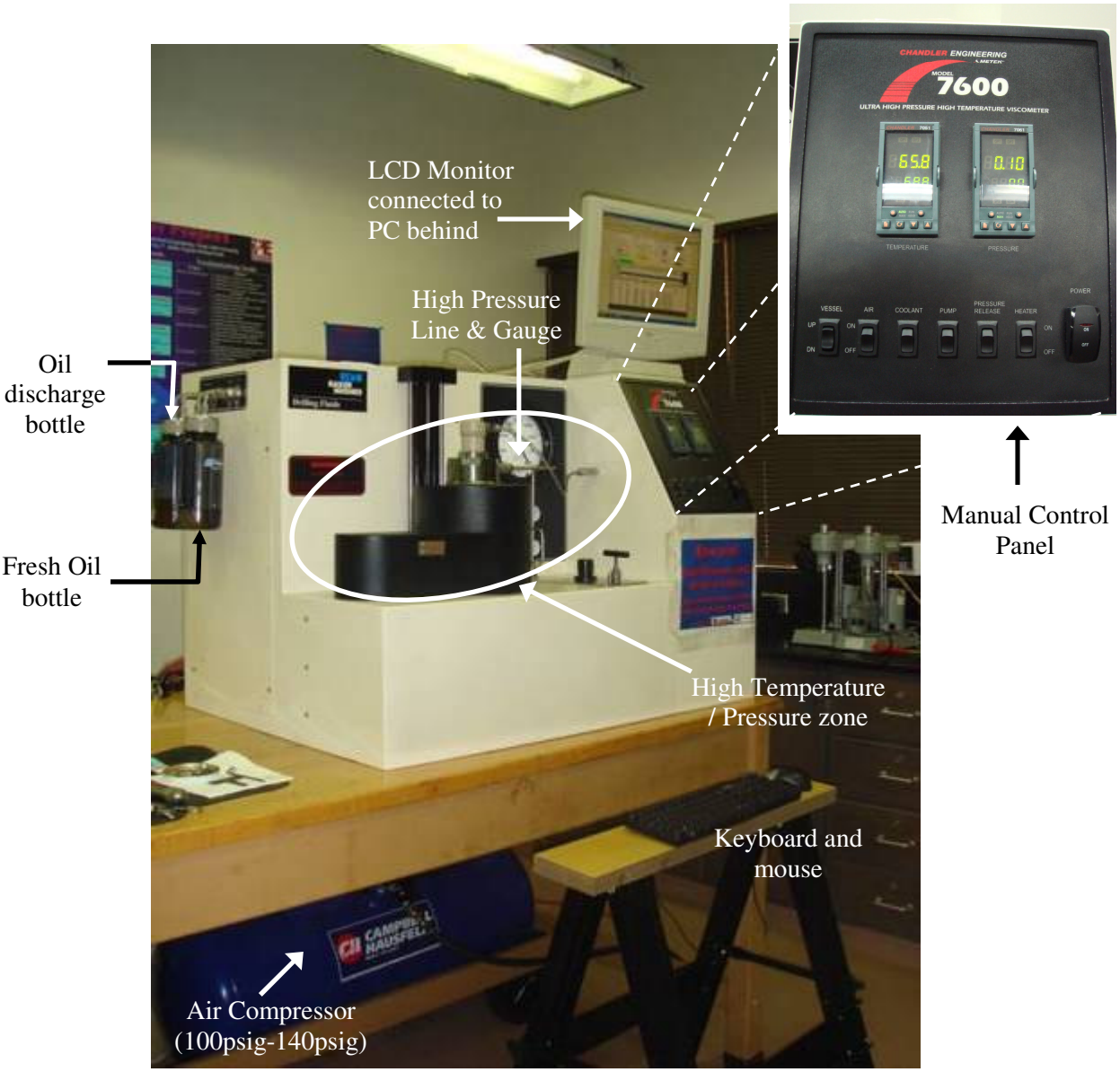

Fig. 4.5–Chandler model 7600 XHP/HT viscometer

Dimensions and Weight: W x D x H: 40 in x 28 in x 28.5 in and 250 lbs

This viscometer will be referred to as "the XHP/HT viscometer" for the remaining part of this thesis.

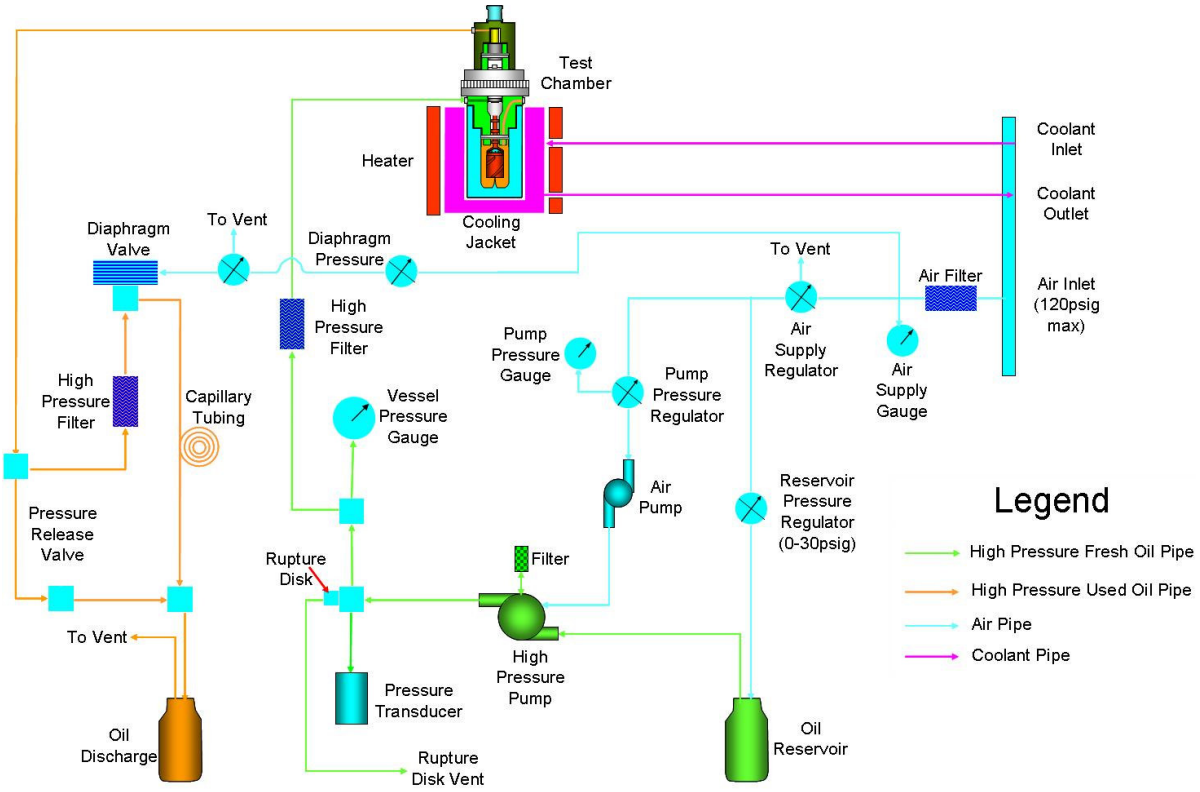

Fig. 4.6–Fluid flow diagram

Fig.4.6 above illustrates the flow path of various fluids through the XHP/HT viscometer. The high pressure pump uses compressed air (in blue rated 100 to 140 psig) to pump fresh hydraulic oil (in green) into the test chamber which compresses the drilling fluid sample. The rupture disc is a safety device that is designed to fail when the pressure in the system is excessive (say >45,000 psig). For a typical test were temperature is increased at constant pressure, thermal expansion causes additional compression. The system reacts by bleeding-off some hydraulic fluid through the discharge line (in orange) to normalize the pressure. For rapid cooling and better temperature control, there is provision for a coolant (in pink) to be circulated through an inlet and outlet tube connected to cooling jacket which surrounds the test chamber. All these activities can either be done manually using the control panel shown in Fig. 4.5 or automatically according to a pre-designed test schedule.

4.2.5 Utilities in Place

- Main Power to instrument: 230 VAC, ±10%, 50/60Hz, 15A – used for high current components.
- Instrument Power to Instrument: 115/230 VAC, ±10%, 50/60Hz, 5A – used for data acquisition components.
- Air: Filtered, dry compressed air; 100 to140 psig. During the experiments, it was observed that a minimum supply of 120 psig is required to achieve and sustain a 40,000 psig pressure.
- Drain: Suitable for steam.

4.3 DESIGN OF EXPERIMENTS

In general *factorial designs* are the most efficient way of investigating experiments that involve the study of the effects of two or more factors. Primarily factorial designs allow the effects of a factor to be estimated at several levels of other factors yielding in results that are valid over a range of experimental conditions. A factorial design is necessary especially when interactions may be present to avoid misleading conclusions. Temperature and pressure are the two factors being investigated in this research using factorial experiments.

Factorial Experiment: In statistics, a factorial experiment is an experiment whose design consists of two or more factors, each with discrete possible values or "levels", and whose experimental units take on all possible combinations of these levels across all such factors,[26]. Such an experiment allows studying the effect of each factor on the response variable, as well as the effects of interactions between factors on the response variable. Factorial designs are widely used in research work and they form the basis of other designs of considerable practical value.

This research by nature is a typical case of a two-factor factorial experiment as will be discussed in details in Chapter VI. The analysis of variance, hypothesis and residuals

calculations will be made using data from the Fluid Type-A tests. Also results will be compared with output from the *FluidStats* program. I developed this program in Visual Basic to facilitate the statistical analyses and modeling of the enormous data often associated with factorial experiments like the ones performed during this research.

4.4 FLUID SAMPLING AND TESTING PROCEDURE

Throughout the course of this research emphasis was placed on proper fluid preparation and sampling as this could result in significant discrepancies given that all the oil-based fluids used are solids laden and hence easily susceptible to sag.

4.4.1 Fluid Types

Two different oil-based fluid formulations were used during this research. For confidentiality they will be referred to as "Fluid Type A" and "Fluid Type B". Below is a brief description of the fluids.

1. **Fluid Type A:** This was the first fluid formulation to be used in this research. The base oil was diesel and it was weighted with barite. The original fluid was obtained from the field and then improved in the lab with some additives. The fluid had a density of 18.8 ppg and an oil/water ratio of 91/9.

2. **Fluid Type B:** This fluid was used extensively in this research. It is a mineral oil-based fluid with a mud density of 18.0 ppg and 93/7 oil/water ratio. Average Electrical Stability (ES) was 950. The primary weighting agent was barite although a different formulation was also tested using manganese tetroxide as weighting agent. This gave better results vis-a-vis thermal stability but was observed to be more abrasive as the wear and tear on the moving parts was significant.

4.4.2 Fluid Preparation

Before shipment to TAMU, freshly-mixed samples were heat-aged at 400ºF for 16 hours at Baker Hughes Drilling Fluids (BHDF) facility in Houston. On arrival in the TAMU lab, the solids (barite) in the fluid are often noticed to have settled. Before testing the fluid with the XHP/HT viscometer these steps are followed:

1. The whole fluid in the bucket is stirred first with a pallet then with two Hamilton Beach mixers at 70 RPM for less than 5 minutes to ensure a homogeneous mixture.
2. A sample (usually 2 lab barrels) is then poured out into a cup and uniformly sheared for 10 minutes. After collecting the sample the remaining fluid in the bucket is properly covered to avoid contamination.
3. Using a syringe 25 ml is extracted and 175 ml poured into the thermowell of the XHP/HT viscometer.
4. The remaining was poured into the thermo-cup for initial rheology check with the Fann 35.

4.4.3 Experimental Procedure

The laboratory experiments for project were executed in phases according to the factorial design concept discussed earlier. In the first phase of testing, temperature and pressure were simultaneously increased and the fluid's plastic viscosity, yield point and gel strengths (10 sec. /10 min.) determined at each increment. The second phase involved the constant pressure increasing temperature schedules while the third phase was the reserve; constant temperature, increasing pressure. The test schedules for the 4^{th} and 5^{th} phases where designed at constant shear rate (100 RPM) while increasing only temperature or only pressure respectively. Nominal 50ºF temperature increments are used initially, however significant changes in viscosity warranted smaller increments (25ºF) from 400- to 600-°F in the first phase of testing.

For each test, the initial rheology check was performed at 150°F and ambient pressure (14.7 psia) using both the XHP/HT and Fann 35 viscometers. The variable speed Fann 286 viscometer was also used. Using two or more viscometers was necessary for proper quality control and to ensure consistency in results.

Finally the results of the tests are analyzed; conclusions and recommendations made. If and when discrepancies occurred, steps were taken to investigate and identify the cause(s) and where necessary re-calibrate the affected viscometer(s) according to standard API procedures. A simple workflow process for a typical test using the XHP/HT viscometer is presented in **Fig. 4.7** below:

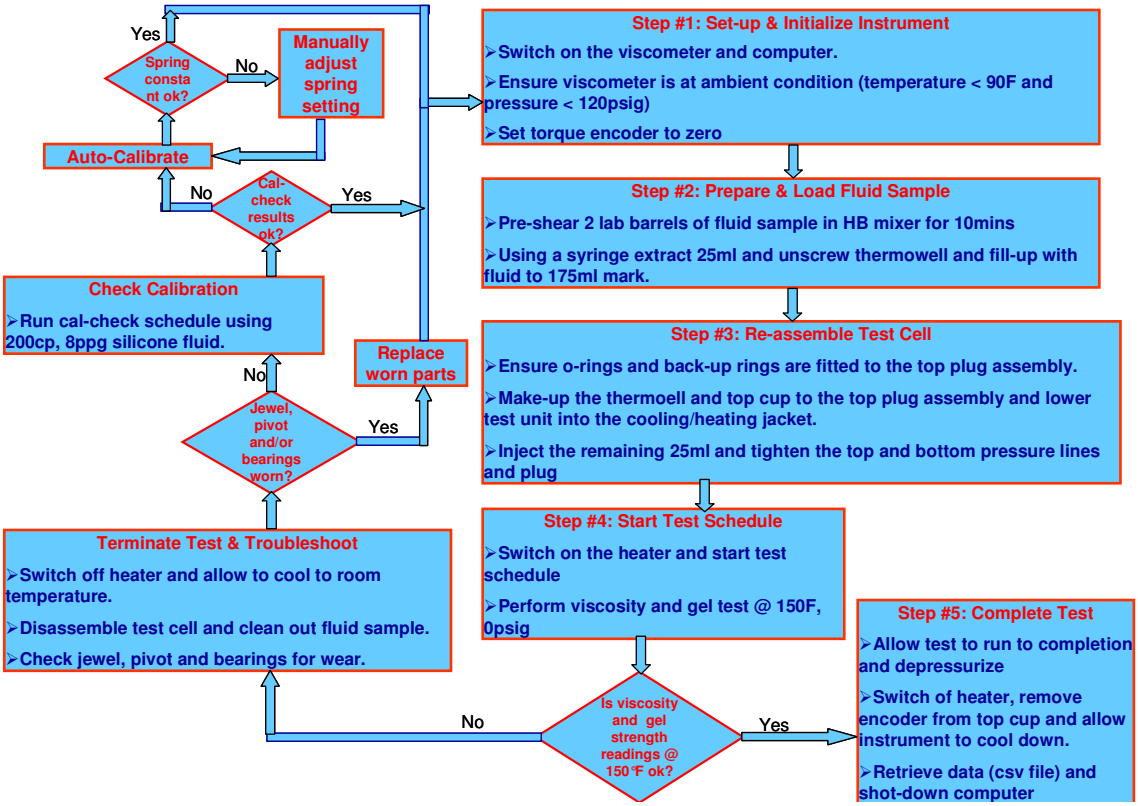

Fig. 4.7–Work flow process

4.5 SAFETY

The XHP/HT viscometer is designed with operator safety in mind. Any instrument that is capable of high temperatures and pressures should always be operated with CAUTION!! I use this opportunity recognize the good safety record of the TAMU XHP/HT team for the over 365 days of operation without any safety-related incident or injury. This was made possible by a strict adherence to safety standards.

4.5.1 Safety Procedures

To guarantee safety, the following measures were implemented:

- Posted caution signs near the instrument to warn non-operating personnel
- Read all instructions manuals before attempting to operate instrument.
- Observed all caution notes and warning labels on the instrument.
- Never exceeded the instrument maximum temperature and pressure ratings.
- Always disconnected main power to the instrument before attempting any repair.
- Turned OFF the heater, power switch, air compressor at completion of each test.
- Located appropriately rated fire extinguishers within close proximity to the instrument.
- Removed oil on the heated surfaces that may pose a hazard to starting a test that will exceed 400°F.
- Never open the pressure vessel before the temperature is below 100ºF
- The pressure vessel was visually inspected prior to any test.

4.5.2 Materials Handling

The following personal protective equipments were worn when working with the drilling fluids and lifting heavy equipment:

- Chemical resistant clothing with a protective apron
- Organic vapor respirator when exposed to mists or vapors
- Chemical splash goggles
- Nitrile hand gloves

- Rubber-soled safety boots.

For every material, MSDS was obtained and read prior to storage or use. All waste fluids and materials are safely contained and appropriately disposed.

4.5.3 Emergency and First Aid Instructions

All emergency exit and first aid procedures as contained in the lab safety manual were studied. In the event of a spill as was the case when the rupture disc failed, the following was done:

- Source of spill was located and stopped while wearing appropriate personal protective gears.
- An absorbent material was then used to soak up the spilled hydraulic oil and then disposed in accordance with state regulations.
- The floor was cleaned properly with a scrub and allowed to dry to avoid slipping.

4.6 CHALLENGES

As is typical with a project of this nature, several challenges have arisen while performing the lab experiments. Most of them where equipment related as discussed below.

4.6.1 Equipment Problems

4.6.1.1 Rotor Shaft Design

This was a major challenge as the original shaft delivered with the XHP/HT viscometer was made of an alloy that was not thermally stable at the high-temperatures in which tests were carried-out. As a result it was very difficult backing-off the shaft from the rotor cup especially after a test at 600°F. The shaft had to be sent back twice to the manufacturer for re-threading but this was only a temporary solution to the problem. Eventual a new shaft had to be built from a more thermally stable alloy and since then this has problem has not repeated.

4.6.1.2 Lift Mechanism Problem

By design, the top or bottom infra sensor automatically stops the motion of the carriage when it senses the top or bottom stopper respectively. The stoppers attached to the traveling block of the lift (carriage) system have been observed to shift with time. So when the stopper is displaced, motion of the carriage continues until it gets to the slide block causing the deformation of the helical coupling. A new coupling was supplied by the manufacturer.

4.6.1.3 Rupture Disc Failure

This happened while testing a fluid to 40,000 psig. The pressure was 35,000 psig at the time of the failure which caused a leakage of hydraulic oil through the discharge vent. **Fig. 4.8** shows a picture of the failed rupture disc.

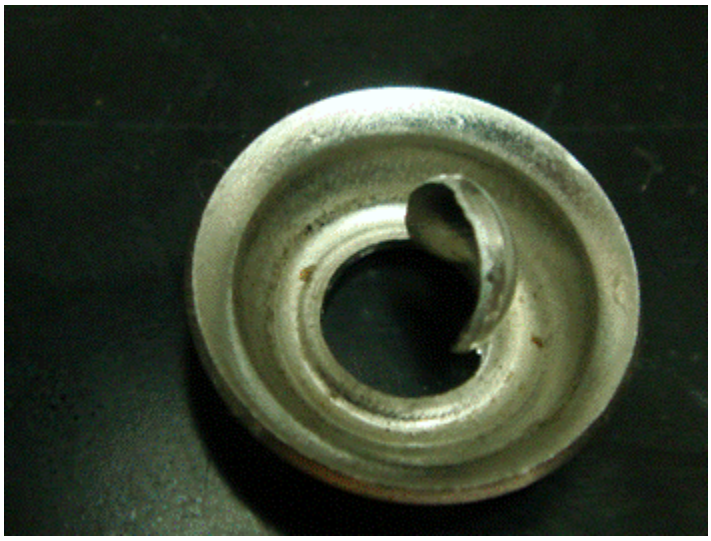

Fig. 4.8–Failed rupture disc

This particular rupture disc is rated to 47,275 psig. This was clearly a fatigue failure because the burst rating was not exceeded during the test or on any previous test. A replacement rupture disc was provided by BHDF.

4.6.1.4 Spring Slippage

Deviations in dial readings from the initial calibration setting have been noticed with repeated testing. Technically, the magnetic drive excites the spring because of its strong magnetic field. Also depending on the transmissibility curve characteristics, for a given spring constant and system mass, there is a speed at which the spring oscillation will increase dramatically. To remedy this we have had to recalibrate and/or manually readjust the spring setting.

4.6.2 Future Improvements

4.6.2.1 Better Temperature Control

It will be necessary to install cooling system to ensure better temperature control. At the moment, the sample is allowed to cool naturally if readings are to be taken while cooling down.

4.6.2.2 Rheo 7000 Software

The Rheo 7000 software is the platform through which all automatic controls are sent to the XHP/HT viscometer. The program has been noticed to skip a step ahead of the desired step when jumping steps on a pre-designed test schedule. This needs to be addressed in subsequent versions of the software. Also there needs to be a pop-up decision box to guard against accidentally quitting the program especially when running a test.

4.6.2.3 Seal Design

The Viton O-ring has been observed to deform permanently beyond 450°F (shown in **Fig. 4.9**) thereby compromising the seal's integrity. I suggest a re-inspection and re-calibration of heating jacket and pressure transducer in line with the 6-month maintenance schedule.

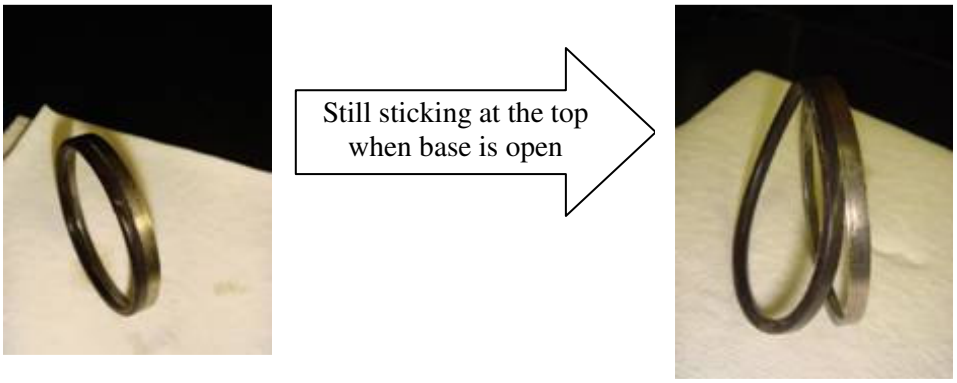

Fig. 4.9–Viton O-ring deformed and stuck to back-up ring after a max. 450°F test

4.6.2.4 Tight Back-Up ring

Usually while taking the cell apart after a test, the metallic back-up ring is found to be stuck to the bottom pressure vessel. On a particular instance, the diameter of the bottom ring was measured to be 2.250 in, slightly more than that of the top metallic ring which was 2.245 in. This small increase might be responsible for the difficulty in removing the ring. Also a close inspection of the diameter of the bore of the thermowell is recommended.

4.6.2.5 Oil Leakage

After each test, there is usually fluid (hydraulic oil) leaking from under the viscometer. Future equipment design should improve the containment of oils coming from the pump muffler and hoses.

4.6.3 Fluid Thickening

During the experiments, it was noticed that baseline rheology was slightly different for each fluid batch. A total of 4 batches of the Fluid Type B were used in performing the factorial experiments. **Table 4.2** below gives details of each batch.

Table 4.2–Rheology of different Fluid Type B batches

Fluid Type B Batches								
	Batch #1		***Batch #2***		***Batch #3***		***Batch #4***	
Date	2 to 20-Mar-07		24-Mar to 9-Apr-07		2-May to 24-Jul-07		25-Jul to 10-Aug-07	
Tests	T1 to T11		T12 to T17		T18 to T28		T29 to T32	
RPM	***Chandler***	***Fann-35***	***Chandler***	***Fann-35***	***Chandler***	***Fann-35***	***Chandler***	***Fann-35***
600	133	139	156	155	154	155	130	142
300	76	78	91	88	88	89	78	85
200	57	57	68	64	65	66	60	65
100	36	34	43	39	41	41	39	42
6	11	8	13	9	12	10	13	12
3	10	6	6	7	10	9	11	10
Gels 10s/10m	11/33	9/21	13/35	10/20	12/24	11/20	15/31	13/26
PV	57	61	65	67	66	66	52	57
YP	19	17	26	21	22	23	26	29
ES	965		950		962		940	

The dial readings indicated above are the average values obtained with each viscometer in a given fluid batch. There is a close match between the average Fann 35 and XHP/HT viscometer readings.

A comparison of the results of the initial rheology check (at 150°F and ambient pressure) for each test in a batch show an apparent thickening of the fluid with time for both the Fann 35 and XHP/HT viscometers. To illustrate this, plots of the initial rheology check with both viscometers (for batch #1) are shown in **Figs. 4.10** and **4.11** below.

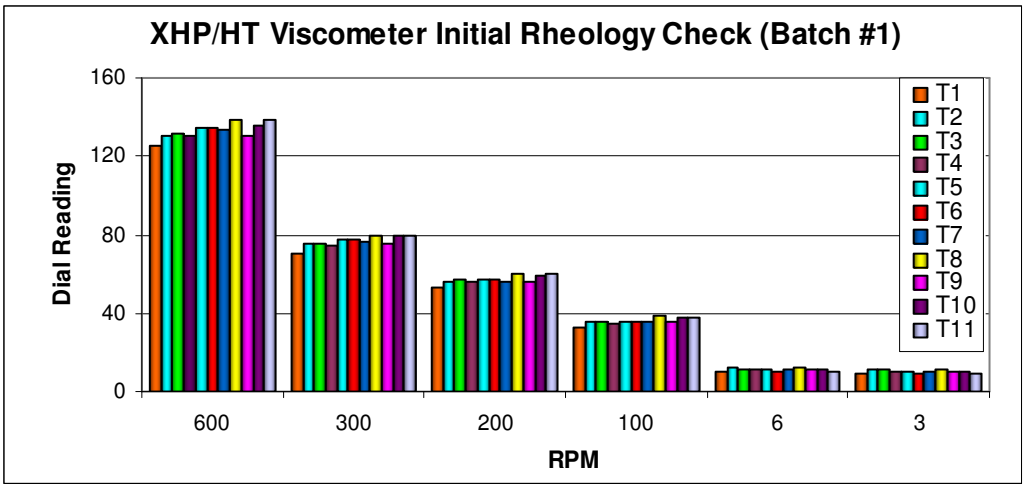

Fig. 4.10–XHP/HT viscometer initial rheology check for batch #1

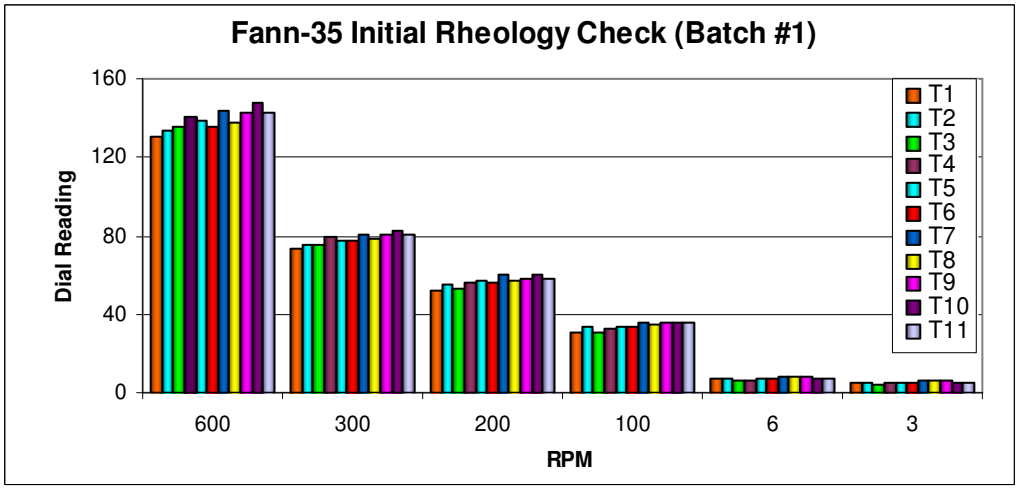

Fig. 4.11–Fann 35 viscometer initial rheology check for batch #1

Clearly we can see an overall upward trend in dial reading from T1 to T11. This behavior was also noticed in the other three batches. However the plastic viscosity and yield point values were relatively stable as presented in **Figs. 4.12** and **4.13**.

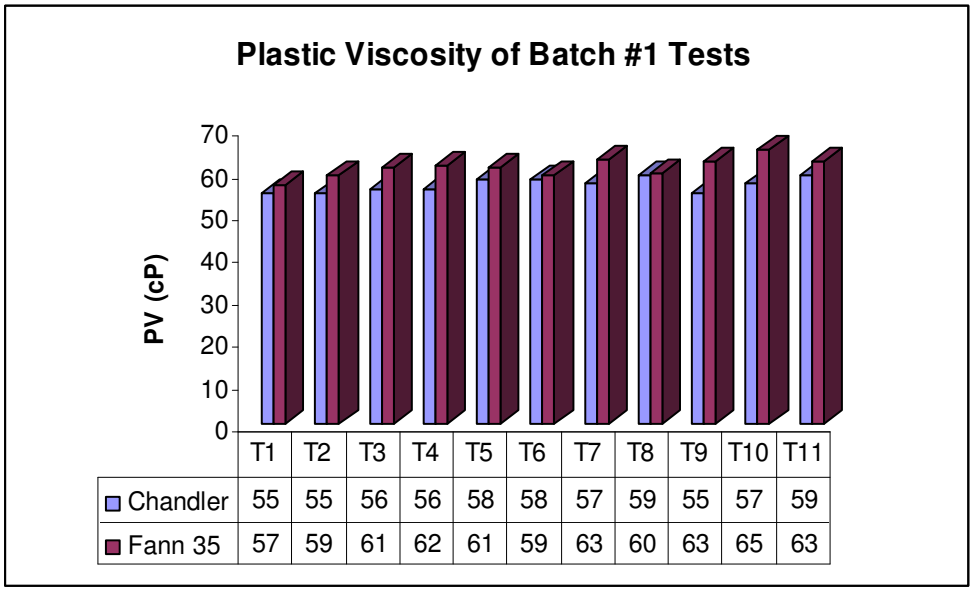

Fig. 4.12–Plastic viscosity of batch #1 tests

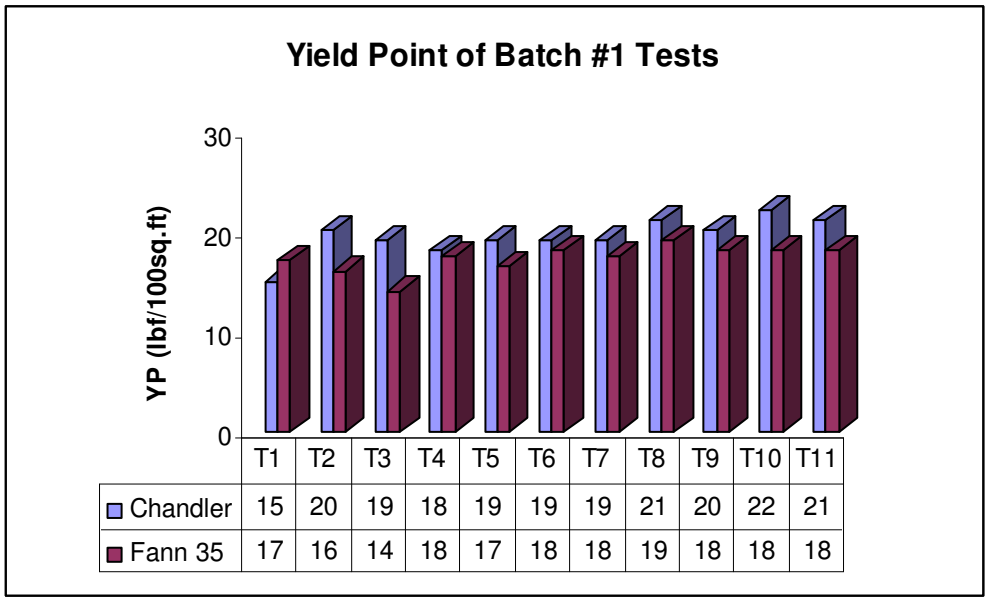

Fig. 4.13–Yield point of batch #1 tests

CHAPTER V

RESULTS OF EXPERIMENTS

5.1 FLUID TYPE A

A total of four (4) conclusive pilot tests were performed with this fluid from 18 October 2006 to 22 November 2006.

5.1.1 Pilot Test 1

This test schedule was designed according to the baseline format (ie simultaneously increasing temperature and pressure). The test was later aborted due to equipment problems after pressuring up to 14,000 psig. This baseline test was repeated on the 19th using the same fluid formulation.

5.1.2 Pilot Test 2

The same test schedule as in Pilot Test 1 was used but different fluid sample resulting in slightly lower viscosity readings. A plot of dial reading, temperature and pressure versus time is shown in **Fig. 5.1** below. See how the dial reading (viscosity) increases rapidly after 425°F and 25,000 psig.

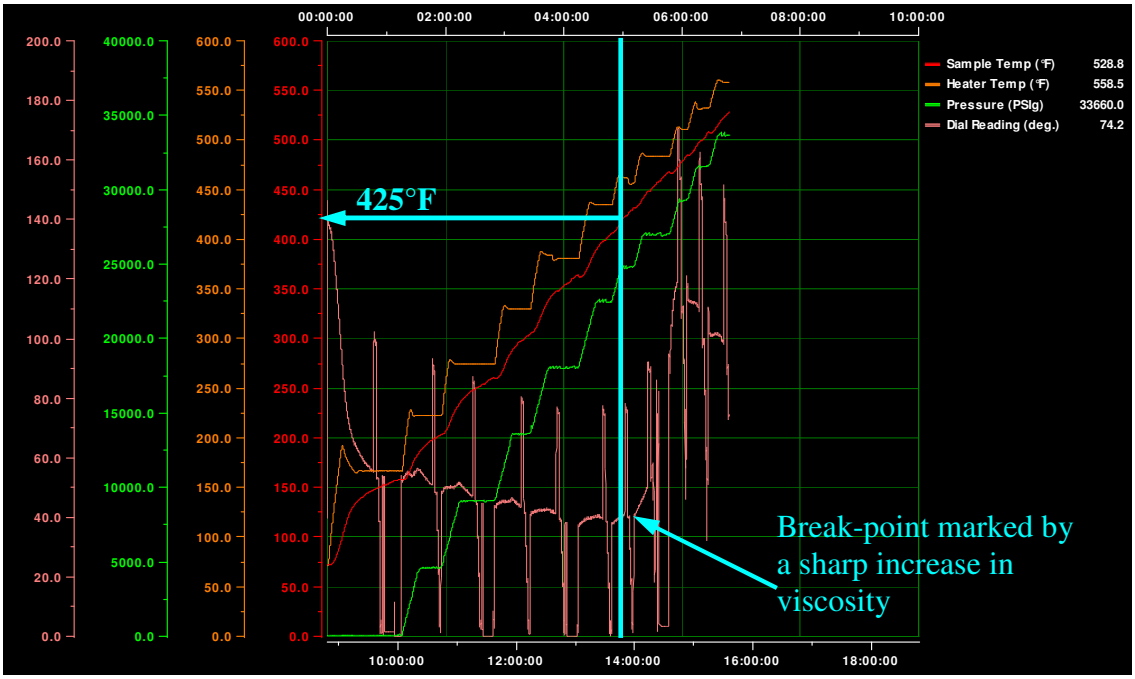

Fig. 5.1–Pilot Test 2 result (final stage)

5.1.3 Pilot Test 3

On 2 November 2006, a different schedule was used by keeping pressure constant at 10,000 psig and varying temperature from 150 to 600°F. The viscosity increased sharply at about 425°F, same for the earlier tests. The viscosity data at 150°F from the Fann 286 were close to those of the XHP/HT viscometer. It was noticed that the 6 RPM and 3 RPM readings from the XHP/HT viscometer were low.

5.1.4 Pilot Test 4

This test was performed on 9 November 2006 to investigate the effect of constant shear rate on the fluid's viscosity over time. The result is similar to that of Pilot Test 2 with the viscosity increasing sharply at about 425°F. However it was noticed that the viscosity profile is slightly higher than that of Pilot Test 2. See details in **Figs. 5.2** and **5.3**

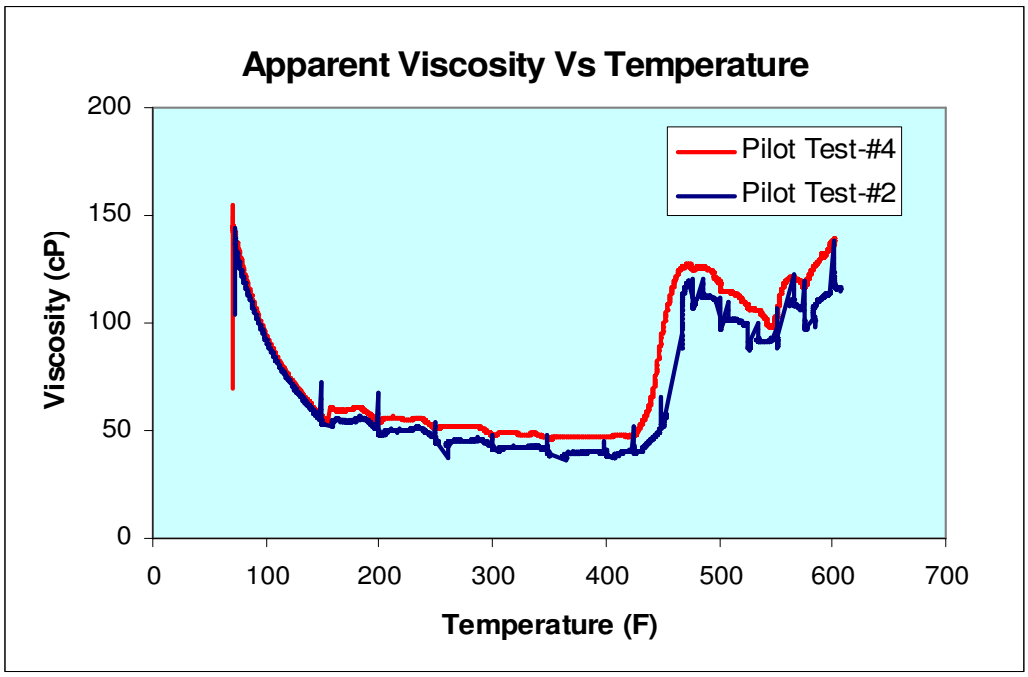

Fig. 5.2–Apparent viscosity versus temperature for Pilot Tests 2 and 4

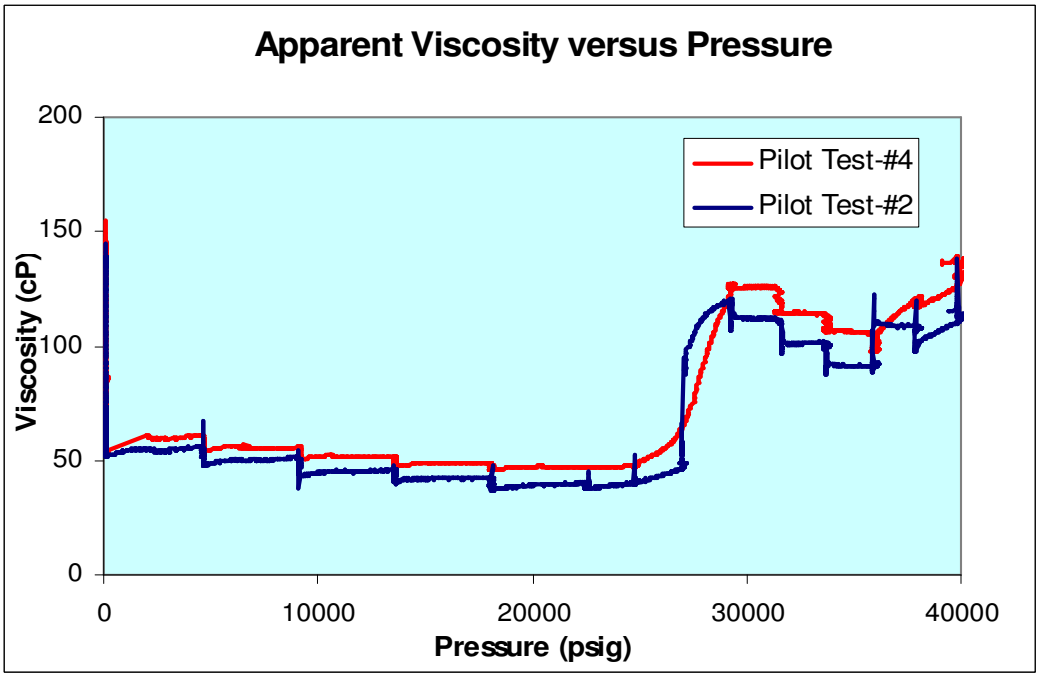

Fig. 5.3–Apparent viscosity versus pressure for Pilot Tests 2 and 4

Pilot Test 2 is the full test run for temperatures between (150°F and 600°F) and pressures up to 40,000 psig while taking 600 to 3 RPM dial readings and gels strengths at intervals. In Pilot Test 4 all variables were the same except the speed which was set constant at 300 RPM through out the test. For this test no gel strength readings were taken.

As is obvious from the viscosity decline profile for the two tests, the general trend is the same with both tests breaking-out at 425°F. However notice that beyond 150°F the viscosity profile for Pilot Test 2 is lower than that of Pilot Test 4. Also the spikes in viscosity readings of Pilot Test 2 are due to the gel effect when revving back to 300RPM after each gel strength test. Also notice that at 27,000 psig and 29,000 psig the viscosity plots of the two tests cross.

5.1.5 Summary of Findings

The following was observed from the pilot tests with the Fluid Type-A:

- There is a close match of the data from Pilot Tests 2 and 4 before 150°F and thereafter there is a gradual separation in the two curves up to 7 cP at 425°F. Beyond this point the trend is still maintained but the separation increases up to 15 cP.
- Results from Pilot Tests 2 and 4 have revealed that a variation in shear rate over time leads to a net reduction in apparent viscosity for the Fluid Type-A formulation.
- Fluid Type-A has been shown to disintegrate beyond 425°F and its rheological behavior becomes inconsistent as reflected in the non-uniform increase in viscosity.
- The fluid's apparent viscosity was observed to peak (at 125 cP for Pilot Test 2 and 120 cP for Pilot Test 4) shortly after thermal degradation (at 425°F) and then decreases and increases again up to the original peak level at 600°F.

The initial rheology check for Pilot Tests 2, 3 and 4 was similar and slightly lower than that of Pilot Test 1 since they are of different batches. See **Table 5.1**.

Table 5.1–Initial rheology check for the various pilot tests with Fluid Type-A

Dial Reading Comparison at 150ºF								
	Pilot Test 1		Pilot Test 2		Pilot Test 3		Pilot Test 4	
RPM	Chandler	Fann 286	Chandler	Fann 286	Chandler	Fann 286	Chandler	Fann 286
600	122	124	98	111	105	111	N/A	103
300	67	68	53	63	56	60	57	55
200	48	48	39	41	40	45	N/A	40
100	28	27	--	23	23	27	N/A	25
6	5	6	4	6	2	5	N/A	6
3	3	4	3	4	1	4	N/A	4
Gels 10s/10m	8/11	7/12	5/12	7/14	8/11	7/14	N/A	7/14
ES	1243		1281		1190		1245	

5.2 COMPARISON OF TWO WEIGHTING AGENTS

Still using Fluid Type A, two tests where performed (between 15 and 17 November 2006) to investigate the effects of two different weighting agents (barite and manganese tetroxide – Mn_3O_4) on the thermal stability of the fluid. Both fluid formulations have a density of 18.9 ppg and the base line test schedule was based on the temperature and pressure profile of a Gulf of Mexico XHP/HT well. The maximum temperature and pressure attained was 600°F and 33,000 psig. No gel strength readings were taken. In summary, the results of these tests showed that:

- For similar pressure and temperature conditions, the manganese tetroxide formulation had lower plastic viscosity and yield strength values.
- The manganese tetroxide formulation also had better thermal stability (up to 600°F) when compared with the barite option which could only hold up to 450°F.

It was more difficult cleaning out the test cell with manganese tetroxide (weighting agent) as it was very “muddy” and bright red like hematite. Also the wear on the moving parts inside the test cell was very significant. Raw data have been withheld for confidentiality. **Figs. 5.4** and **5.5** show plots of plastic viscosity and yield point versus temperature. These were similar to the pressure plots.

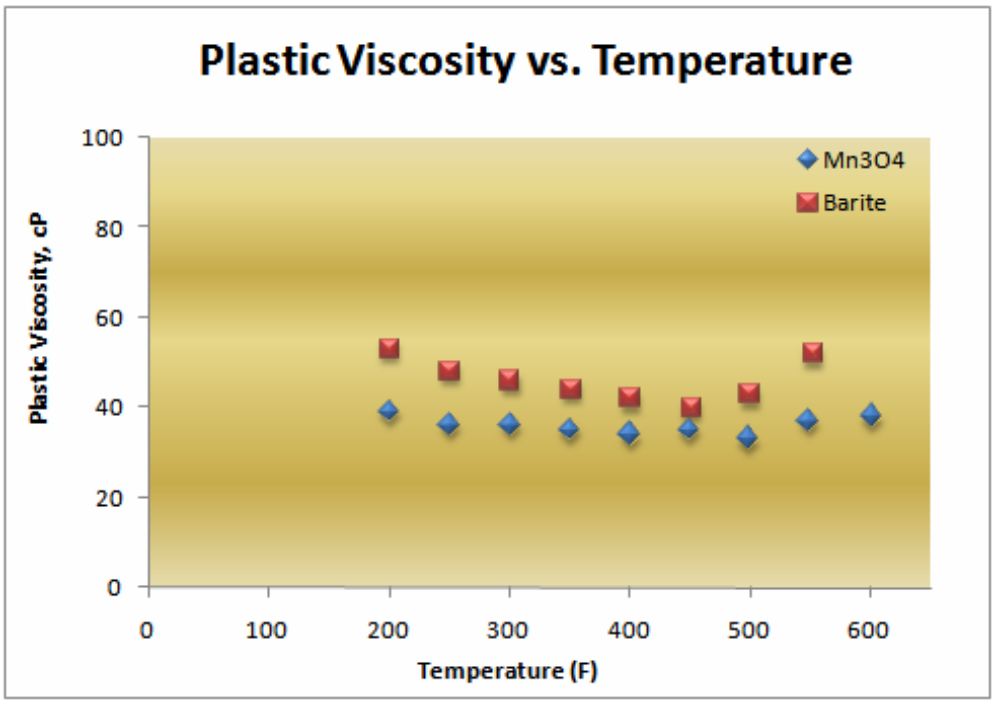

Fig. 5.4–Plastic viscosity versus temperature for barite and Mn_3O_4

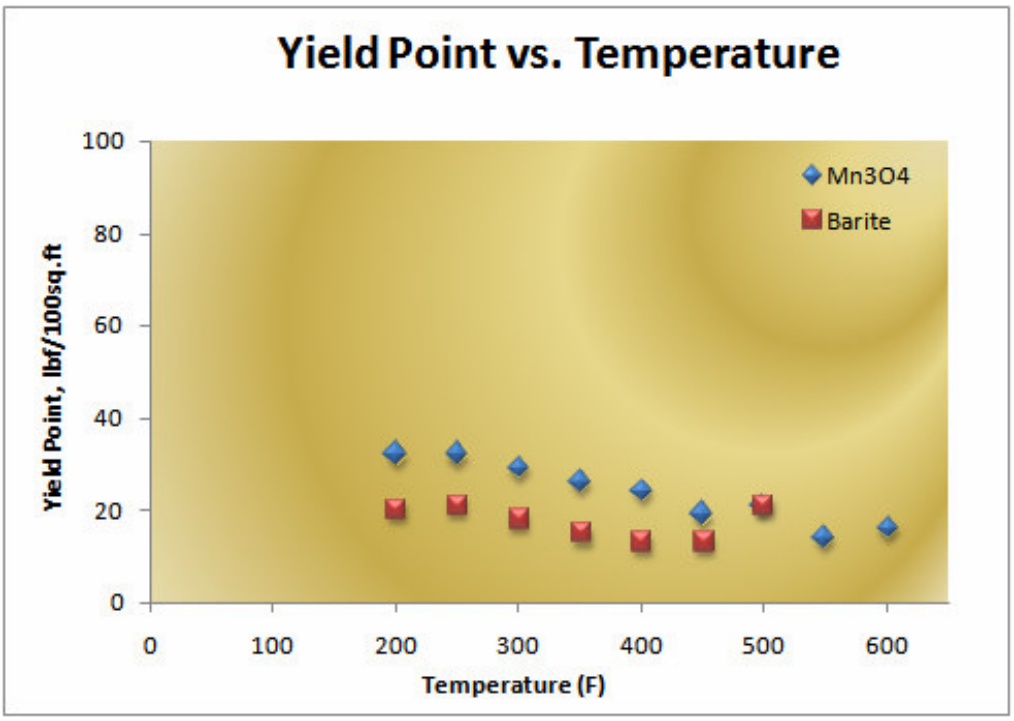

Fig. 5.5–Yield point versus temperature for barite and Mn_3O_4

5.3 FLUID TYPE B

Preliminary testing with Fluid Type B started on 18 November 2006. This fluid is a fresh lab formulation with 93/7 oil/water ratio and density of 18.0 ppg. The base is mineral oil. Initially several tests were run amidst equipment problems ranging from, calibration issues to rupture disc failure as discussed earlier. These problems no doubt caused some delays but were eventually addressed and definitive testing began on 2 March 2007. For the purpose of this report we shall present these tests starting with the baseline test.

5.3.1 Baseline Test

Temperature and pressure was simultaneously increased from 150 to 600°F and 0 to 40,000 psig respectively. The schedule was designed by increasing temperature by 50°F from 150 to 400°F and then by 25 to 600°F. Pressure increments ranged from 3,000 to 5,000 psig. This schedule was designed to replicate conditions in a typical Gulf of Mexico XHP/HT well. Gel strength readings were taken at each increment. For this test it was kind of difficult to see the break-point (ie where viscosity sharply increases with increase in temperature) because of the combined pressure effect. See Appendix C for more details. The initial rheology check showed that both the Fann 35 and Chandler XHP/HT viscometers were within ±5% of the mean dial reading values.

5.3.2 Variable Temperature, Constant Pressure Tests

The schedules for these tests where designed by keeping pressure constant while increasing temperature from 150 to 600°F. As a standard, before proceeding with each test schedule, an initial rheology check was performed to compare and ensure consistency in the results from both the XHP/HT and Fann 35 viscometers. A total of eight (8) tests were performed in this stage for pressures ranging from 5,000 to 40,000 psig in 5,000 psig increments. **Figs 5.6**, **5.7, 5.8** and **5.9** are plots of 600 RPM, 300 RPM dial readings plastic viscosity and yield point versus temperature respectively.

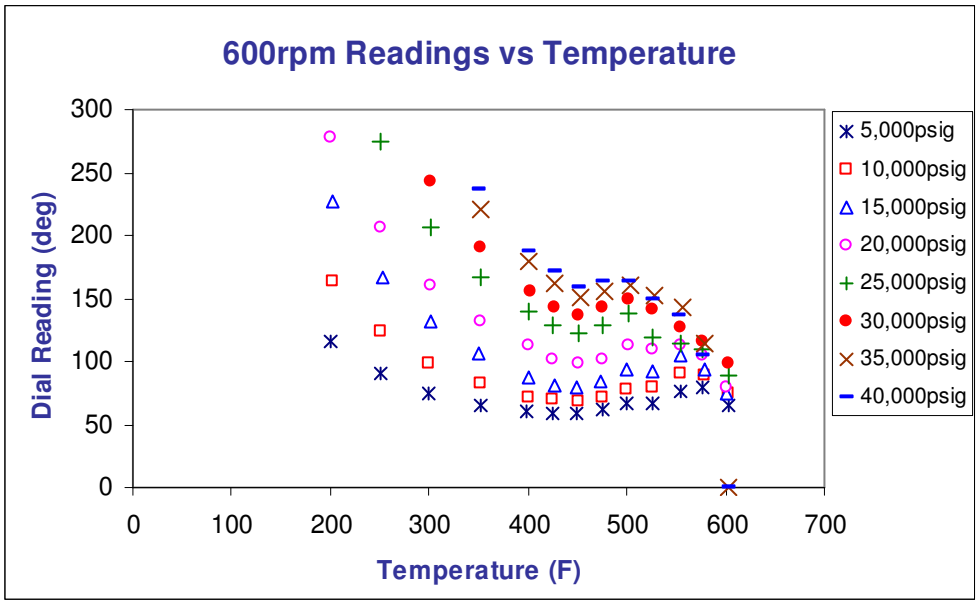

Fig. 5.6–600 RPM dial readings versus temperature

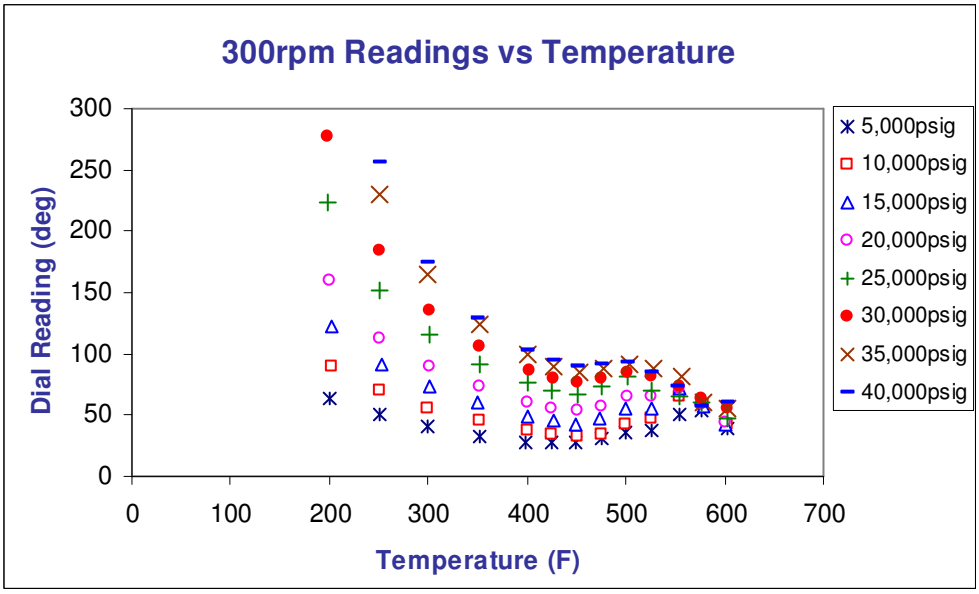

Fig. 5.7–300 RPM dial readings versus temperature

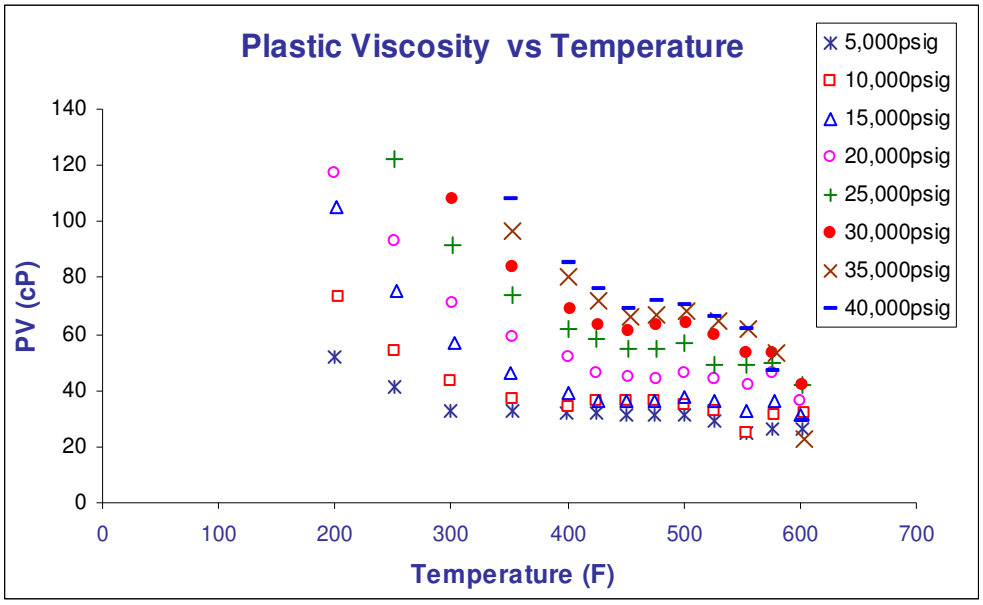

Fig.5.8–Plastic viscosity versus temperature

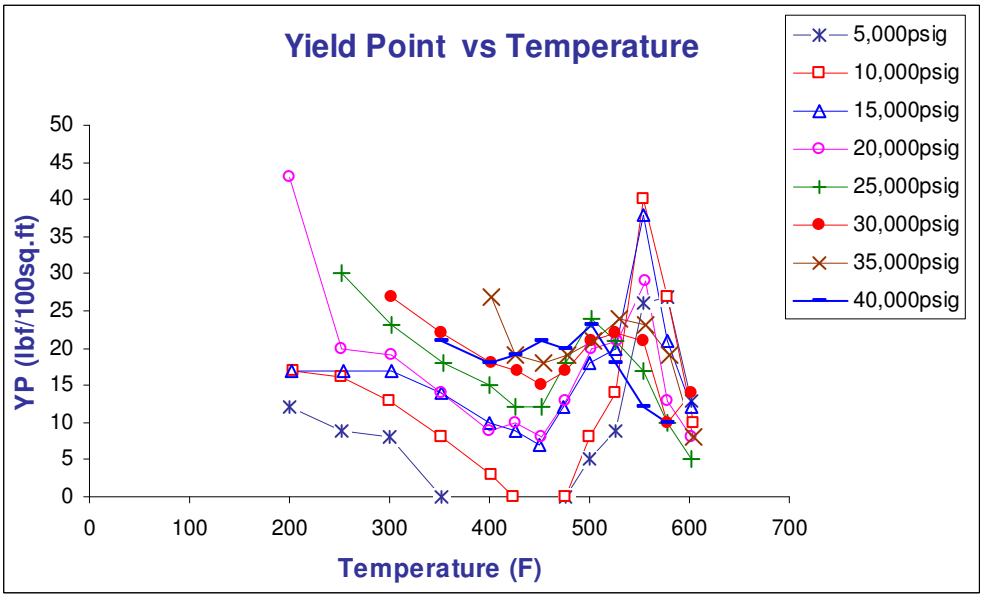

Fig. 5.9–Yield point versus temperature

5.3.3 Summary of Findings

The following conclusions can be drawn from analysis of the plots above:

- For all the tests, there is uniform exponential decline in rheological properties with temperature until 450°F.
- Beyond 450°F there is a slight increase in viscosity, 600 RPM and 300 RPM readings which plateau at 500°F and then decline to 600°F. This is also true for yield point data in Fig. 5.7, the difference being the magnitude of the increase and decrease.
- All the data show a convergence at 600°F. This indicates that irrespective of the prevailing pressure, the fluid behavior is similar at 600°F. In other words, pressure has little effect at 600°F. The effect of pressure is strongest at low temperature.
- Yield point data for the 5,000 psig and 10,000 psig curves become negative between 350°F and 475°F so those sections have been omitted. This is unrealistic and indicates non-Bingham behavior of the fluid. To illustrate this point, **Fig. 5.10** compares an ideal Bingham plastic fluid and a fictitious fluid having negative yield point.

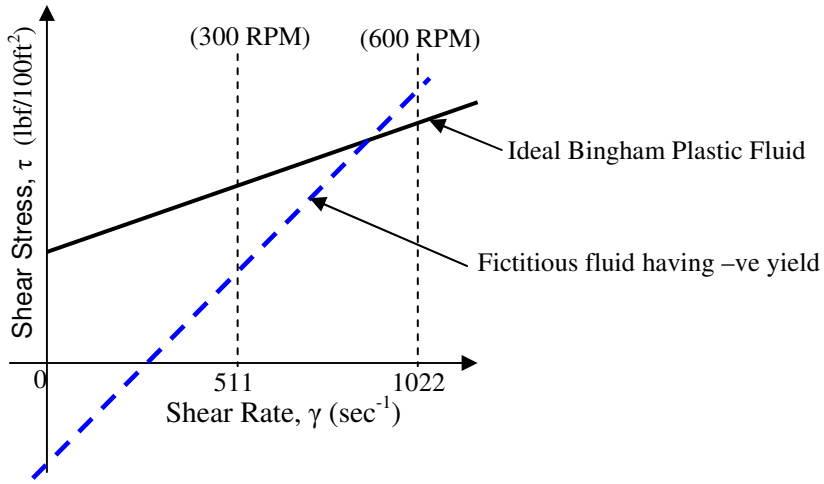

Fig. 5.10–Ideal Bingham Plastic and a fictitious fluid

Interpreting the diagram above, a fictitious fluid would have zero shear stress when being sheared at a given rate which is most unlikely. This is why the negative values have been ignored.

Table 5.2 shows a set of 5 by 5 data of plastic viscosity collected from these experiments to be used later in chapter four for statistical analysis.

Table 5.2: Plastic viscosity data for constant pressure varying temperature tests

		Temperature (°F)				
Pressure (psig)		**300**	**350**	**400**	**450**	**500**
	10,000	43	37	34	36	35
	15,000	57	46	39	36	38
	20,000	71	59	52	45	46
	25,000	92	74	62	55	57
	30,000	108	84	69	61	64

5.3.4 Constant Temperature, Variable Pressure Tests

This is the opposite of the previous test schedule. Here temperature was kept constant while increasing pressure. For this stage, nine (9) tests were performed. **Figs 5.11**, **5.12, 5.13** and **5.14** illustrate the results.

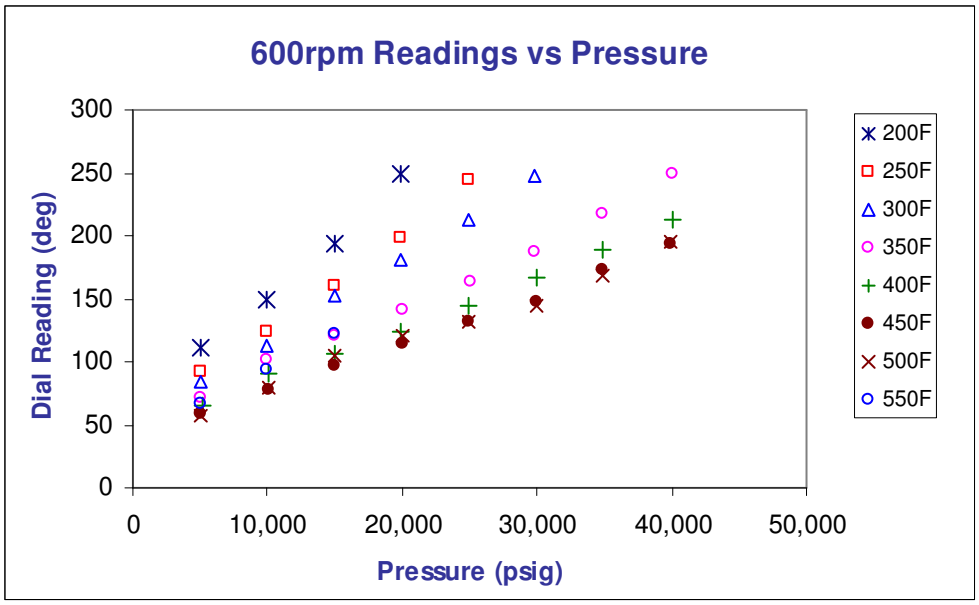

Fig. 5.11–600 RPM dial readings versus pressure

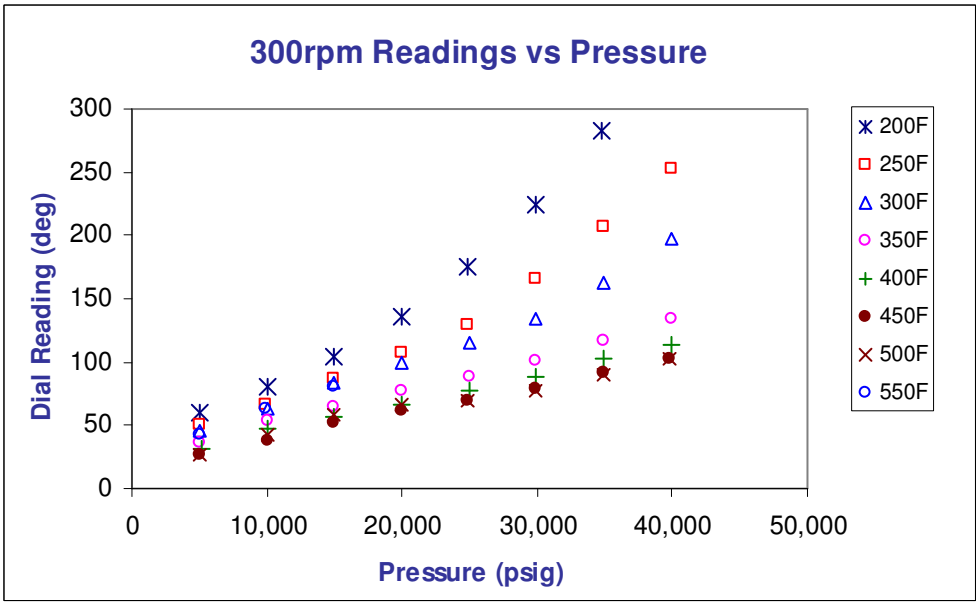

Fig. 5.12–300 RPM dial readings versus pressure

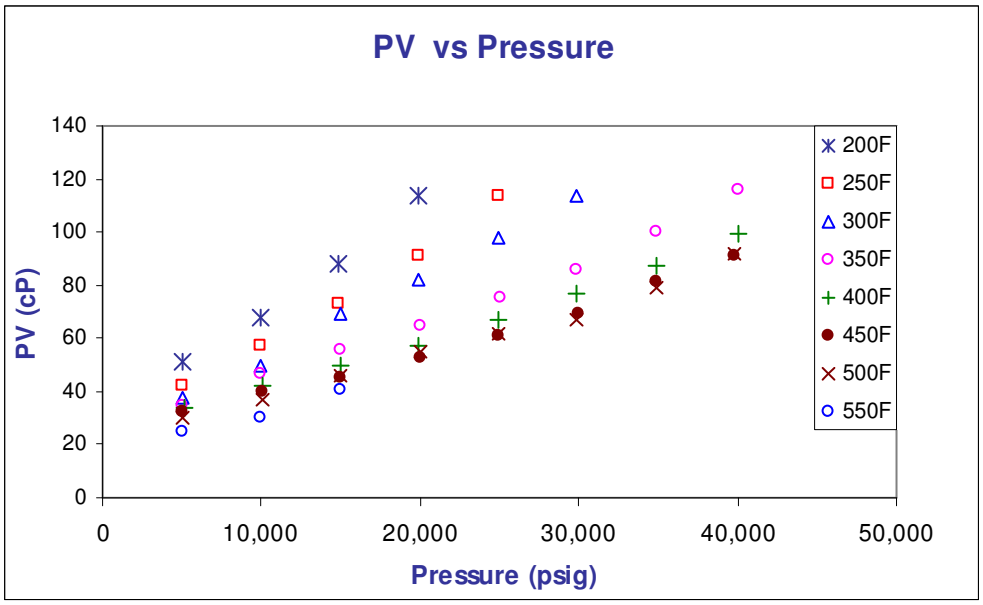

Fig. 5.13–Plastic viscosity versus pressure

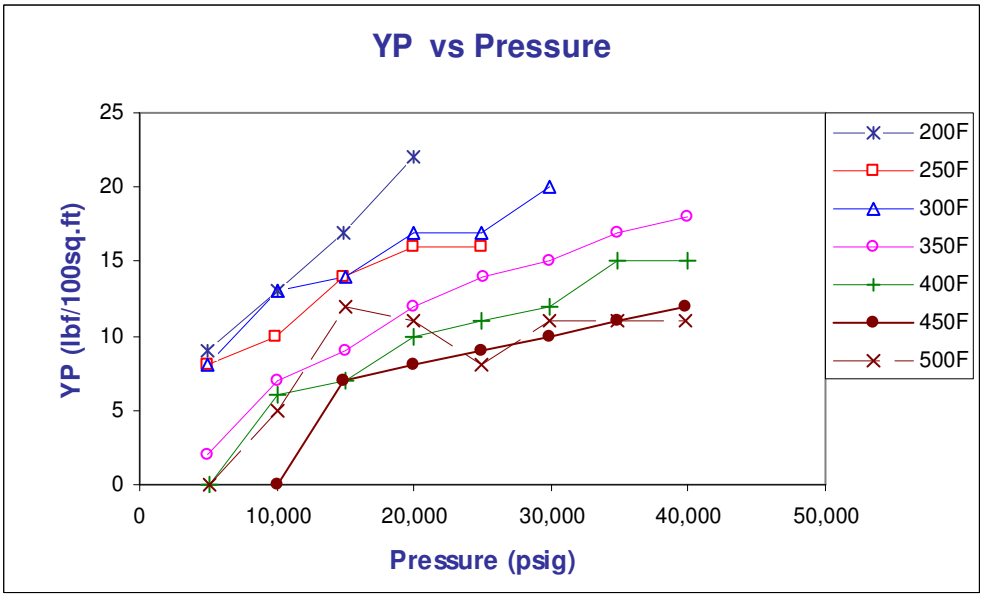

Fig. 5.14–Yield point versus pressure

5.3.5 Summary of Findings

The following can be deduced from of the plots above:

- Results from the plastic viscosity and dial reading plots confirms that temperature effect is minimal at lower pressures (ie < 15,000 psig) compared to the broader variation at higher pressures.
- At higher temperatures (350 to 550°F), there is a linear relationship between plastic viscosity, 600 RPM, 300 RPM dial readings and pressure. The relationship is exponent at lower temperatures. This means that the viscosity of Fluid Type B increases more rapidly at lower temperatures for a given constant pressure.
- Yield point values are less uniform but they consistently increase with increasing pressure or decreasing temperature. Just like in the previous tests some negative yield point values were obtained for the 400°F, 450°F and 500°F curves. Similarly, these points were omitted in the plot since they are unrealistic.

Just as in the previous phase of experiments, a 5 by 5 plastic viscosity data was collected for statistical analyses.

Table 5.3–Plastic viscosity data for constant temperature varying pressure tests

		Temperature (°F)				
Pressure (psig)		**300**	**350**	**400**	**450**	**500**
	10,000	50	47	42	40	37
	15,000	69	56	50	45	46
	20,000	82	65	57	53	55
	25,000	98	75	67	61	62
	30,000	114	86	77	69	67

5.3.6 Constant Shear Rate Tests

Here shear rate was maintained constant at 170sec^{-1} (ie 100 RPM), typical for annular flow as illustrated in Table 4.1. These tests were carried out in two phases:

5.3.6.1 Variable Temperature, Constant Pressure Tests

All the test schedules for this phase were designed so that the 100 RPM readings could be taken while heating and again when cooling down. **Fig. 5.15** below shows a combined plot (of dial readings versus temperature) for seven (7) tests.

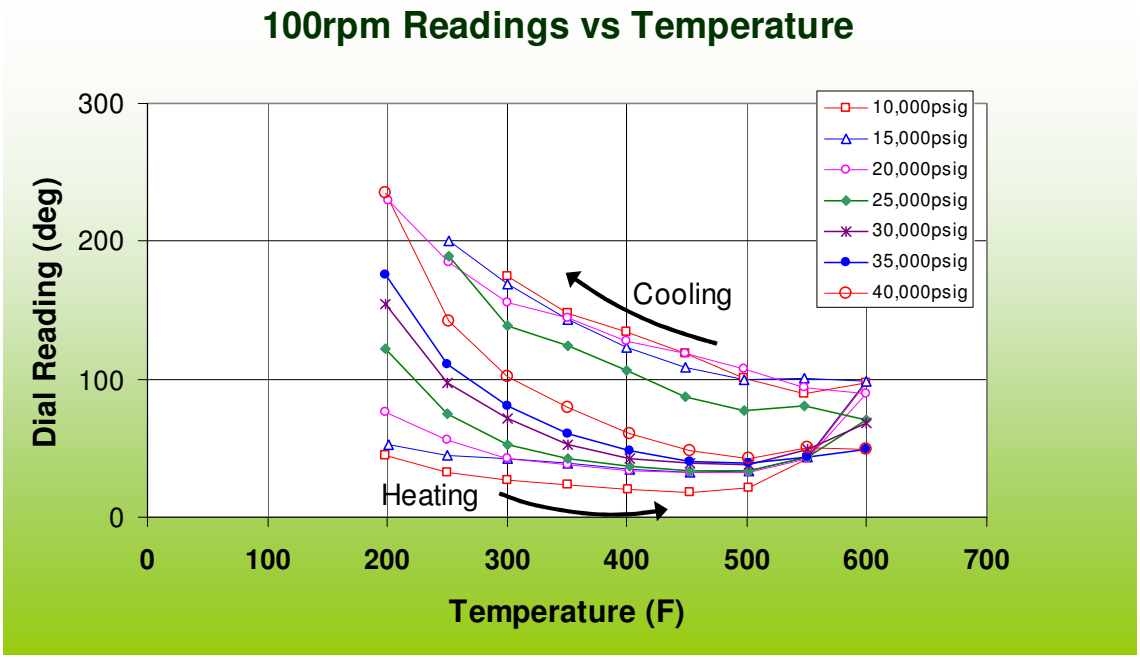

Fig. 5.15–100 RPM dial readings versus temperature

The following conclusions can be drawn from analysis of Fig. 5.15:

- At lower temperatures (<350°F), the effect of pressure is very noticeable from the spread in the "Heating" curves.
- The relationship between temperature and dial readings is exponential just as found earlier from the multiple shear rates, variable temperature and constant pressure tests.
- There is a general convergence of all the "Heating" curves at 550°F which then deviate slightly at 600°F.
- The "Cooling" curves tend to align to each other regardless of pressure. This goes to indicate that the behavior of the thermally degraded fluid is essentially the same for the different pressure profiles.

5.3.6.2 Variable Pressure, Constant Temperature tests

Seven (7) tests were performed as presented in **Fig 5.16**. Results of these tests are analogous to those of the multiple shear rates, variable pressure and constant temperature tests. As observed earlier, linear relationship exists between shear rate and pressure at constant temperature.

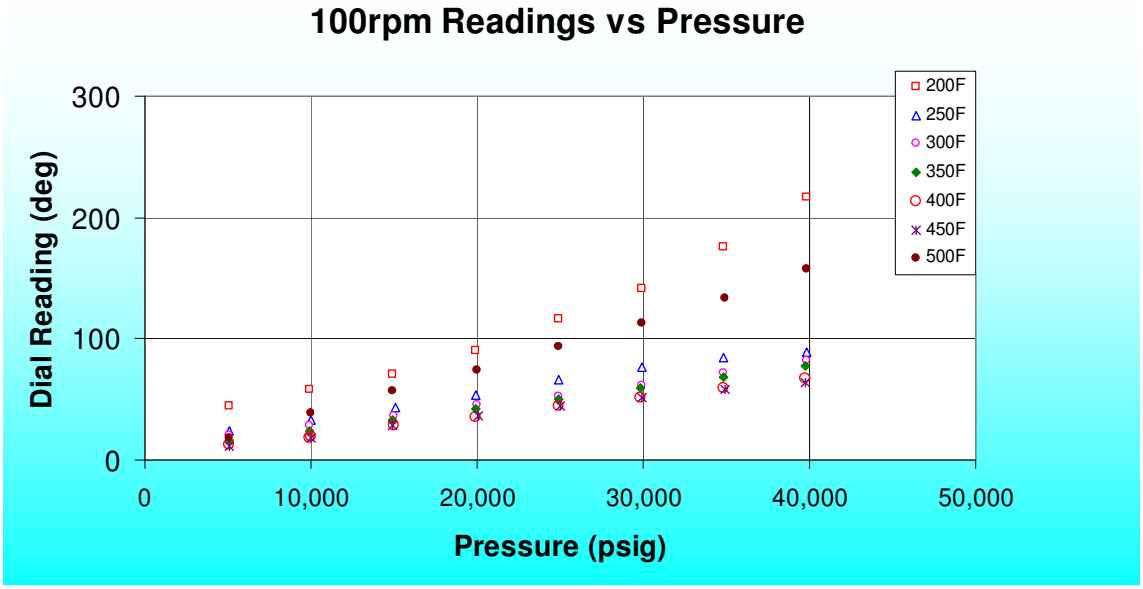

Fig. 5.16–100 RPM dial readings versus pressure

5.3.7 TX Test Series

The TX-1 to 4 series of tests were performed to further investigate the behavior of the same Fluid Type B beyond 450°F at high shear rates (300 RPM and 600 RPM) and constant pressure of 10,000 psig. A total of eight (8) tests where carried out. One original and then a repeat for each test schedule. A brief description of the four test schedules is given below:

- TX-1: (300 RPM at max 600°F and 10,000 psig)
- TX-2: (300 RPM at max 450°F and 10,000 psig)
- TX-3: (600 RPM at max 450°F and 10,000 psig)
- TX-4: (600 RPM at max 600°F and 10,000 psig)

The test schedules for this series were designed so that initial readings can be taken while heating and repeat readings when cooling down. **Fig. 5.17** shows the TX-4 test result while **Figs. 5.18** and **5.19** are plots of the original and repeat tests respectively.

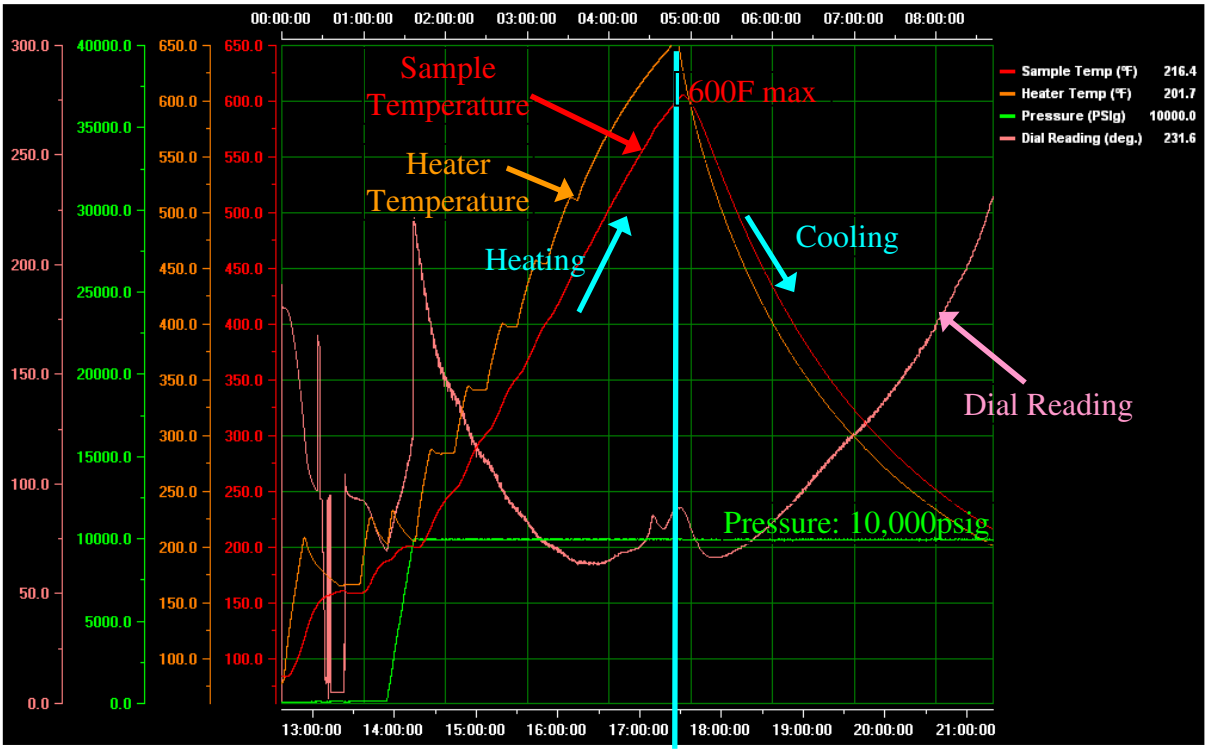

Fig. 5.17–TX-4 (600 RPM at max. 600°F and 10,000 psig) test result

Due to the considerable change in composition of the original fluid sample beyond 450°F, there is increase in viscosity while cooling down from 600°F as shown in Fig. 5.15 above.

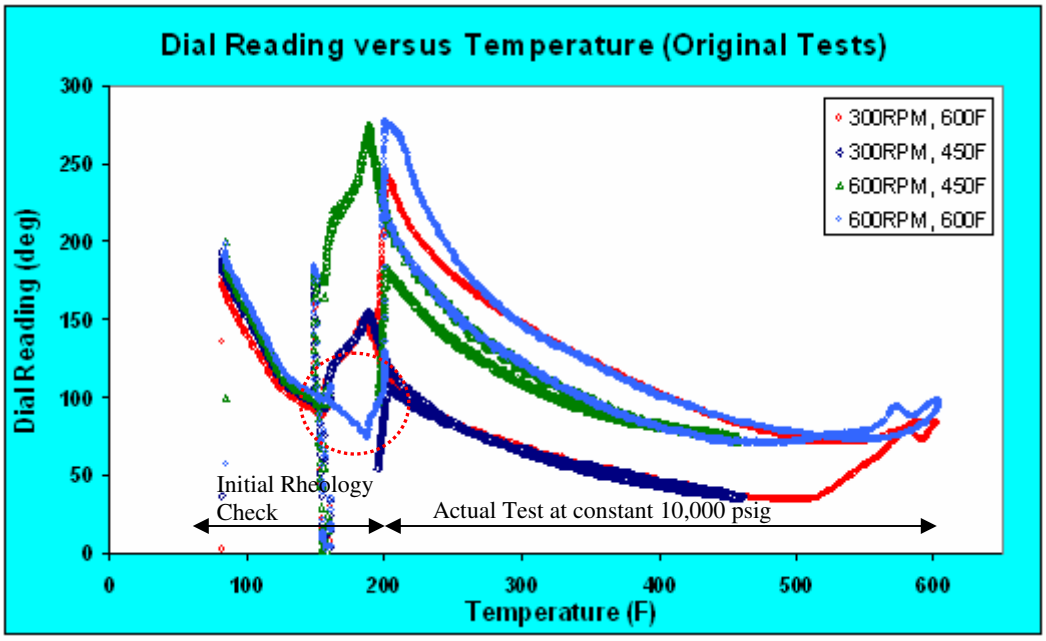

Fig. 5.18–Dial reading versus temperature for TX-tests (original)

The drop in dial reading in the section circled red was caused by low constant pressure (<200 psig) while increasing temperature.

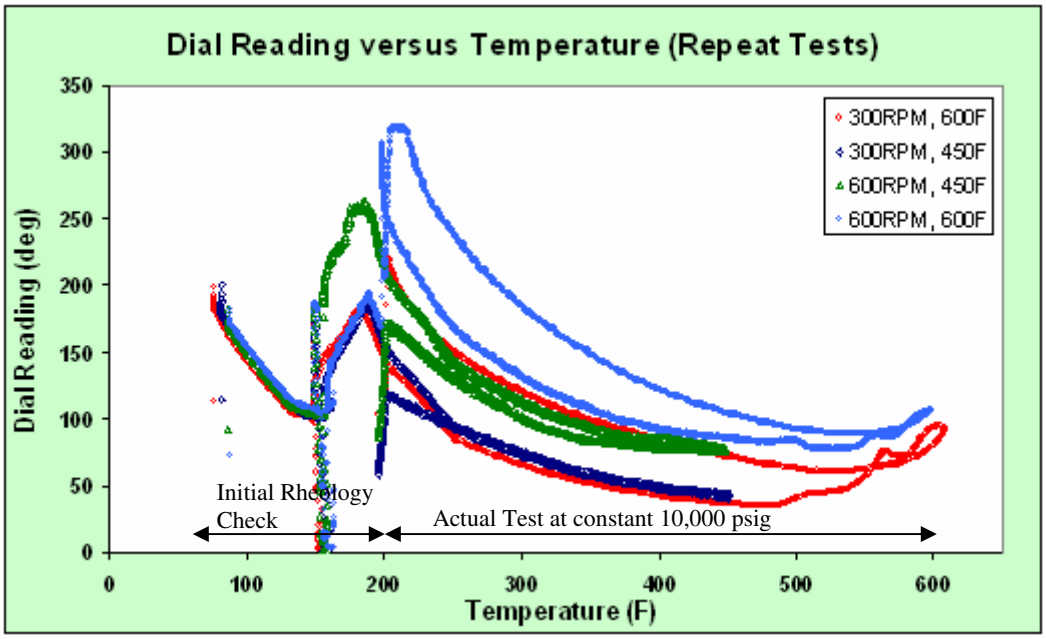

Fig. 5.19–Dial reading versus temperature for TX-tests (repeat)

The repeat experiments were performed to ensure reproducibility of the original results. The plots are quite similar. The major difference is in the higher dial reading response of TX-4 repeat test. This could have been caused by fluid thickening with time as the TX-4 was the last to be done in the series. The initial rheology check involves measuring the 600, 300, 200, 100, 6, and 3 RPM readings and gel strengths at 10 seconds and 10 minutes. These measurements were carried-out at 150°F and ambient pressure. Then between 150°F and 200°F pressure was increased to 10,000 psig and stabilized.

5.3.7.1 Summary of Findings

From the results above, the following can be deduced:

- Below 450°F, there is no significant change in the viscosity profile of Fluid Type-B for a given shear rate. The values measured when heating are quite similar to those obtained when cooling down especially for the 300 RPM test.
- The slight decrease in viscosity in the 450°F tests is attributable to the thixotropic nature of the fluid.
- Due to thermally degradation beyond 450°F, dial reading response is higher when cooling down from 600°F for both the 300 RPM and 600 RPM tests.

CHAPTER VI

STATISTICAL ANALYSES

6.1 TWO-FACTOR FACTORIAL DESIGNS

The simplest types of factorial experiments involve only two factors or sets of treatments. Given that there are *a* levels of factor *A* and *b* levels of factor *B*, all arranged in a factorial design; that is, each of the *n* replicates of the experiment contains *ab* treatment combinations. Suppose an engineer wishes to study the total power used by each of two different motors, *X* and *Y*, each running at two different speeds, 2000 or 3000 RPM. The factorial experiment would consist of four experimental units: motor *X* at 2000 RPM, motor *Y* at 2000 RPM, motor *X* at 3000 RPM, and motor *Y* at 3000 RPM. Each combination of a single level selected from every factor is present once. This experiment is an example of a 2^2 (or 2 x 2) factorial experiment, so named because it considers two levels (the base) for each of two factors (the superscript), producing $2^2 = 4$ factorial points.

Let y_{ijk} be the observed response when factor *A* is at the *i*th level (i = 1, 2, …, a) and factor *B* is at the *j*th level (j = 1, 2, ..., b) for the *k*th replicate (k = 1, 2, …, n). The order in which the *abn* observations are taken is selected at random so that the design is a completely randomized design. The observations can be described by the linear statistical model,[27]:

$$y_{ijk} = \mu + \tau_i + \beta_j + (\tau\beta)_{ij} + \varepsilon_{ijk} \begin{cases} i = 1,2,...,a \\ j = 1,2,...,b \\ k = 1,2,...,n \end{cases} \quad \text{..... (6.1)}$$

Where μ is the overall mean effect, τ_i is the effect of the *i*th level of the row factor *A*, β_j is the effect of the *j*th level of the column factor *B*, $(\tau\beta)_{ij}$ is the effect of the interaction between τ_i and β_j, ε_{ijk} is a random error component having a normal

distribution with a mean zero and variance, σ^2. We are interested in testing the hypotheses of no main effect for factor *A*, no main effect for *B*, and no *AB* interaction effect.

6.2 ANALYSIS OF VARIANCE

The analysis of variance or ANOVA can be used to test hypotheses about the main factor effects of *A* and *B* and the *AB* interaction. To present the ANOVA, we will need some symbols, some of which are illustrated in **Table 6.1**.

Table 6.1–Data Arrangement for a Two-Factor Factorial design

		Factor *B*				**Totals**	**Averages**
		1	**2**	**…**	***b***		
Factor *A*	**1**	$y_{111}, y_{112}, \ldots, y_{11n}$,	$y_{121}, y_{122}, \ldots, y_{12n}$,		$y_{1b1}, y_{1b2}, \ldots, y_{1bn}$,	$y_{1..}$	$\bar{y}_{1..}$
	2	$y_{211}, y_{212}, \ldots, y_{21n}$,	$y_{221}, y_{222}, \ldots, y_{22n}$,		$y_{2b1}, y_{2b2}, \ldots, y_{2bn}$,	$y_{2..}$	$\bar{y}_{2..}$
	. . .						
	a	$y_{a11}, y_{a12}, \ldots, y_{a1n}$,	$y_{a21}, y_{a22}, \ldots, y_{a2n}$,		$y_{ab1}, y_{ab2}, \ldots, y_{abn}$,	$y_{a..}$	$\bar{y}_{a..}$
Totals		$y_{.1.}$	$y_{.2.}$		$y_{.b.}$	$y\ldots$	
Averages		$\bar{y}_{.1..}$	$\bar{y}_{.2.}$		$\bar{y}_{.b.}$		$\bar{y}...$

Let $y_{i..}$ denote the total of the observations taken at the *i*th level of factor *A*; $y_{.j.}$ denote the total of the observations taken at the *j*th level of factor *B*; $y_{ij.}$ denote the total of the observations in the *ij*th cell as shown above; and *y*... denote the grand total of all the observations. Define $\bar{y}_{i...}$, $\bar{y}_{.j.}$, $\bar{y}_{ij.}$ and $\bar{y}...$ as the corresponding row, column, cell, and grand averages. That is,

$$\left.\begin{array}{lll} y_{i..} = \sum_{j=1}^{b}\sum_{k=1}^{n} y_{ijk} & \bar{y}_{i..} = \dfrac{y_{i..}}{bn} & i = 1, 2,..., a \\ y_{.j.} = \sum_{i=1}^{a}\sum_{k=1}^{n} y_{ijk} & \bar{y}_{.j.} = \dfrac{y_{.j.}}{an} & j = 1, 2,..., b \\ y_{ij.} = \sum_{k=1}^{n} y_{ijk} & \bar{y}_{ij.} = \dfrac{y_{ij.}}{n} & i = 1, 2,..., a \text{ and } j = 1, 2,..., b \\ y_{...} = \sum_{i=1}^{a}\sum_{j=1}^{b}\sum_{k=1}^{n} y_{ijk} & \bar{y}_{...} = \dfrac{y_{...}}{abn} & \end{array}\right\} \quad \text{... (6.2)}$$

In a two-factor experiment, we will use a two-way ANOVA in order to conduct formal tests for hypotheses of no interaction, and hypotheses of no main effect for each factor. Basically the ANOVA tests these hypotheses by decomposing the total variability in the data into component parts and then comparing the various elements in this decomposition. The total variability is measured by the total sum of squares of the observations given as:

$$\begin{aligned} \sum_{i=1}^{a}\sum_{j=1}^{b}\sum_{k=1}^{n}(y_{ijk} - \bar{y}...)^2 &= bn\sum_{i=1}^{a}(\bar{y}_{i..} - \bar{y}...)^2 \\ &+ an\sum_{j=1}^{b}(\bar{y}_{.j.} - \bar{y}...)^2 \\ &+ n\sum_{i=1}^{a}\sum_{j=1}^{b}(\bar{y}_{ij.} - \bar{y}_{i..} - \bar{y}_{.j.} + \bar{y}...)^2 \\ &+ \sum_{i=1}^{a}\sum_{j=1}^{b}\sum_{k=1}^{n}(y_{ijk} - \bar{y}_{ij.})^2 \quad \text{..... (6.3)} \end{aligned}$$

Or symbolically as: $SS_T = SS_A + SS_B + SS_{AB} + SS_E$ ..... (6.4)

Where SS_A is the sum of squares for the row factor A, SS_B is the sum of squares for the column factor B, SS_{AB} is the sum of squares for the interaction between A and B, and SS_E is the error sum of squares. In summary, the sums of squares in a two-factor ANOVA are computed as follows:

$$SS_T = \sum_{i=1}^{a}\sum_{j=1}^{b}\sum_{k=1}^{n} y_{ijk}^2 - \frac{y_{...}^2}{abn} \quad \text{(6.5)}$$

$$SS_A = \sum_{i=1}^{a} \frac{y_{i..}^2}{bn} - \frac{y_{...}^2}{abn} \quad \text{(6.6)}$$

$$SS_B = \sum_{j=1}^{b} \frac{y_{.j.}^2}{an} - \frac{y_{...}^2}{abn} \quad \text{(6.7)}$$

$$SS_{AB} = \sum_{i=1}^{a}\sum_{j=1}^{b} \frac{y_{ij.}^2}{n} - \frac{y_{...}^2}{abn} - SS_A - SS_B \quad \text{(6.8)}$$

And finally we can calculate SS_E by making it the subject of Eq. 6.4

$$SS_E = SS_T - SS_A - SS_B - SS_{AB} \quad \text{(6.9)}$$

For a two-factor ANOVA, there are $abn-1$ total degrees of freedom. The main effects *A* and *B* have $a-1$ and $b-1$ degrees of freedom, while the interaction effect *AB* has $(a-1)(b-1)$ degrees of freedom. Within each of the *ab* cells in Table 6.1 there are $n-1$ degrees of freedom between the *n* replicates, and observations in the same cell can differ only because of random error. Therefore, there are $ab(n-1)$ degrees of freedom for error and all the degrees of freedom are partition as follows:

$$abn-1 = (a-1)+(b-1)+(a-1)(b-1)+ab(n-1) \quad \text{(6.10)}$$

By dividing each of the sums of squares on the right-hand side of equation 6.4 by the corresponding number of degrees of freedom, we obtain the mean squares for A, B, the interaction and error;

$$MS_A = \frac{SS_A}{a-1}, \quad MS_B = \frac{SS_B}{b-1}, \quad MS_{AB} = \frac{SS_{AB}}{(a-1)(b-1)}, \quad MS_E = \frac{SS_E}{ab(n-1)} \quad \text{(6.11)}$$

6.2.1 Fixed-Effects Model

Suppose that *A* and *B* are fixed factors. That is, the *a* levels of factor *A* and the *b* levels of factor *B* are specifically chosen by the experimenter, and inferences are confined to

these levels only. In this model, it is customary to define the effects τ_i, β_j and $(\tau\beta)_{ij}$ as deviations from the mean, so that $\sum_{i=1}^{a}\tau_i = 0$, $\sum_{j=1}^{b}\beta_j = 0$, $\sum_{i=1}^{a}(\tau\beta)_{ij} = 0$ and $\sum_{j=1}^{b}(\tau\beta)_{ij} = 0$. **Table 6.2** shows all the ANOVA parameters for a two-factor factorial, fixed-effects model

Table 6.2–ANOVA table for a Two-Factor Factorial, Fixed-Effects Model[27]

Source of Variation	Sum of Squares	Degrees of Freedom	Mean Square	F_0
Factor, A	SS_A	$a-1$	$MS_A = \frac{SS_A}{a-1}$	$F_0 = \frac{MS_A}{MS_E}$
Factor, B	SS_B	$b-1$	$MS_B = \frac{SS_B}{b-1}$	$F_0 = \frac{MS_B}{MS_E}$
Interaction	SS_{AB}	$(a-1)(b-1)$	$MS_{AB} = \frac{SS_{AB}}{(a-1)(b-1)}$	$F_0 = \frac{MS_{AB}}{MS_E}$
Error	SS_E	$ab(n-1)$	$MS_E = \frac{SS_E}{ab(n-1)}$	
Total	SS_T	$abn-1$		

6.2.2 Random-Effects Model

Consider a more practical situation were the levels of both factors *A* and *B* are randomly selected from larger populations of factor levels, and we wish to extend our conclusion to the entire population. The observations are represented by the same model as defined in Eq. 6.1. Here the parameters τ_i, β_j, $(\tau\beta)_{ij}$ and ε_{ijk} are normally and independently distributed random variables with means zero and variances σ_τ^2, σ_β^2, $\sigma_{\tau\beta}^2$, and σ^2 respectively. Just like the fixed effects model the basis of analysis of variance remains unchanged; that is, SS_A, SS_B, SS_{AB}, SS_T, and SS_E are calculated as in the fixed effects case. The ANOVA parameters for a two-factor factorial, random-effects model are presented in **Table 6.3.** The only difference from the fixed effects model is in the expression for

calculating the F_0 (test statistic) of factors *A* and *B*. The denominator here is the interaction mean square (MS_{AB}) instead of the error mean square (MS_E).

Table 6.3–ANOVA table for a Two-Factor Factorial, Random-Effects Model[27]

Source of Variation	**Sum of Squares**	**Degrees of Freedom**	**Mean Square**	***F₀***
Factor, A	SS_A	$a-1$	$MS_A = \frac{SS_A}{a-1}$	$F_0 = \frac{MS_A}{MS_{AB}}$
Factor, B	SS_B	$b-1$	$MS_B = \frac{SS_B}{b-1}$	$F_0 = \frac{MS_B}{MS_{AB}}$
Interaction	SS_{AB}	$(a-1)(b-1)$	$MS_{AB} = \frac{SS_{AB}}{(a-1)(b-1)}$	$F_0 = \frac{MS_{AB}}{MS_E}$
Error	SS_E	$ab(n-1)$	$MS_E = \frac{SS_E}{ab(n-1)}$	
Total	SS_T	$abn-1$		

6.2.3 Mixed-Effects Models

In the context of this research this could be either of two models: a Random Pressure, Fixed Temperature or a Random Temperature, Fixed Pressure model. Thus one factor is fixed while the other is random. For a given model, the F_0 statistic of the random factor is calculated using MS_{AB} as the denominator whereas MS_E is used as the denominator in estimating the F_0 statistic of the fixed factor. Both the interaction $(\tau\beta)_{ij}$ and error ε_{ijk} terms are random variables having zero mean and variance σ^2 but the error term is independently distributed.

6.2.4 Illustration

The plastic viscosity data of Fluid Type B for both the constant pressure-variable temperature and constant temperature-variable pressure tests contained in Tables 5.2 and 5.3 are combined in the **Table 6.4** below. The first value is from the constant pressure-variable temperature test while the second is from the corresponding constant temperature-variable pressure test. These data were sampled from a larger population of temperature and pressure ranging from 200 to 600°F and 10,000 to 40,000 psig respectively.

Table 6.4–Combined plastic viscosity data from Fluid Type B tests

		Temperature (°F)				
Pressure (psig)		**300**	**350**	**400**	**450**	**500**
	10,000	43/50	37/47	34/42	36/40	35/37
	15,000	57/69	46/56	39/50	36/45	38/46
	20,000	71/82	59/65	52/57	45/53	46/55
	25,000	92/98	74/75	62/67	55/61	57/62
	30,000	108/114	84/86	69/77	61/69	64/67

From the above data set, $n = 2$ since we have two sets of data. So k will range from 1 to 2. Also $a = b = 5$, representing 5 levels each for pressure and temperature. Using the sums and averages formulas defined in Eq. 6.2, the following calculations are made:

6.2.4.1 Calculate Totals and Averages

For the first row representing (10,000 psig data):

$$y_{1..} = \sum_{j=1}^{5}\sum_{k=1}^{2} y_{1jk} = 43 + 50 + 37 + 47 + 34 + 42 + 36 + 40 + 35 + 37 = 401$$

And $\bar{y}_{1..} = \dfrac{y_{1..}}{bn} = \dfrac{401}{5 \times 2} = 40.1$

Similarly for other rows;

$$y_{2..} = \sum_{j=1}^{5}\sum_{k=1}^{2} y_{2jk} = 482, \qquad \bar{y}_{2..} = \frac{y_{2..}}{bn} = \frac{482}{5 \times 2} = 48.2$$

$$y_{3..} = \sum_{j=1}^{5}\sum_{k=1}^{2} y_{3jk} = 585, \qquad \bar{y}_{3..} = \frac{y_{3..}}{bn} = \frac{585}{5\times 2} = 58.5$$

$$y_{4..} = \sum_{j=1}^{5}\sum_{k=1}^{2} y_{4jk} = 703, \qquad \bar{y}_{4..} = \frac{y_{4..}}{bn} = \frac{703}{5\times 2} = 70.3$$

$$y_{5..} = \sum_{j=1}^{5}\sum_{k=1}^{2} y_{5jk} = 799, \qquad \bar{y}_{5..} = \frac{y_{5..}}{bn} = \frac{799}{5\times 2} = 79.9$$

This process is also true for the column operations. So for the first column:

$$y_{.1.} = \sum_{i=1}^{5}\sum_{k=1}^{2} y_{i1k} = 43+50+57+69+71+82+92+98+108+114 = 784$$

And $\bar{y}_{.1.} = \frac{y_{.1.}}{an} = \frac{784}{5\times 2} = 78.4$

Similarly

$$y_{.2.} = \sum_{i=1}^{5}\sum_{k=1}^{2} y_{i2k} = 629, \qquad \bar{y}_{.2.} = \frac{y_{.2.}}{an} = \frac{629}{5\times 2} = 62.9$$

$$y_{.3.} = \sum_{i=1}^{5}\sum_{k=1}^{2} y_{i3k} = 549, \qquad \bar{y}_{.3.} = \frac{y_{.3.}}{an} = \frac{549}{5\times 2} = 54.9$$

$$y_{.4.} = \sum_{i=1}^{5}\sum_{k=1}^{2} y_{i4k} = 501, \qquad \bar{y}_{.4.} = \frac{y_{.4.}}{an} = \frac{501}{5\times 2} = 50.1$$

$$y_{.5.} = \sum_{i=1}^{5}\sum_{k=1}^{2} y_{i5k} = 507, \qquad \bar{y}_{.5.} = \frac{y_{.5.}}{an} = \frac{507}{5\times 2} = 50.7$$

To calculate the sum and average of cell (1, 1), we use;

$$y_{ij.} = y_{11.} = \sum_{k=1}^{n} y_{11k} = 43+50 = 93 \qquad \text{and} \qquad \bar{y}_{11.} = \frac{y_{11.}}{n} = \frac{93}{2} = 46.5$$

This was done for all the cells and the results used later in the analysis of residuals.

Finally, the grand sum and average are given as:

$$y_{...} = \sum_{i=1}^{5}\sum_{j=1}^{5}\sum_{k=1}^{2} y_{ijk} = 43+50+....+64+67 = 2970 \quad \text{and} \quad \bar{y}_{...} = \frac{y_{...}}{abn} = \frac{2970}{5\times 5\times 2} = 59.4$$

6.2.4.2 Estimate ANOVA Parameters

Using Eq. 6.4 through to 6.9 we have that:

$$SS_T = \sum_{i=1}^{a}\sum_{j=1}^{b}\sum_{k=1}^{n} y_{ijk}^2 - \frac{y_{...}^2}{abn} = 194{,}110 - \frac{2970^2}{5\times 5\times 2} = 17{,}692$$

$$SS_A = \sum_{i=1}^{a}\frac{y_{i..}^2}{bn} - \frac{y_{...}^2}{abn} = \frac{1{,}867{,}960}{5\times 2} - \frac{2970^2}{5\times 5\times 2} = 10{,}378$$

$$SS_B = \sum_{j=1}^{b}\frac{y_{.j.}^2}{an} - \frac{y_{...}^2}{abn} = \frac{1{,}819748}{5\times 2} - \frac{2970^2}{5\times 5\times 2} = 5{,}556.8$$

$$SS_{AB} = \sum_{i=1}^{a}\sum_{j=1}^{b}\frac{y_{ij.}^2}{n} - \frac{y_{...}^2}{abn} - SS_A - SS_B = \frac{386{,}850}{2} - \frac{2970^2}{5\times 5\times 2} - 10{,}378 - 5{,}556.8 = 1{,}072.2$$

$$SS_E = SS_T - SS_A - SS_B - SS_{AB} = 685$$

$$MS_A = \frac{SS_A}{a-1} = \frac{10{,}378}{5-1} = 2{,}594.5, \qquad MS_B = \frac{SS_B}{b-1} = \frac{5{,}556.8}{5-1} = 1{,}389.2$$

$$MS_{AB} = \frac{SS_{AB}}{(a-1)(b-1)} = \frac{1{,}072.2}{(5-1)(5-1)} = 67.0 \qquad MS_E = \frac{SS_E}{ab(n-1)} = \frac{685}{25(2-1)} = 27.4$$

6.3 HYPOTHESIS TESTING

The random effects model discussed earlier will be used in hypothesis testing because the data used for illustration was obtained from a larger population. Thus we are treating both pressure and temperature as random factors. The three hypotheses to be evaluated are as follows:

1. $H_0 : \tau_1 = \tau_2 = ... = \tau_a = 0$ (no main effect of factor *A* - Pressure)……..…..(6.12)

   H_1 : at least one $\tau_i \neq 0$

To test that the row factor (pressure) effects are all equal to zero, we would use the ratio:

$$F_0 = \frac{MS_A}{MS_{AB}} = \frac{2594.5}{67.0} = 38.7 \quad \text{...……..……..……..... (6.13)}$$

This is an F-distribution with $a-1$ and $(a-1)(b-1)$ degrees of freedom if $H_0 : \tau_i = 0$ is true. This null hypothesis is rejected at the α level of significance if $f_0 > f_{\alpha,a-1,(a-1)(b-1)}$.

Assuming a significance level of $\alpha = 0.05$, then $f_{\alpha,a-1,(a-1)(b-1)} = f_{0.05,4,16} = 3.01$. Since $38.7 > 3.01$, the null is rejected, meaning that at $\alpha = 0.05$ (ie 95% confidence level), the effects of pressure on plastic viscosity of the fluid is not negligible.

2. $H_0 : \beta_1 = \beta_2 = ... = \beta_b = 0$ (no main effect of factor *B* - Temperature)…..... (6.14)

   H_1 : at least one $\beta_j \neq 0$

Similarly, to test the hypothesis that all the column factor (temperature) effects are equal to zero $H_0 : \beta_j = 0$, we would use the ratio

$$F_0 = \frac{MS_B}{MS_{AB}} = \frac{1389.2}{67.0} = 20.7 \quad \text{…….……..…….……..…….....} \quad (6.15)$$

This F-distribution has $b-1$ and $(a-1)(b-1)$ degrees of freedom if $H_0 : \beta_j = 0$ is true. This null hypothesis is rejected at the α level of significance if $f_0 > f_{\alpha,b-1,(a-1)(b-1)}$. For the case at hand, the null hypothesis is still rejected at $\alpha = 0.05$ since; $f_{\alpha,b-1,(a-1)(b-1)} = f_{0.05,4,16} = 3.01 < 20.7$

3. $H_0 : (\tau\beta)_{11} = (\tau\beta)_{12} = ... = (\tau\beta)_{ab} = 0$ (no interaction effect between *A* & *B*)…...(6.16)

   H_1 : at least one $(\tau\beta)_{ij} \neq 0$

Finally, to test the hypothesis that all interaction effects are equal to zero $H_0 : (\tau\beta)_{ij} = 0$, we would use the ratio:

$$F_0 = \frac{MS_{AB}}{MS_E} = \frac{67.0}{27.4} = 2.45 \quad \text{…….……..…….……..……..} \quad (6.17)$$

This has an F-distribution with $(a-1)(b-1)$ and $ab(n-1)$ degrees of freedom if $H_0 : \beta_j = 0$ is true. This null hypothesis is rejected at the α level of significance if $f_0 > f_{\alpha,(a-1)(b-1),ab(n-1)}$. Performing the calculations; $f_{\alpha,(a-1)(b-1),ab(n-1)} = f_{0.05,16,25} = 2.07$

Clearly for $\alpha = 0.05$ (level of significance) there is strong evidence to conclude that estimates of the slope τ_i, β_j and $(\tau\beta)_{ij}$ are not equal to zero. This implies that the main

and interaction effects of pressure and temperature on the plastic viscosity of the Fluid Type-B are not negligible

Note that if the hypothesis of no interaction between two factors is rejected, that is, if interaction exists, then the two hypotheses of no factor main effects are irrelevant, since both factors clearly do affect the response variable through the interaction effect. However if there is no interaction, and if only one of the factor main effects is significant, the two-way ANOVA model reduces to a one-way ANOVA model. The data analysis can be continued with a one-way ANOVA.

In some cases involving a two-factor factorial experiment, we may have only one replicate that is, only one observation per cell. In this situation, there are exactly as many parameters in the analysis of variance model as observations, and the error degrees of freedom are zero. Thus, we cannot test hypotheses about the main effects and interactions unless some additional assumptions are made. One possible assumption is to assume the interaction effect is negligible and use the interaction mean square as an error mean square. Thus, the analysis is equivalent to the analysis used in the randomized block design. This no-interaction assumption can be dangerous, and the experimenter should carefully examine the data and the residuals for indications as to whether or not interaction is present.

6.4 ANALYSIS OF RESIDUALS

Residuals from a factorial experiment play an important role in determining the model adequacy. By definition,[27] the residuals from a two-factor factorial experiment are just the difference between the observations and the corresponding cell averages:

$$e_{ijk} = y_{ijk} - \bar{y}_{ij.} \quad \text{(6.18)}$$

Recall $\bar{y}_{ij.}$ has been calculated earlier. **Table 6.5** presents the residuals of the plastic viscosity data for the Fluid Type B.

Table 6.5: Residuals of plastic viscosity data for Fluid Type B

		Temperature (°F)				
		300	**350**	**400**	**450**	**500**
Pressure (psig)	**10,000**	-3.5/3.5	-5/5	-4/4	-2/2	-1/1
	15,000	-6/6	-5/5	-5.5/5.5	-4.5/4.5	-4/4
	20,000	-5.5/5.5	-3/3	-2.5/2.5	-4/4	-4.5/4.5
	25,000	-3/3	-0.5/0.5	-2.5/2.5	-3/3	-2.5/2.5
	30,000	-3/3	-1/1	-4/4	-4/4	-1.5/1.5

The normal probability plot of these residuals is shown in **Fig. 6.1**. The tails do not exactly follow a straight line trend indicating some deviation from normality. There is noticeably a wave-pattern in the distribution of the residuals. However the deviation is not severe.

Figs. 6.2, **6.3** and **6.4** plot the residuals versus pressure, temperature and predicted values respectively. There is more variability in the data measure at 15,000 psig pressure and 300°F. Generally, the variation reduces with increase in temperature and pressure. Measurements taken independently at 25,000 psig and 450°F have the least variations.

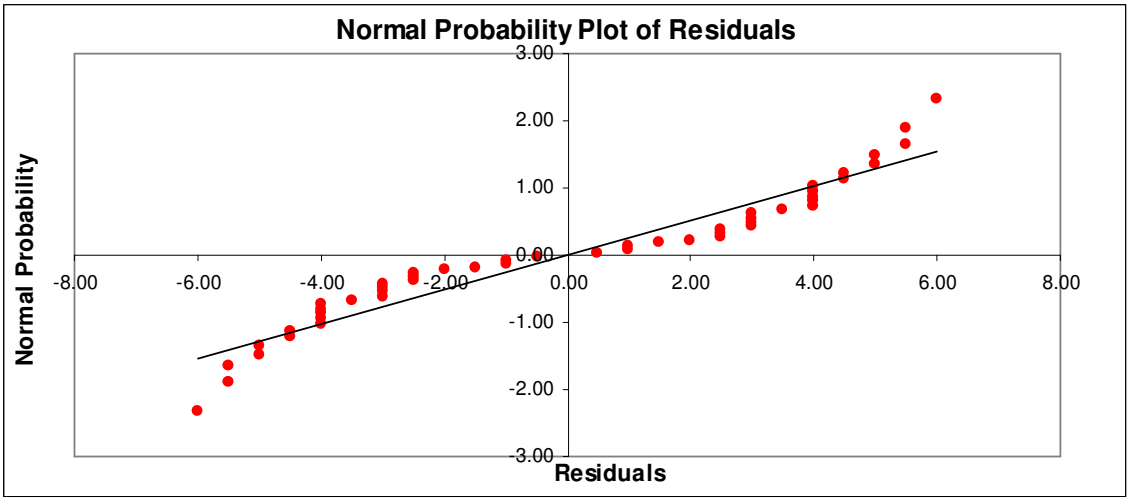

Fig. 6.1–Normal probability plot of residuals

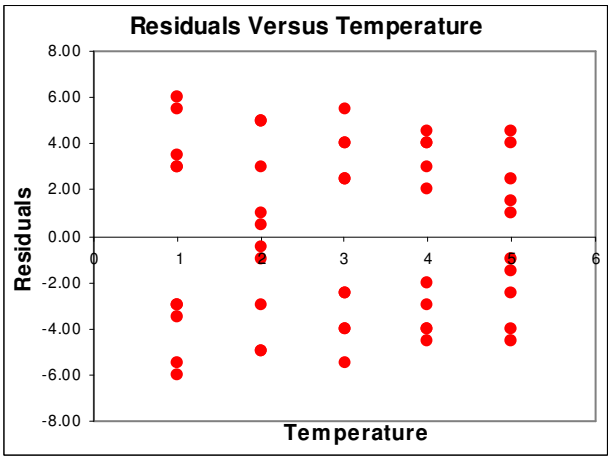

Fig. 6.2–Residuals versus temperature

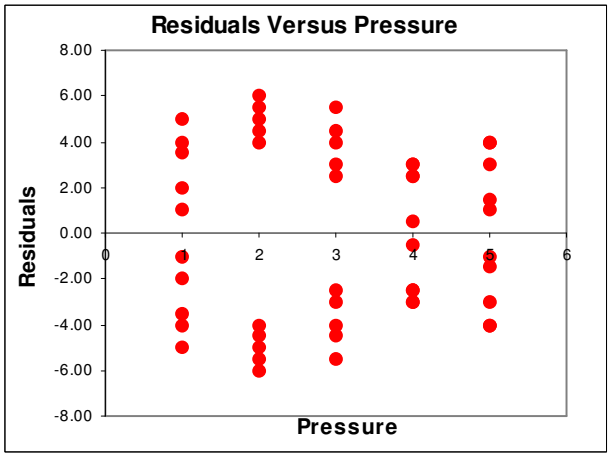

Fig. 6.3–Residuals versus pressure

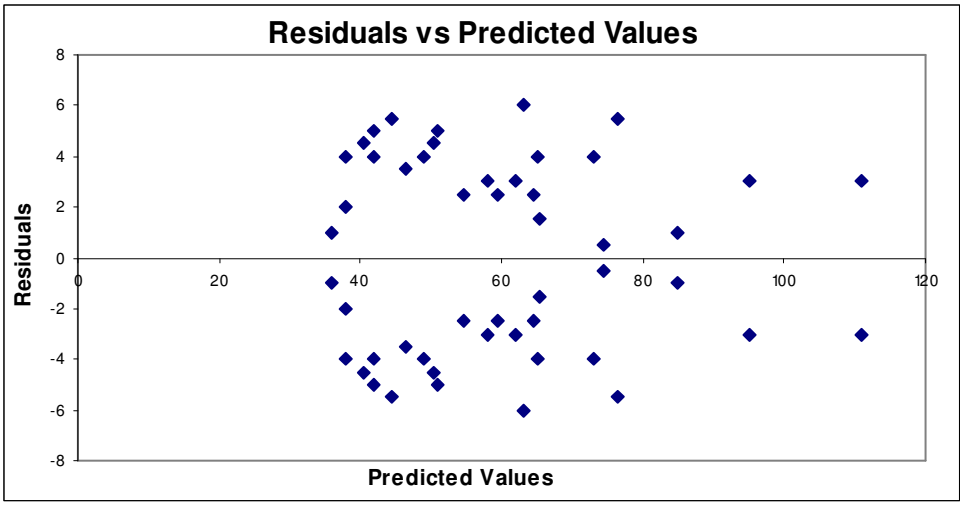

Fig. 6.4–Residuals versus predicted values

6.5 MODELING

In general, a model mathematically describes the relationship between a dependent variable (say plastic viscosity) and its regressor variables (temperature and pressure). For the purpose of this research, the multiple linear regression technique was adopted based on the intrinsic linearity existing between rhelogical properties and pressure-temperature effects.

6.5.1 Multiple Linear Regression

A regression model containing more than one regressor variable is called a multiple regression model. In theory, the dependent variable can be related to the regressor variables as follows,[27]:

$$Y = \beta_0 + \beta_1 x_1 + \beta_2 x_2 + ... + \beta_k x_k + \varepsilon \quad \text{..... (6.19)}$$

Where the parameters β_j, $j = 0,1,....,k,$ are know as the regression coefficients. They represent the expected change in the response Y per unit change in x_j when all the remaining regressors are kept constant. Multiple linear regression is also applicable to models with interaction effects as is typical of this research. The interaction between the two variables can be represented by a cross-product in the model:

$$Y = \beta_0 + \beta_1 x_1 + \beta_2 x_2 + \beta_{12} x_1 x_2 + \varepsilon \quad \text{..... (6.20)}$$

And by setting $x_3 = x_1 x_2$ and $\beta_3 = \beta_{12}$, Eq. 6.20 can be written as:

$Y = \beta_0 + \beta_1 x_1 + \beta_2 x_2 + \beta_3 x_3 + \varepsilon$ which is a linear model like Eq. 6.19.

Based on fundamental principles and experimental results from this research, pressure and temperature are directly and inversely proportional to viscosity respectively. So a simple algebraic model can be written as:

$$PV = \beta_0 + \beta_1 P + \beta_2 T^{-1} + \beta_3 PT^{-1} \quad \text{..... (6.21)}$$

Logarithmic, exponential and polynomial model options are also explored to obtain a better fit. These model options are all incorporated in the *FluidStats* program with a flexibility to choose the parameter forms.

6.5.2 Matrix Notations

The mathematical operations involved in fitting a multiple linear regression model are best expressed using matrix notations. Given that there are *k* regressor variables and *n* observations i.e.: $(x_{i1}, x_{i2}, ..., x_{ik}, y_i), i = 1,2,...,n$, then the model relating the regressor variables to the response is,[27]:

$$Y = \beta_0 + \beta_1 x_{i1} + \beta_2 x_{i2} + ... + \beta_k x_{ik} + \varepsilon \qquad i = 1,2,...,n \quad \text{..... (6.22)}$$

This model represents a system of *n* equations that can be expressed in matrix form as:

$$\mathbf{y} = \mathbf{X}\boldsymbol{\beta} + \boldsymbol{\varepsilon} \quad \text{..... (6.23)}$$

Where:

$$\mathbf{y} = \begin{bmatrix} y_1 \\ y_2 \\ \vdots \\ y_n \end{bmatrix} \quad \mathbf{X} = \begin{bmatrix} 1 & x_{11} & x_{12} & \cdots & x_{1k} \\ 1 & x_{21} & x_{22} & \cdots & x_{2k} \\ \vdots & \vdots & \vdots & & \vdots \\ 1 & x_{n1} & x_{n2} & \cdots & x_{nk} \end{bmatrix} \quad \boldsymbol{\beta} = \begin{bmatrix} \beta_0 \\ \beta_1 \\ \vdots \\ \beta_k \end{bmatrix} \quad \text{and} \quad \boldsymbol{\varepsilon} = \begin{bmatrix} \varepsilon_1 \\ \varepsilon_2 \\ \vdots \\ \varepsilon_n \end{bmatrix}$$

Here **y** is an (n x 1) vector of the observations, **X** is an (n x p) matrix of levels of the independent variables, **β** is an (p x 1) vector of regression coefficients, and **ε** is a (n x 1) vector of random errors with zero mean and variance, σ^2. Using the least squares approach, estimate of the coefficients matrix **β** is given as:

$$\hat{\boldsymbol{\beta}} = (\mathbf{X}^{\mathbf{T}}\mathbf{X})^{-1}\,\mathbf{X}^{\mathbf{T}}\mathbf{y} \quad \text{..... (6.24)}$$

Where the superscripts T and -1 stand for transpose and inverse respectively. The fitted regression model is given as:

$$\hat{y}_i = \hat{\beta}_0 + \sum_{j=1}^{k} \hat{\beta}_j x_{ij} \qquad i = 1,2,...,n \quad \text{..... (6.25)}$$

Or $\hat{\mathbf{y}} = \mathbf{X}\hat{\boldsymbol{\beta}}$ in matrix notation.

From Eq. 6.25 note that there are $p = k + 1$ normal equations in $p = k + 1$ unknowns or parameters (ie the values of ($\hat{\beta}_0, \hat{\beta}_1, ..., \hat{\beta}_k$). Also the matrix $\mathbf{X}^{\mathbf{T}}\mathbf{X}$ is always non-singular with p x p dimension.

In multiple linear regression, the residual is defined as the difference between the observation y_i and the fitted value $\hat{y}_i$. That is: $e_i = y_i - \hat{y}_i$. The (n x 1) vector of residuals is defined as:

$$\mathbf{e} = \mathbf{y} - \hat{\mathbf{y}} \quad \text{..... (6.26)}$$

Calculations involving matrix operations are often very rigorous and are best done using a computer program. For this reason, I will only present results obtained using my *FluidStats* program later.

6.5.3 Check for Model Adequacy

The coefficient of multiple determination R^2 is vital for estimating the fit of a model. It is calculated as,[27]:

$$R^2 = \frac{SS_R}{SS_T} = 1 - \frac{SS_E}{SS_T} \quad \text{..... (6.27)}$$

Where SS_R is the regression sum of squares defined as:

$$SS_R = \hat{\beta}^T X^T y - \frac{\left(\sum_{i=1}^{n} y_i\right)^2}{n} \quad \text{..... (6.28)}$$

The total and error sums of squares are given as:

$$SS_T = y^T y - \frac{\left(\sum_{i=1}^{n} y_i\right)^2}{n} \quad \text{..... (6.29)}$$

$$SS_E = SS_T - SS_R \quad \text{..... (6.30)}$$

It is also important to estimate σ^2, which is the variance of the error term ε, in the multiple linear regression model. The unbiased estimator of σ^2 is defined as:

$$\hat{\sigma}^2 = \frac{\sum_{i=1}^{n} e_i^2}{n-p} = \frac{SS_E}{n-p} \quad \text{..... (6.31)}$$

This is the same expression used for the error mean square (MS_E) which is defined as the error or residual sum of squares, SS_E divided by the error degrees of freedom, $n - p$.

To better investigate the usefulness of adding more variables to a model, many regression users prefer to use an adjusted R^2 statistic:

$$R^2_{adj} = 1 - \frac{SS_E/(n-p)}{SS_T/(n-1)} \quad \text{..... (6.32)}$$

From Eq. 6.32, $SS_E/(n-p)$ is the error mean square and $SS_T/(n-1)$ is a constant. Hence R^2_{adj} will only increase when a variable that reduces the error mean square is added to the model.

The criterion for selecting the best model from a set of options is to choose the one with the highest R^2 value but lowest MS_E. I will now discuss the results from the *FluidStats* program.

6.6 THE *FluidStats* PROGRAM

I developed the *FluidStats* program to facilitate the statistical analyses of the effects of temperature and pressure on the rhelogical properties of drilling fluids. *FluidStats* is a Visual Basic two-factor factorial analyzer and modeling software. It is user-friendly and very handy for manipulating large factorial data. Other features include:

- Performs ANOVA, hypothesis testing and analysis of residuals calculations at the click of a button for up to 3 sets of 10 by 10 data size.
- Flexibility to implement any of: Fixed-, Random- and Mixed-Effects Models.
- Inbuilt F-distribution and normal probability plotting capability.
- Adequate for analyzing any other two-factor factorial experiment.
- Modeling capability using multiple linear regression technique.
- Enables 2- and 3-parameter model options.
- In-built input error checks and controls.

The *FluidStats* program is presented here to show the ease with which these calculations can be done and its potential to be used for the analyses of other two-factor factorial experiments. It is not intended to be a substitute to other more elaborate, statistical programs like SAS or Minitab. Suffice to say results obtained with the *FluidStats* program are accurate and have been validated with results from SAS. The Visual Basic code of the *FluidStats* program is listed in Appendix B.

6.6.1 Two-Factor Factorial Analysis Results

To demonstrate the ANOVA and hypothesis testing concepts explained earlier, data from Tables 5.2 and 5.3 are entered into the *FluidStats* program. We now proceed to

show a summary of the ANOVA table and test of hypothesis of the Fluid Type-B data. **Fig. 6.5** shows the ANOVA and hypothesis result tables.

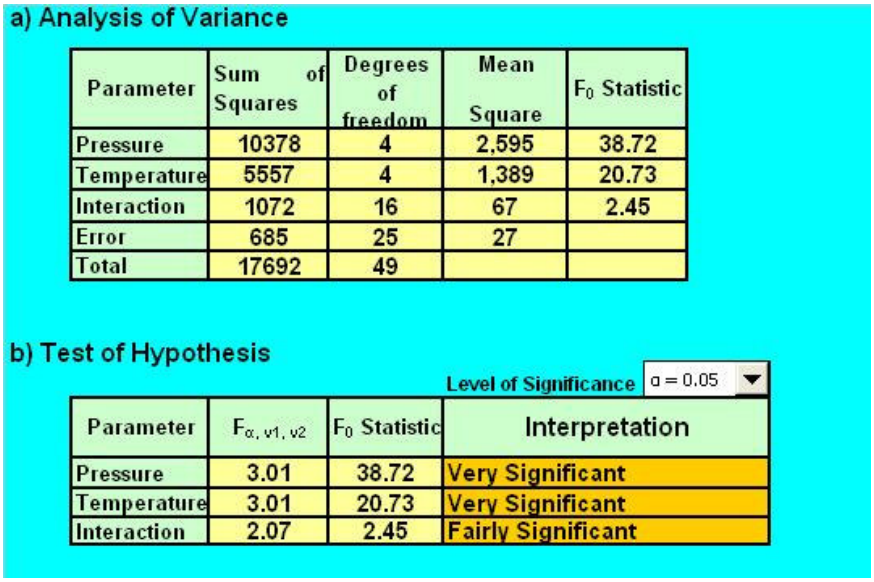

a) Analysis of Variance

Parameter	Sum of Squares	Degrees of freedom	Mean Square	F_0 Statistic
Pressure	10378	4	2,595	38.72
Temperature	5557	4	1,389	20.73
Interaction	1072	16	67	2.45
Error	685	25	27	
Total	17692	49		

b) Test of Hypothesis

Level of Significance α = 0.05

Parameter	$F_{\alpha, v1, v2}$	F_0 Statistic	Interpretation
Pressure	3.01	38.72	Very Significant
Temperature	3.01	20.73	Very Significant
Interaction	2.07	2.45	Fairly Significant

Fig. 6.5–ANOVA table from *FluidStats* Program

By design, the program allows the user to specify five (5) levels of significance (i.e. $\alpha = 0.01, 0.025, 0.05, 0.10,$ and 0.25. After every run, the interpretation column displays either of three (3) pre-programmed categories of significance. Conditions for these categories are defined as follows:

- **Very Significant**: When the F_0 test statistic is greater than 1.5 times the $f_{\alpha,v1,v2}$ calculated from the F-distribution table.
- **Fairly Significant**: When $f_{\alpha,v1,v2} < F_0$ statistic $< 1.5\, f_{\alpha,v1,v2}$
- **Not Significant**: When the F_0 test statistic is less than the $f_{\alpha,v1,v2}$ calculated from the F-distribution table.

This information is very necessary in deciding which parameter or effects should be included or ignored in adequately fitting a multiple linear regression. **Fig. 6.6** is a full screen print out of the two-factor factorial analysis window of the *FluidStats* program.

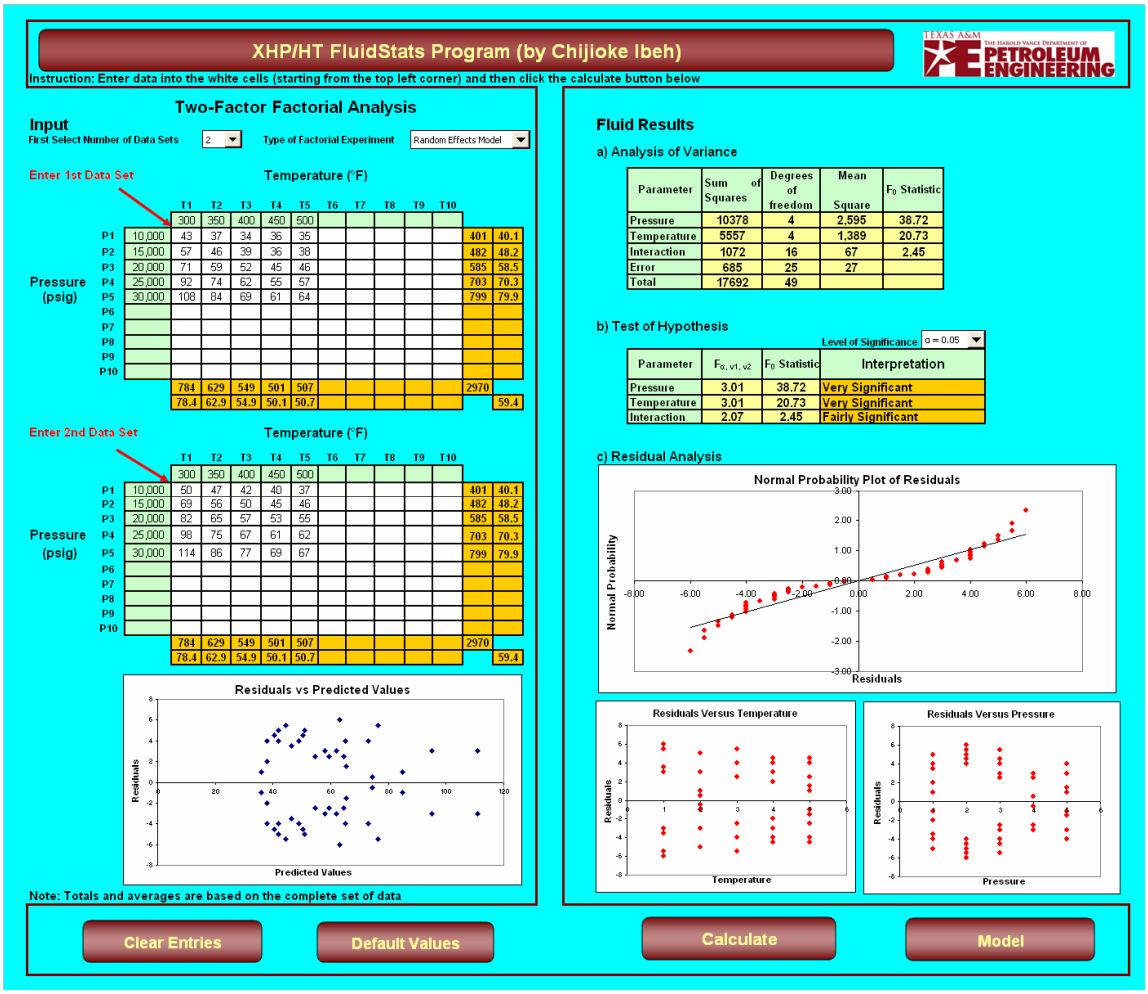

Fig. 6.6–Two-factor factorial analysis using the *FluidStats* program

From the results above we conclude as before that:

- For $\alpha = 0.05$, level of significance (ie $100(1-\alpha) = 95\%$ confidence level), the main effects of temperature and pressure on the plastic viscosity of the Fluid Type-B (18.0ppg, 93/7) formulation is very significant. Though the interaction effect is fairly significant.
- When we choose a higher confidence level say 99% (or $\alpha = 0.01$) we notice that the interaction effect becomes insignificant.

6.6.2 Multiple Linear Regression Results

Four types of models (algebraic, logarithmic, exponential and polynomial) where considered in developing the multiple regression code in the *FluidStats* program. Generally the response (e.g. plastic viscosity, yield point) has direct and inverse relationship with pressure and temperature respectively. This is in line with the concept of exclusive pressure or temperature effect on rheology as discussed earlier. **Fig. 6.7** shows the results of the four models using the mean response from the factorial data sets. The predicted response is a mathematical expression involving pressure, temperature and interaction terms together with their coefficients and an intercept.

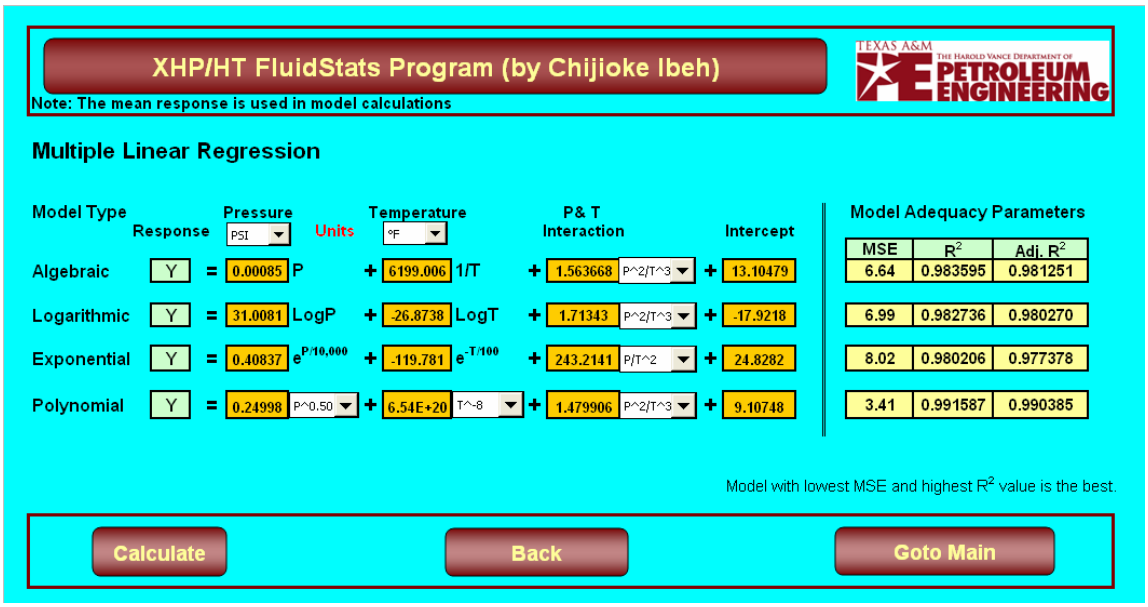

Fig. 6.7–Multiple linear regression using the *FluidStats* program

Thus the polynomial model is selected as the best because it has the lowest *MSE* value of 3.41 and highest R^2 value of 0.991587. An R^2 value of 0.991587 means that the model represents at least 99% of the data which is desirable. The model is written as:

$$PV = 9.10748 + 0.24998P^{0.5} + 6.54\times10^{20}T^{-8} + 1.479906P^{2}T^{-3} \quad \text{..... (6.33)}$$

Plastic viscosity is in cP, pressure in psig and temperature in °F. Note that Eq. 6.33 is only valid for pressure and temperature ranging from 10,000- to 30,000-psig and 300- to 500°F respectively.

To validate the results above, a separate run was made using SAS, a well-known commercial statistical analysis software. The results are given in **Table 6.6**. The number of observations used is 25, the same as the number of mean responses from the plastic viscosity data. As expected, all the results (circled) are the same as those obtained with the *FluidStats* program.

Table 6.6–Multiple linear regression using SAS program

SAS Output – Polynomial Model of Plastic Viscosity Data

The REG Procedure
Model: MODEL1
Dependent Variable: y Plastic Viscosity

Number of Observations Read	25
Number of Observations Used	25

Analysis of Variance

Source	DF	Sum of Squares	Mean Square	F Value	Pr > F
Model	3	8431.96253	2810.65418	825.07	<.0001
Error	21	71.53747	3.40655		
Corrected Total	24	8503.50000			

Root MSE	1.84568	R-Square	0.9916
Dependent Mean	59.40000	Adj R-Sq	0.9904
Coeff Var	3.10721		

Parameter Estimates

Variable	Label	DF	Parameter Estimate	Standard Error	t Value	Pr > |t|	Variance Inflation
Intercept	Intercept	1	9.10748	3.24410	2.81	0.0106	0
x3	P^0.5	1	0.24998	0.02622	9.53	<.0001	3.36619
x4	T^-8	1	6.541974E20	1.085407E20	6.03	<.0001	2.72267
x5	P^2/T^3	1	1.47991	0.10729	13.79	<.0001	5.08886

CHAPTER VII

CONCLUSIONS AND RECOMMENDATIONS

7.1 CONCLUSIONS

To say the least, this research effort has led to a better appreciation of the great impact extreme pressure and temperature could have on the rheology of an oil-based drilling fluid. Based on the results of the experiments contained in this report, the following conclusions are pertinent:

1. An effective method for quantitatively estimating the effects of temperature and pressure on the rheological properties of drilling fluids has been developed.
2. I have developed a useful statistical tool (called the *FluidStats* program) that is quick, easy to use and accurate for analyzing and modeling factorial experimental data. It is designed to be a handy tool for the drilling fluids design engineer.
3. A truly representative polynomial model has been developed for Fluid Type-B using the *FluidStats* program. The model relates plastic viscosity to pressure and temperature from 10,000 to 30,000 psig and 300 to 500°F respectively.
4. Proper evaluation of the pressure-temperature interaction effect on the rheology of a fluid is vital to achieving a good model fit.
5. All experimental data on Fluid types A and B suggest a linear relationship between pressure and viscosity while that of temperature is exponential.
6. The effects of temperature on viscosity of the oil-based fluids have been observed to be dominant at higher pressures. (>20,000 psig) while pressure effects prevail at lower temperatures (<350°F).
7. An active factor is more influential in determining the responses in a factorial experiment. For instance when pressure is increased at constant temperature, the viscosity obtained is higher than that at constant pressure and varying temperature.
8. It has been shown that thermal degradation occurs faster at low pressures (<10,000 psig) than at higher pressures given the same shear history.

9. Accurate determination of the thermal breakpoint of a fluid is very important in predicting its rheological behavior. The thermal breakpoints for Fluid Types-A and B were found to be 425°F and 450°F respectively.
10. Results from Pilot Tests 2 and 4 indicate that a variation in shear rate over time results in a net reduction in the apparent viscosity of Fluid Type-A.
11. The oil-based fluid formulation with manganese tetroxide as weighting agent has been shown to have better thermal stability and lower rheology (up to 600°F) than the barite-weighted OBM.
12. Fluid Type-B constant shear rate experiments data converge at 600°F. This implies that irrespective of the prevailing pressure, the fluid behavior is similar at 600°F. In other words, pressure has little effect at 600°F. As stated earlier, the effect of pressure is strongest at low temperature. For $\alpha = 0.05$, level of significance (ie $100(1-\alpha) = 95\%$ confidence level), the main and interaction effects of temperature and pressure on the plastic viscosity of the Fluid Type-B formulation is significant. At a higher confidence level (say 99% or $\alpha = 0.01$) we notice that the interaction effect becomes insignificant.
13. There is a close match between the Fann-35 and XHP/HT viscometer readings obtained during initial rheology checks at 150°F and ambient pressure. Generally the XHP/HT viscometer dial readings were within ±5% from those of the Fann-35.

7.2 RECOMMENDATIONS

1. Other XHP/HT fluid types (WBM, synthetic fluids, formate brines e.t.c) and property variations (density, oil/water ratio, weighting agent, viscosifiers e.t.c) should be investigated using the methodology presented in this report.
2. A cooling system should be installed in the XHP/HT viscometer for better temperature control.
3. Consider other better sealing methods as the present seal configuration seems to be ineffective beyond 450°F.

4. For future factorial experimentation, it is desirable to obtain all the test samples from the same fluid batch to minimize bias. Barite sag and fluid thickening also need to be addressed.
5. Measurements could not be made at low temperatures (<300°F) and high pressures (>25,000 psig) because with the F1 spring, the dial spins fully (>300 deg) at these conditions. A different spring type should be considered for future measurements in these situations.

As we drill into the future, all components of the drilling process (drilling fluids, logging tools, BOP and other rig equipment) have to be upgraded to withstand XHP/HT conditions else the effort put into formulating an XHP/HT drilling fluid will be of little benefit.

NOMENCLATURE

Abbreviations

AIME	American Institute of Mining, Metallurgical and Petroleum Engineers
ANN	Artificial Neural Network
ANOVA	Analysis of Variance
API	American Petroleum Institute
ASTM	American Society for Testing and Materials
BHDF	Baker Hughes Drilling Fluids
BHP	Bottom Hole Pressure
BHT	Bottom Hole Temperature
BML	Below Mud Line
BOPE	Blow-Out Prevention Equipment
ECD	Equivalent Circulating Density
ES	Electric Stability
GOM	Gulf of Mexico
HP/HT	High Pressure-High Temperature
HSE	Health Safety and Environment
LWD	Logging While Drilling
MASP	Maximum Anticipated Surface Pressure
MMS	Minerals Management Service
MMscf	Million standard cubic feet
MSDS	Material Safety and Data Sheet
MWD	Measuring While Drilling
OBM	Oil-Based Mud
P	Pressure
PDC	Polycrystalline Diamond Compact
PV	Plastic Viscosity

RPM	Revolutions Per Minute
SAE	Society of Automotive Engineers
SAS	Statistical Analysis Software
SG	Specific Gravity
SITP	Shut-in Tubing Pressure
TAMU	Texas A&M University
T	Temperature
Tcf	Trillion Cubic Feet
YP	Yield Point
WBM	Water-Based Mud
XHP/HT	Extreme High-Pressure, High Temperature

Greek Letters

μ, η	fluid viscosity (cP)
μ_p	plastic viscosity (cP)
η_0	viscosity at zero shear (cP)
v	kinematic viscosity (cSt)
ρ	fluid density (ppg)
τ_y, τ_0	yield stress (dynes/cm^2)
γ	shear rate (sec^{-1})
λ	time index
θ	angular deviation (deg)
θ_{600}	600RPM dial reading
θ_{300}	300RPM dial reading
v_i	velocity in *i*-coordinate direction (m/s)
ω, Ω	angular velocity (rad/sec)

Statistical Parameters

A	factor A, Pressure
B	factor B, Temperature
a	number of levels of factor A
b	number of levels of factor B
n	number of data replicates (in factorial data analyses)
	number of observations (in modeling)
k	number of regressor variables
p	number of parameters ($p = k + 1$)
μ	sample mean
σ^2	variance
τ_i	effects of factor A at various i levels
β_j	effects of factor B at various j levels
$\boldsymbol{\beta}$	vector of regression coefficients
$\hat{\boldsymbol{\beta}}$	least squares estimate of $\boldsymbol{\beta}$
$(\tau\beta)_{ij}$	interaction effects of factors A and B
ε_{ijk}	random error component
$\boldsymbol{\varepsilon}$	random error vector
e_{ijk}	residual of factorial data
e_i	residual of fitted model
R^2	coefficient of multiple determination
R^2_{adj}	adjusted R^2
$\mathbf{X}$	matrix of the levels of independent variables
y_{ijk}	individual observation (response)
$y_{i..}$	total of the observations taken at the ith level of factor A
$y_{.j.}$	total of the observations taken at the jth level of factor B
$y_{ij.}$	total of the observations in the ijth cell

$\bar{y}_{i\ldots}$, $\bar{y}_{.j.}$, $\bar{y}_{ij.}$	row and column averages
$y\ldots$	grand total
$\bar{y}\ldots$	grand average
$\hat{\mathbf{y}}$	response vector
$\mathbf{y}$	least square estimate of $\mathbf{y}$
SS_A	sum of squares for the row factor A
SS_B	sum of squares for the row factor B
SS_{AB}	sum of squares for the interaction between A and B
SS_E	error sum of squares
SS_R	regression sum of squares
MS_A	mean square for the row factor A
MS_B	mean square for the row factor B
MS_{AB}	mean square for the interaction between A and B
MS_E	error mean squares
F_A	F-ratio for the row factor A
F_B	F-ratio square for the row factor B
F_{AB}	F-ratio for the interaction between A and B
F_0	F-statistic
H_0	null hypothesis
H_1	alternative hypothesis

Subscripts

A	factor A, Pressure
B	factor B, Temperature
AB	factors A & B interaction
i	range from 1 to a
j	range from 1 to b
k	range from 1 to n

Other Symbols

k	consistency index
L	bob height (cm)
M	torque on Bob shaft (dyne-cm)
n	flow behavior index
r	radial distance from centerline (cm)
R_i	bob Radius (cm)
R_o	rotor Radius (cm)
u	average flow velocity, ft/s
N_{re}	Reynolds Number
D	diameter of the flow channel (in)

REFERENCES

1. Bartlett, L.E.: "Effects of Temperature on the Flow Properties of Drilling Fluids," paper SPE 1861 presented at the 1967 SPE Annual Meeting of AIME, Houston, Texas, 1-4 October.

2. Casson, N.: "A Flow Equation for Pigment-oil Suspensions of the Printing Ink Type," *Rheology of Disperse Systems*, Mill C.C (ed.), Pergamon, London (1959) 84.

3. Karstad, E. and Aadnoy, B.: "Analysis of Temperature Measurements during Drilling," paper SPE 38603 presented at the 1997 SPE Annual Technical Conference and Exhibition, San Antonio, Texas, 5-8 October.

4. DeepStar CTR 7501 Drilling and Completion Gaps for HPHT Wells in Deep Water Final Report. Mineral Management Service, www.mms.gov/tarprojects/519/HPHTGaps-FinalReport.pdf, Downloaded 4 March 2007.

5. Alderman, N.J. Gavignet, A. Guillot, D. and Maitland, G.C.: "High-Temperature, High-Pressure Rheology of Water-Based Muds," paper SPE 18035 presented at the 1988 SPE Annual Technical Conference and Exhibition, Houston, Texas, 2-5 October.

6. Combs, G.D. and Whitemire, L.D.: "Capillary Viscometer Simulates Bottom-Hole Conditions," *Oil & Gas Journal* (September 1968) 108-113.

7. McMordie, W.C., Bennet, R.B., and Bland, R.G., "The Effect of Temperature and Pressure on the Viscosity of Oil-Base Muds," *Journal of Petroleum Technology* (July 1975) 884-886.

8. De Wolf, R.C., Coffin, G.B., and Byrd, R.V.: "Effects of Temperature and Pressure on Rheology of less Toxic Oil Muds," paper SPE 11892 presented at the 1983 Offshore Europe Conference, Aberdeen, 6-9 September.

9. Houwen, O.H.: "Rheology of Oil-Based Muds," paper SPE 15416 presented at the 1986 SPE Annual Technical Conference and Exhibition, New Orleans, 5-8 October.

10. Babu, D.R.: "Effects of p-ρ-T Behavior of Muds on Static Pressures during Deep Well Drilling," paper SPE 27419 presented at the 1996 SPE Drilling and Completions Conference, 24 January.

11. Karstad, E. and Aadnoy, B.: "Density Behavior of Drilling Fluids during High Pressure High Temperature Drilling Operations," paper SPE 47806 presented at the 1998 SPE Drilling Technology Conference, Jakarta, Indonesia, 7-8 September.

12. Osman, E.A. and Aggour, M.A.: "Determination of Drilling Mud Density Change with Pressure and Temperature Made Simple and Accurate by ANN," paper SPE 81422 presented at the 2003 SPE Middle East Oil Show and Conference, Bahrain, 5-8 April.

13. Downs, J.D. Blaszczynski, M. Turner, J. and Harris. M.: "Drilling and Completing Difficult HPHT Wells with the Aid of Cesium Formate Brines – A Performance Review," paper IADC/SPE 99068 presented at the 2006 IADC/SPE Drilling Conference, Miami, Florida, 21-23 February.

14. Viscosity. Transtronics, http://xtronics.com/reference/viscosity.htm. Downloaded 10 May 2007.

15. Rheological Models. Schlumberger, http://www.glossary.oilfield.slb.com/. Downloaded 2 July 2007.

16. Ayeni, K.: "Drilling Fluid Hydraulic Simulator with Emphasis on Rheological Models," MS thesis, Oklahoma U., Norman, Oklahoma (2003).

17. Weidner, D.E. and Schwartz, L.W.: "Contact-line motion of shear thinning liquids," *Physical Fluids* (November 1994), **No. 6, 11**

18. *Rheology Technical Bulletin*, Kelco Oilfield Group, Monsanto Company Publication, (1996) **1-15**.

19. Lummus, J.L. and Azar, J.J.: *Drilling Fluids Optimization: A Practical Field Approach*, Pennwell Corporation, Tulsa, Oklahoma (December 1986).

20. Moore, P. L.: *Drilling Practices Manual*, The Petroleum Publishing Company, Tulsa, Oklahoma (1974).

21. Marsh Funnel. Schlumberger, http://www.glossary.oilfield.slb.com/search.cfm. Downloaded 21 July 2007.

22. Viscosity. Wikipedia, http://en.wikipedia.org/wiki/Viscosity. Downloaded 7 August 2007.

23. Macosko, C.W.: *Rheology: Principles, Measurements, and Applications*, New York City (1994)

24. Gusler, W., Pless, M., Maxey, J., Grover, and P., Perez, J.: "A New Extreme-HP/HT Viscometer for New Drilling Fluid Challenges," paper SPE 99009 presented at the 2006 IADC/SPE Drilling Conference, Miami, Florida, 21-23 February.

25. HPHT Viscometer, Chandler Engineering, Ametek, http://www.chandlereng.com/products/drilingfluids.cfm. Downloaded 10 August 2007.

26. Montgomery, D.C.: *Design and Analysis of Experiments*, third edition, John Wiley & Sons, New York City (1991).

27. Montgomery, D.C. and Runger, G.C.: *Applied Statistics and Probability for Engineers*, third edition, John Wiley & Sons, New York City (2003).

APPENDIX A

FLUID TYPE B BATCH INFORMATION

Initial Rheology Check Data for Batch #1 (T1 to T11)

	Chandler Model 7600 XHP/HT Viscometer Dial Readings										
RPM	***T1***	***T2***	***T3***	***T4***	***T5***	***T6***	***T7***	***T8***	***T9***	***T10***	***T11***
600	125	130	131	130	135	135	133	139	130	136	139
300	70	75	75	74	77	77	76	80	75	79	80
200	53	56	57	56	57	57	56	60	56	59	60
100	33	36	36	35	36	36	36	39	36	38	38
6	10	12	11	11	11	10	11	12	11	11	10
3	9	11	11	10	10	9	10	11	10	10	9
Gels 10s/10m	10/26	13/29	11/30	11/30	12/31	10/34	13/30	11/39	11/33	11/38	10/38
PV	55	55	56	56	58	58	57	59	55	57	59
YP	15	20	19	18	19	19	19	21	20	22	21

	Fann 35 Viscometer Dial Readings										
RPM	***T1***	***T2***	***T3***	***T4***	***T5***	***T6***	***T7***	***T8***	***T9***	***T10***	***T11***
600	130	134	136	141	139	136	144	138	143	148	143
300	74	75	75	79	78	77	81	79	81	83	81
200	52	55	53	57	57	57	61	57	59	60	59
100	31	34	31	33	34	34	36	35	36	36	36
6	8	8	7	7	8	8	9	8	9	8	8
3	6	6	5	5	6	6	6	6	7	6	6
Gels 10s/10m	8/17	9/22	7/15	7/14	8/16	8/25	9/25	8/24	11/29	9/16	8/21
PV	57	59	61	62	61	59	63	60	63	65	63
YP	17	16	14	18	17	18	18	19	18	18	18

Initial Rheology Check Data for Batch #2 (T12 to T17)

	Chandler XHP/HT Viscometer Data					
RPM	T12	T13	T14	T15	T16	T17
600	154	153	157	156	154	161
300	89	90	92	90	90	93
200	66	68	69	67	67	69
100	42	43	44	43	42	43
6	13	13	13	13	12	12
3	11	11	11	11	11	10
Gels 10s/10m	12/32	14/34	12/37	15/35	12/35	12/35
PV	65	63	65	66	64	68
YP	24	27	27	24	26	25

	Fann 35 Viscometer Dial Readings					
RPM	T12	T13	T14	T15	T16	T17
600	154	156	158	152	152	160
300	84	86	91	88	88	92
200	61	62	66	65	65	67
100	36	37	40	40	40	41
6	7	8	9	9	9	9
3	5	6	7	7	7	8
Gels 10s/10m	8/16	9/16	10/19	10/24	10/24	11/21
PV	70	70	67	64	64	68
YP	14	16	24	24	24	24

Initial Rheology Check Data for Batch #3 (T18 to T28)

	Chandler Model 7600 XHP/HT Viscometer Dial Readings										
RPM	T18	T19	T20	T21	T22	T23	T24	T25	T26	T27	T28
600	148	150	150	153	157	158	148	155	160	152	159
300	86	86	86	88	91	91	84	86	89	87	92
200	64	65	65	65	68	67	62	64	66	65	68
100	41	41	41	42	42	42	38	39	40	40	42
6	13	13	13	13	13	13	11	10	10	11	11
3	12	11	11	12	11	11	9	8	8	8	9
Gels 10s/10m	14/34	14/30	12/32	14/33	14/22	13/22	11/20	10/19	11/16	11/17	11/16
PV	62	64	64	65	66	67	64	69	71	65	67
YP	24	22	22	23	25	24	20	17	18	22	25

	Fann 35 Viscometer Initial Dial Readings										
RPM	T18	T19	T20	T21	T22	T23	T24	T25	T26	T27	T28
600	158	151	149	157	147	156	154	157	159	159	176
300	92	85	86	91	85	89	87	90	92	92	103
200	68	63	63	68	62	65	64	67	68	68	76
100	42	38	39	43	38	40	40	42	42	42	48
6	11	9	9	11	10	10	10	11	11	11	12
3	9	7	8	10	8	8	8	9	9	9	10
Gels 10s/10m	11/26	9/17	10/21	12/26	11/18	10/18	10/18	11/18	11/19	11/19	12/19
PV	66	66	63	66	62	67	67	67	67	67	73
YP	26	19	23	25	23	22	20	23	25	25	30

Initial Rheology Check Data for Batch #4 (T29 to T32)

	Chandler XHP/HT Viscometer Data			
RPM	T29	T30	T31	T32
600	128	124	134	133
300	78	74	79	80
200	60	57	61	61
100	40	37	40	40
6	13	11	13	13
3	11	9	11	11
Gels 10s/10m	16/30	14/28	13/34	16/32
PV	50	50	55	53
YP	28	24	24	27

	Fann 35 Viscometer Data			
RPM	T29	T30	T31	T32
600	144	134	143	145
300	86	80	86	88
200	66	60	67	66
100	43	39	44	43
6	13	11	12	12
3	11	9	10	10
Gels 10s/10m	14/26	11/25	13/29	14/25
PV	58	54	57	57
YP	28	26	29	31

APPENDIX B

VISUAL BASIC CODE OF THE FLUIDSTATS PROGRAM

```
'Dimension Variables
Public Ftype, Nrep, Ysums, Ybars, Ysmj, Ysmi, Ysuma, Ysumb, Yav, P4, T4, alpha, beta As Double
Public Y(100, 100, 100), Resid(1000), Pred(1000), Ysumi(100), Ysumj(100), T(1000), P(1000) As Variant
Public Ysumk(100, 100), Ybari(100), Ybarj(100), Yave(1000), Temp(1000), Press(1000), PT(1000) As Variant
Public Ysq, Yssa, Yssb, Yssab, SST, SSA, SSB, SSAB, SSE, DFA, DFB, DFAB, DFE, DFT As Double
Public MSA, MSB, MSAB, MSE, FA, FB, FAB, LS, FATest, FBTest, FABTest, alpha1 As Double
Public B10, B11, B12, B13, B20, B21, B22, B23, B30, B31, B32, B33, B40, B41, B42, B43 As Double
Public SSE1, SSR1, SST1, SSE2, SSR2, SST2, SSE3, SSR3, SST3, SSE4, SSR4, SST4, pp As Double
Public MSE1, MSE2, MSE3, MSE4, R1, R2, R3, R4, aR1, aR2, aR3, aR4, PT1, PT2, PT3, PT4 As Double
Public i, j, k, a, b, n, en, m, Counta, Countb As Integer
Public Msg, Style, Title, Help, Ctxt, Response, MyString As String


Sub Master() 'Input Data, Validation & Calculations'

    'Clear Screen
    Worksheets("FDist").Range(" B3:D5").ClearContents
    Worksheets("Plot Data").Range(" B2:C1000, E2:K1000").ClearContents
    Worksheets("Main").Range(" O15:P26, E25:N26, V14:Y18,V25:Z27").ClearContents
    Worksheets("Main2").Range(" O15:P26, E25:N26, O32:P43,E42:N43, V14:Y18,V25:Z27").ClearContents
    Worksheets("Main3").Range(" O15:P26, E25:N26, O32:P43,E42:N43,O48:P59,E58:N59, V14:Y18,V25:Z27").ClearContents

    'Input Variables

    'Type of Experiments and number of replicates
    Ftype = Cells(8, 15)                    'Factorial Experiment type
    Nrep = Cells(8, 6)                      'Number of Replicates
```

```
   If Nrep = 1 Then n = 1: GoTo 10
   If Nrep = 2 Then n = 2: GoTo 20
   If Nrep = 3 Then n = 3: GoTo 30

10  'Call ClearSheet1
   With ThisWorkbook.Worksheets("Main") 'Case I: No replicates (ie only one set of
data)
   Counta = 100: Countb = 100

   'Count total Data rows and columns (ie determine the values of a and b)
   For i = 1 To Counta
   If .Cells(14 + i, 5) = 0 Then GoTo 1
   Next i
1   Counta = i - 1
   For j = 1 To Countb
   If .Cells(15, 4 + j) = 0 Then GoTo 2
   Next j
2   Countb = j - 1
   i = 0: j = 0: k = 0
   Call Initial_Calculations
   Call ANOVA
   End With: GoTo 40

20  'Call ClearSheet2
   With ThisWorkbook.Worksheets("Main2") 'Case II: Two replicates (ie two sets of
data)
   Counta = 100: Countb = 100
   'Count total Data rows and columns (ie determine the values of a and b)
   For i = 1 To Counta
   If .Cells(14 + i, 5) = 0 Then GoTo 3
   Next i
3   Counta = i - 1
   For j = 1 To Countb
   If .Cells(15, 4 + j) = 0 Then GoTo 4
   Next j
4   Countb = j - 1
   i = 0: j = 0: k = 0
   Call Initial_Calculations
   Call ANOVA
   End With
   Call Hypothesis: GoTo 40

30  'Call ClearSheet3
```

```
With ThisWorkbook.Worksheets("Main3") 'Case III: Three replicates (ie 3 sets of data)

Counta = 100: Countb = 100
'Count total Data rows and columns (ie determine the values of a and b)
For i = 1 To Counta
If .Cells(14 + i, 5) = 0 Then GoTo 5
Next i
5  Counta = i - 1
For j = 1 To Countb
If .Cells(15, 4 + j) = 0 Then GoTo 6
Next j
6  Countb = j - 1
i = 0: j = 0: k = 0
Call Initial_Calculations
Call ANOVA
End With
Call Hypothesis
40
Call Display_Results
Call Residuals
End Sub
```

Sub Initial_Calculations()

```
'Input First Set of Data
a = Counta: b = Countb
alpha1 = a: beta = b
Call Error_Check  'Error Check / Data Validation
For i = 1 To a
For j = 1 To b
For k = 1 To n
If k = 1 Then Y(i, j, k) = Cells(14 + i, 4 + j)
If k = 2 Then Y(i, j, k) = Cells(31 + i, 4 + j)
If k = 3 Then Y(i, j, k) = Cells(47 + i, 4 + j)
alpha1 = Y(i, j, k)
Call Error_Check   'Error Check / Data Validation
Next k
Next j
Next i

'Estimate Totals and Averages for factor A - Pressure
For i = 1 To a
Ysmi = 0
```

```
For j = 1 To b
Ysuma = 0
For k = 1 To n
Ysuma = Y(i, j, k) + Ysuma
Next k
Ysumk(i, j) = Ysuma
Ysmi = Ysumk(i, j) + Ysmi
Next j
Ysumi(i) = Ysmi
Ybari(i) = Ysumi(i) / (b * n)
Next i

'Estimate Totals and Averages for factor B - Temperature
For j = 1 To b
Ysmj = 0
For i = 1 To a
Ysumb = 0
For k = 1 To n
Ysumb = Y(i, j, k) + Ysumb
Next k
Ysumk(i, j) = Ysumb
Ysmj = Ysumk(i, j) + Ysmj
Next i
Ysumj(j) = Ysmj
Ybarj(j) = Ysumj(j) / (b * n)
Next j

'Estimate Global Totals and Averages
Ysums = 0: Ybars = 0
For i = 1 To a
For j = 1 To b
For k = 1 To n
Ysums = Y(i, j, k) + Ysums
Next k
Next j
Next i
Ybars = Ysums / (a * b * n)
End Sub

Sub ANOVA()

'ANALYSIS OF VARIANCE CALCULATIONS

'Calculate Total Sum of Squares (SST)
```

```
Ysq = 0
For i = 1 To a
For j = 1 To b
For k = 1 To n
Ysq = Y(i, j, k) ^ 2 + Ysq
Next k
Next j
Next i
SST = Ysq - Ysums ^ 2 / (a * b * n)

'Calculate Sum of Squares for Factor A - Pressure (SSA)
Yssa = 0
For i = 1 To a
Yssa = Ysumi(i) ^ 2 + Yssa
Next i
SSA = Yssa / (b * n) - Ysums ^ 2 / (a * b * n)

'Calculate Sum of Squares for Factor B - Temperature (SSB)
Yssb = 0
For j = 1 To b
Yssb = Ysumj(j) ^ 2 + Yssb
Next j
SSB = Yssb / (a * n) - Ysums ^ 2 / (a * b * n)

'Calculate Sum of Squares for Interaction between A & B (SSAB)
Yssab = 0
For i = 1 To a
For j = 1 To b
Yssab = Ysumk(i, j) ^ 2 + Yssab
Next j
Next i
SSAB = Yssab / n - Ysums ^ 2 / (a * b * n) - SSA - SSB

'Calculate Sum of Squares for Error (SSE)
If n > 1 Then SSE = SST - SSA - SSB - SSAB Else SSE = SSAB: SSAB = 0

'Calculate Degrees of Freedom
DFA = a - 1              'Degrees of freedom for factor A
DFB = b - 1              'Degrees of freedom for factor B
If n > 1 Then DFAB = (a - 1) * (b - 1) Else DFAB = 0  'Degrees of freedom for A - B
Interaction
If n > 1 Then DFE = a * b * (n - 1) Else DFE = (a - 1) * (b - 1) 'Degrees of freedom
for Error
DFT = a * b * n - 1        'Total Degrees of freedom
```

```
    'Calculate Mean Squares
    MSA = SSA / DFA          'Mean Square for factor A
    MSB = SSB / DFB          'Mean Square for factor B
    If n > 1 Then MSAB = SSAB / DFAB Else MSAB = 0      'Mean Square for A & B
intercation
    MSE = SSE / DFE          'Mean Square for Error

    'Calculate F - Statistics
    If Ftype = 1 Then FA = MSA / MSE: FB = MSB / MSE        'F-statistic for Fixed
Effects Model
    If Ftype = 2 Then FA = MSA / MSAB: FB = MSB / MSAB      'F-statistic for Random
Effects Model
    If Ftype = 3 Then FA = MSA / MSAB: FB = MSB / MSE       'F-statistic for Random
Pressure and Fixed Temperature Model
    If Ftype = 4 Then FA = MSA / MSE: FB = MSB / MSAB       'F-statistic for Random
Temperature and Fixed Pressure Model
    If n > 1 Then FAB = MSAB / MSE Else FAB = 0             'F-statistic for A & B
interaction
    End Sub

Sub Hypothesis ()

  'TEST OF HYPOTHESIS

    'Determine level of significance
    LS = Cells(22, 26)
    If LS = 1 Then alpha = 0.25
    If LS = 2 Then alpha = 0.1
    If LS = 3 Then alpha = 0.05
    If LS = 4 Then alpha = 0.025
    If LS = 5 Then alpha = 0.01

    With ThisWorkbook.Worksheets("FDist")

    'Estimate F-statistics for Factor A (Pressure)
    .Cells(3, 2) = alpha
    .Cells(4, 2) = a - 1
    If Ftype = 1 Then .Cells(5, 2) = a * b * (n - 1)
    If Ftype = 3 Then .Cells(5, 2) = a * b * (n - 1)
    If Ftype = 2 Then .Cells(5, 2) = (a - 1) * (b - 1)
    If Ftype = 4 Then .Cells(5, 2) = (a - 1) * (b - 1)
    FATest = .Cells(6, 2)
```

```
'Estimate F-statistics for Factor B (Temperature)
.Cells(3, 3) = alpha
.Cells(4, 3) = b - 1
If Ftype = 1 Then .Cells(5, 3) = a * b * (n - 1)
If Ftype = 4 Then .Cells(5, 3) = a * b * (n - 1)
If Ftype = 2 Then .Cells(5, 3) = (a - 1) * (b - 1)
If Ftype = 3 Then .Cells(5, 3) = (a - 1) * (b - 1)
FBTest = .Cells(6, 3)

'Estimate F-statistics for Interaction between A & B
.Cells(3, 4) = alpha
.Cells(4, 4) = (a - 1) * (b - 1)
.Cells(5, 4) = a * b * (n - 1)
FABTest = .Cells(6, 4)
End With

'Interpretation
If FA > FATest And FA > 1.5 * FATest Then Cells(25, 24) = "Very Significant"
If FA > FATest And FA <= 1.5 * FATest Then Cells(25, 24) = "Fairly Significant"
If FA <= FATest Then Cells(25, 24) = "Not Significant"
If FB > FBTest And FB > 1.5 * FBTest Then Cells(26, 24) = "Very Significant"
If FB > FBTest And FB <= 1.5 * FBTest Then Cells(26, 24) = "Fairly Significant"
If FB <= FBTest Then Cells(26, 24) = "Not Significant"
If FAB > FABTest And FAB > 1.5 * FABTest Then Cells(27, 24) = "Very Significant"
If FAB > FABTest And FAB <= 1.5 * FABTest Then Cells(27, 24) = "Fairly Significant"
If FAB <= FABTest Then Cells(27, 24) = "Not Significant"
'Show Other Results
Cells(25, 22) = FATest: Cells(25, 23) = FA
Cells(26, 22) = FBTest: Cells(26, 23) = FB
Cells(27, 22) = FABTest: Cells(27, 23) = FAB

End Sub

Sub Display Results ()

If n = 2 Then GoTo 60
If n = 3 Then GoTo 70
50
With ThisWorkbook.Worksheets("Main")  'Case I: No replicates (ie only one set of data)
For i = 1 To a
For j = 1 To b
```

```
   .Cells(14 + i, 15) = Ysumi(i): .Cells(14 + i, 16) = Ybari(i)
   .Cells(25, 4 + j) = Ysumj(j): .Cells(26, 4 + j) = Ybarj(j)
   Next j
   Next i
   .Cells(25, 15) = Ysums
   .Cells(26, 16) = Ybars

   'ANOVA Results
   .Cells(14, 22) = SSA: .Cells(14, 23) = DFA: .Cells(14, 24) = MSA: .Cells(14, 25) =
FA
   .Cells(15, 22) = SSB: .Cells(15, 23) = DFB: .Cells(15, 24) = MSB: .Cells(15, 25) =
FB
   .Cells(16, 22) = SSAB: .Cells(16, 23) = DFAB: .Cells(16, 24) = MSAB: .Cells(16, 25)
= FAB
   .Cells(17, 22) = SSE: .Cells(17, 23) = DFE: .Cells(17, 24) = MSE
   .Cells(18, 22) = SST: .Cells(18, 23) = DFT
   End With: GoTo 80
60
With ThisWorkbook.Worksheets("Main2")  'Case II: One replicate (ie two sets of data)
   For i = 1 To a
   For j = 1 To b
   .Cells(14 + i, 15) = Ysumi(i): .Cells(14 + i, 16) = Ybari(i)
   .Cells(31 + i, 15) = Ysumi(i): .Cells(31 + i, 16) = Ybari(i)
   .Cells(25, 4 + j) = Ysumj(j): .Cells(26, 4 + j) = Ybarj(j)
   .Cells(42, 4 + j) = Ysumj(j): .Cells(43, 4 + j) = Ybarj(j)
   Next j
   Next i
   .Cells(25, 15) = Ysums: .Cells(42, 15) = Ysums
   .Cells(26, 16) = Ybars: .Cells(43, 16) = Ybars

   'ANOVA Results
   .Cells(14, 22) = SSA: .Cells(14, 23) = DFA: .Cells(14, 24) = MSA: .Cells(14, 25) =
FA
   .Cells(15, 22) = SSB: .Cells(15, 23) = DFB: .Cells(15, 24) = MSB: .Cells(15, 25) =
FB
   .Cells(16, 22) = SSAB: .Cells(16, 23) = DFAB: .Cells(16, 24) = MSAB: .Cells(16, 25)
= FAB
   .Cells(17, 22) = SSE: .Cells(17, 23) = DFE: .Cells(17, 24) = MSE
   .Cells(18, 22) = SST: .Cells(18, 23) = DFT
   End With: GoTo 80
70
   With ThisWorkbook.Worksheets("Main3")  'Case III: Three replicates (ie three sets of
data)
   For i = 1 To a
```

```
   For j = 1 To b
   .Cells(14 + i, 15) = Ysumi(i): .Cells(14 + i, 16) = Ybari(i)
   .Cells(31 + i, 15) = Ysumi(i): .Cells(31 + i, 16) = Ybari(i)
   .Cells(47 + i, 15) = Ysumi(i): .Cells(47 + i, 16) = Ybari(i)
   .Cells(25, 4 + j) = Ysumj(j): .Cells(26, 4 + j) = Ybarj(j)
   .Cells(42, 4 + j) = Ysumj(j): .Cells(43, 4 + j) = Ybarj(j)
   .Cells(58, 4 + j) = Ysumj(j): .Cells(59, 4 + j) = Ybarj(j)
   Next j
   Next i
   .Cells(25, 15) = Ysums: .Cells(42, 15) = Ysums: .Cells(58, 15) = Ysums
   .Cells(26, 16) = Ybars: .Cells(43, 16) = Ybars: .Cells(59, 16) = Ybars

   'ANOVA Results
   .Cells(14, 22) = SSA: .Cells(14, 23) = DFA: .Cells(14, 24) = MSA: .Cells(14, 25) =
FA
   .Cells(15, 22) = SSB: .Cells(15, 23) = DFB: .Cells(15, 24) = MSB: .Cells(15, 25) =
FB
   .Cells(16, 22) = SSAB: .Cells(16, 23) = DFAB: .Cells(16, 24) = MSAB: .Cells(16, 25)
= FAB
   .Cells(17, 22) = SSE: .Cells(17, 23) = DFE: .Cells(17, 24) = MSE
   .Cells(18, 22) = SST: .Cells(18, 23) = DFT
   End With
80
   End Sub
```

Sub Residuals()

```
   'Estimate Residuals for each block
   m = 0
   For i = 1 To a
   For j = 1 To b
   For k = 1 To n: m = m + 1
   Resid(m) = Y(i, j, k) - Ysumk(i, j) / n
   Pred(m) = Ysumk(i, j) / n
   Next k
   Next j
   Next i

   'Assign data cells in Plot Data and calculate normal probability
   With ThisWorkbook.Worksheets("Plot Data")
   For m = 1 To a * b * n
   .Cells(1 + m, 2) = Resid(m): .Cells(1 + m, 10) = Resid(m)
   .Cells(1 + m, 11) = Pred(m)
   .Cells(1 + m, 3) = (m - 0.5) / (a * b * n)
```

```
Next m


'Sort residuals in ascending order
Worksheets("Plot Data").Range("B2:B1000").Sort _
Key1:=Worksheets("Plot Data").Range("B2")

'Calculate Residuals versus Pressure Data
m = 0
For i = 1 To a
For j = 1 To b
For k = 1 To n: m = m + 1
.Cells(1 + m, 5) = Y(i, j, k) - Ysumk(i, j) / n
.Cells(1 + m, 6) = i
Next k
Next j
Next i

'Calculate Residuals versus Temperature Data
m = 0
For j = 1 To b
For i = 1 To a
For k = 1 To n: m = m + 1
.Cells(1 + m, 7) = Y(i, j, k) - Ysumk(i, j) / n
.Cells(1 + m, 8) = j
Next k
Next i
Next j
End With
End Sub

Sub Modeling()

'MULTIPLE LINEAR REGRESSION
pp = 4
If MyString = "Yes" Then GoTo 11
If MyString = "No" Then Call Model: GoTo 16
11
'Factorial Data Option

'Calculate and Assign Mean Responses to Corresponding Temperatures and
Pressures
If Nrep = 1 Then GoTo 12
If Nrep = 2 Then GoTo 13
```

```
   If Nrep = 3 Then GoTo 14
12
   With ThisWorkbook.Worksheets("Main")
   m = 0
   For i = 1 To a
   For j = 1 To b: m = m + 1
   Temp(m) = .Cells(14, 4 + j)
   Press(m) = .Cells(14 + i, 4)
   alpha1 = Press(m): beta = Temp(m)
   Call Level_Error   'Check factor levels data for error / completeness
   Next j
   Next i
   End With: en = a * b: GoTo 15
13
   With ThisWorkbook.Worksheets("Main2")
   m = 0
   For i = 1 To a
   For j = 1 To b: m = m + 1
   Temp(m) = .Cells(14, 4 + j)
   Press(m) = .Cells(14 + i, 4)
   alpha1 = Press(m): beta = Temp(m)
   Call Level_Error   'Check factor levels data for error / completeness
   Next j
   Next i
   End With: en = a * b: GoTo 15
14
   With ThisWorkbook.Worksheets("Main3")
   m = 0
   For i = 1 To a
   For j = 1 To b: m = m + 1
   Temp(m) = .Cells(14, 4 + j)
   Press(m) = .Cells(14 + i, 4)
   alpha1 = Press(m): beta = Temp(m)
   Call Level_Error   'Check factor levels data for error / completeness
   Next j
   Next i
   End With:  en = a * b

15
  'Initialize matrix table
   With ThisWorkbook.Worksheets("Matrix Operator")
   For j = 1 To 100
   .Cells(1 + j, 2) = 0: .Cells(1 + j, 3) = 0: .Cells(1 + j, 4) = 0: .Cells(1 + j, 5) = 0:
.Cells(1 + j, 108) = 0
```

```
    Next j


'Calculate Means Responses
    Yav = 0: m = 0
    For i = 1 To a
    For j = 1 To b: m = m + 1
    For k = 1 To n
    Yav = Y(i, j, k) + Yav
    Next k
    Yave(m) = Yav / n: Yav = 0
    .Cells(1 + m, 108) = Yave(m)
    Next j
    Next i
    End With
16
    'Evaluate data size for error
    If en <= pp Then
    Msg = "Data size is too small. Must be at least a 3 x 3 matrix"    ' Define message.
    Style = vbOKOnly + vbExclamation
    Title = "Data Size Error"
    Response = MsgBox(Msg, Style, Title)
    Call SelectSheets2
    End
    Else
    End If

    'Temperature and Pressure Conversions
    With ThisWorkbook.Worksheets("Model")
    For m = 1 To en
    If .Cells(10, 10) = 1 Then Temp(m) = Temp(m)                'Degrees Fahrenheit
    If .Cells(10, 10) = 2 Then Temp(m) = 5 / 9 * (Temp(m) - 32)   'Degrees Celsius
    If .Cells(10, 10) = 3 Then Temp(m) = Temp(m) + 459.67         'Degrees Rankine
    If .Cells(10, 10) = 4 Then Temp(m) = (Temp(m) + 459.67) / 1.8 'Kelvin
    If .Cells(10, 7) = 1 Then Press(m) = Press(m) Else Press(m) = Press(m) / 14.50377
'PSI or Bar
    Next m
    End With

    Call V_Transforms

    '1 - Algebraic Model
    With ThisWorkbook.Worksheets("Matrix Operator")
    For m = 1 To en
```

```
    P(m) = Press(m)
    T(m) = 1 / Temp(m)
    If PT1 = 1 Then PT(m) = 0: pp = 3
    If PT1 = 2 Then PT(m) = Press(m) / Temp(m)
    If PT1 = 3 Then PT(m) = Press(m) / Temp(m) ^ 2
    If PT1 = 4 Then PT(m) = Press(m) ^ 2 / Temp(m) ^ 2
    If PT1 = 5 Then PT(m) = Press(m) ^ 2 / Temp(m) ^ 3
    .Cells(1 + m, 2) = 1: .Cells(1 + m, 3) = P(m): .Cells(1 + m, 4) = T(m): .Cells(1 + m, 5)
= PT(m)
    Next m
    If PT1 = 1 Then SSE1 = .Cells(30, 19): SSR1 = .Cells(28, 19) - .Cells(13, 12) ^ 2 / en:
B10 = .Cells(28, 12): B11 = .Cells(29, 12): B12 = .Cells(30, 12): B13 = 0 Else SSE1 =
.Cells(22, 19): SSR1 = .Cells(20, 19) - .Cells(13, 12) ^ 2 / en: B10 = .Cells(20, 12): B11
= .Cells(21, 12): B12 = .Cells(22, 12): B13 = .Cells(23, 12)
    SST1 = SSE1 + SSR1: MSE1 = SSE1 / (en - pp): R1 = SSR1 / SST1: aR1 = 1 -
((SSE1 / (en - pp)) / (SST1 / (en - 1)))
    pp = 4

    '2 - Logarithmic Model
    For j = 1 To 100
    .Cells(1 + j, 2) = 0: .Cells(1 + j, 3) = 0: .Cells(1 + j, 4) = 0: .Cells(1 + j, 5) = 0
    Next j
    For m = 1 To en
    P(m) = Log(Press(m)) / Log(10#)
    T(m) = Log(Temp(m)) / Log(10#)
    If PT2 = 1 Then PT(m) = 0: pp = 3
    If PT2 = 2 Then PT(m) = Press(m) / Temp(m)
    If PT2 = 3 Then PT(m) = Press(m) / Temp(m) ^ 2
    If PT2 = 4 Then PT(m) = Press(m) ^ 2 / Temp(m) ^ 2
    If PT2 = 5 Then PT(m) = Press(m) ^ 2 / Temp(m) ^ 3
    .Cells(1 + m, 2) = 1: .Cells(1 + m, 3) = P(m): .Cells(1 + m, 4) = T(m): .Cells(1 + m, 5)
= PT(m)
    Next m
    If PT2 = 1 Then SSE2 = .Cells(30, 19): SSR2 = .Cells(28, 19) - .Cells(13, 12) ^ 2 / en:
B20 = .Cells(28, 12): B21 = .Cells(29, 12): B22 = .Cells(30, 12): B23 = 0 Else: SSE2 =
.Cells(22, 19): SSR2 = .Cells(20, 19) - .Cells(13, 12) ^ 2 / en: B20 = .Cells(20, 12): B21
= .Cells(21, 12): B22 = .Cells(22, 12): B23 = .Cells(23, 12)
    SST2 = SSE2 + SSR2: MSE2 = SSE2 / (en - pp): R2 = SSR2 / SST2: aR2 = 1 -
((SSE2 / (en - pp)) / (SST2 / (en - 1)))
    pp = 4

    '3 - Exponential Model
    For j = 1 To 100
    .Cells(1 + j, 2) = 0: .Cells(1 + j, 3) = 0: .Cells(1 + j, 4) = 0: .Cells(1 + j, 5) = 0
```

```
    Next j
    For m = 1 To en
    P(m) = Exp(Press(m) / 10000)
    T(m) = Exp(-Temp(m) / 100)
    If PT3 = 1 Then PT(m) = 0: pp = 3
    If PT3 = 2 Then PT(m) = Press(m) / Temp(m)
    If PT3 = 3 Then PT(m) = Press(m) / Temp(m) ^ 2
    If PT3 = 4 Then PT(m) = Press(m) ^ 2 / Temp(m) ^ 2
    If PT3 = 5 Then PT(m) = Press(m) ^ 2 / Temp(m) ^ 3
    .Cells(1 + m, 2) = 1: .Cells(1 + m, 3) = P(m): .Cells(1 + m, 4) = T(m): .Cells(1 + m, 5)
= PT(m)
    Next m
    If PT3 = 1 Then SSE3 = .Cells(30, 19): SSR3 = .Cells(28, 19) - .Cells(13, 12) ^ 2 / en:
B30 = .Cells(28, 12): B31 = .Cells(29, 12): B32 = .Cells(30, 12): B33 = 0 Else SSE3 =
.Cells(22, 19): SSR3 = .Cells(20, 19) - .Cells(13, 12) ^ 2 / en: B30 = .Cells(20, 12): B31
= .Cells(21, 12): B32 = .Cells(22, 12): B33 = .Cells(23, 12)
    SST3 = SSE3 + SSR3: MSE3 = SSE3 / (en - pp): R3 = SSR3 / SST3: aR3 = 1 -
((SSE3 / (en - pp)) / (SST3 / (en - 1)))
    pp = 4

    '4 - Polynomial Model
    For j = 1 To 100
    .Cells(1 + j, 2) = 0: .Cells(1 + j, 3) = 0: .Cells(1 + j, 4) = 0: .Cells(1 + j, 5) = 0
    Next j
    For m = 1 To en
    If P4 = 1 Then P(m) = Press(m) ^ 0.5
    If P4 = 2 Then P(m) = Press(m) ^ 0.75
    If P4 = 3 Then P(m) = Press(m) ^ 1.25
    If P4 = 4 Then P(m) = Press(m) ^ 1.5
    If P4 = 5 Then P(m) = Press(m) ^ 2

    If T4 = 1 Then T(m) = Temp(m) ^ -2
    If T4 = 2 Then T(m) = Temp(m) ^ -4
    If T4 = 3 Then T(m) = Temp(m) ^ -6
    If T4 = 4 Then T(m) = Temp(m) ^ -8
    If T4 = 5 Then T(m) = Temp(m) ^ -10

    If PT4 = 1 Then PT(m) = 0: pp = 3
    If PT4 = 2 Then PT(m) = Press(m) / Temp(m)
    If PT4 = 3 Then PT(m) = Press(m) / Temp(m) ^ 2
    If PT4 = 4 Then PT(m) = Press(m) ^ 2 / Temp(m) ^ 2
    If PT4 = 5 Then PT(m) = Press(m) ^ 2 / Temp(m) ^ 3
    .Cells(1 + m, 2) = 1: .Cells(1 + m, 3) = P(m): .Cells(1 + m, 4) = T(m): .Cells(1 + m, 5)
= PT(m)
```

```
    Next m

    If PT4 = 1 Then SSE4 = .Cells(30, 19): SSR4 = .Cells(28, 19) - .Cells(13, 12) ^ 2 / en: B40 = .Cells(28, 12): B41 = .Cells(29, 12): B42 = .Cells(30, 12): B43 = 0 Else SSE4 = .Cells(22, 19): SSR4 = .Cells(20, 19) - .Cells(13, 12) ^ 2 / en: B40 = .Cells(20, 12): B41 = .Cells(21, 12): B42 = .Cells(22, 12): B43 = .Cells(23, 12)
    SST4 = SSE4 + SSR4: MSE4 = SSE4 / (en - pp): R4 = SSR4 / SST4: aR4 = 1 - ((SSE4 / (en - pp)) / (SST4 / (en - 1)))
    End With

    '4 - Display Results
    With ThisWorkbook.Worksheets("Model")
    .Cells(12, 7) = B11: .Cells(12, 10) = B12: .Cells(12, 13) = B13: .Cells(12, 16) = B10: .Cells(12, 19) = MSE1: .Cells(12, 20) = R1: .Cells(12, 21) = aR1
    .Cells(14, 7) = B21: .Cells(14, 10) = B22: .Cells(14, 13) = B23: .Cells(14, 16) = B20: .Cells(14, 19) = MSE2: .Cells(14, 20) = R2: .Cells(14, 21) = aR2
    .Cells(16, 7) = B31: .Cells(16, 10) = B32: .Cells(16, 13) = B33: .Cells(16, 16) = B30: .Cells(16, 19) = MSE3: .Cells(16, 20) = R3: .Cells(16, 21) = aR3
    .Cells(18, 7) = B41: .Cells(18, 10) = B42: .Cells(18, 13) = B43: .Cells(18, 16) = B40: .Cells(18, 19) = MSE4: .Cells(18, 20) = R4: .Cells(18, 21) = aR4
    End With
    End Sub

Sub Choose_Option()

Worksheets("Model").Range("G12:G18,J12:J18,M12:M18,P12:P18,S12:U18").ClearContents

    'Select Data Entry Option
    Msg = "Do you want to use factorial data? Enter Yes for factorial data and No for a different set of data"    ' Define message.
    Style = vbYesNo + vbQuestion + vbDefaultButton1
    Title = "Data Choice"
    Response = MsgBox(Msg, Style, Title)
    If Response = vbYes Then MyString = "Yes": Sheets("Model").Select
    If Response = vbNo Then MyString = "No": Sheets("Model Data").Select
    End Sub

Sub Model()

    'Alternative Data Option
    With ThisWorkbook.Worksheets("Model Data")
    Counta = 100
    'Count total data rows and columns
```

```
    For m = 1 To Counta
    If .Cells(3 + m, 2) = 0 Then GoTo 17
    Next m
17  Counta = m - 1
    en = Counta

    'Collect Data
    For m = 1 To en
    Press(m) = .Cells(3 + m, 3)
    Temp(m) = .Cells(3 + m, 4)
    alpha1 = Press(m): beta = Temp(m)
    Call Error_Check   'Check data for error / completeness
    Next m
    For m = 1 To en
    Yave(m) = .Cells(3 + m, 2)
    alpha1 = Yave(m): beta = 1
    Call Error_Check   'Check data for error / completeness
    Next m
    End With

    'Initialize matrix table
    With ThisWorkbook.Worksheets("Matrix Operator")
    For j = 1 To 100
    .Cells(1 + j, 2) = 0: .Cells(1 + j, 3) = 0: .Cells(1 + j, 4) = 0: .Cells(1 + j, 5) = 0:
.Cells(1 + j, 108) = 0
    Next j

    'Enter Response variable
    For m = 1 To en
    .Cells(1 + m, 108) = Yave(m)
    Next m
    End With
    Sheets("Model").Select
    End Sub
```

VITA

Name:	Chijioke Stanley Ibeh
Address:	Harold Vance Department of Petroleum Engineering Texas A&M University 3116 TAMU - 507 Richardson Building College Station, TX 77843-3116
Phone:	979-422-9647
Email Address:	ibehchijiokes@yahoo.com
Education:	B.Eng., Civil Engineering, Federal University of Technology Owerri, Nigeria, 2000 M.S., Petroleum Engineering, Texas A&M University, 2007
Member:	Society of Petroleum Engineers American Association of Drilling engineers Aggie Drilling Research
Interests:	Football, badminton, contemporary music, traveling and making new friends.